

# Numerical methods for nuclear fuel burnup calculations

Maria Pusa



# Numerical methods for nuclear fuel burnup calculations

---

Maria Pusa

*Thesis for the degree of Doctor of Science in Technology to be presented with due permission for public examination and criticism in Auditorium N at Aalto University (Otakaari 1 M, Espoo, Finland), on the 24<sup>th</sup> of May, 2013, at 12 noon.*



ISBN 978-951-38-7999-0 (Soft back ed.)  
ISBN 978-951-38-8000-2 (URL: <http://www.vtt.fi/publications/index.jsp>)

VTT Science 32

ISSN-L 2242-119X  
ISSN 2242-119X (Print)  
ISSN 2242-1203 (Online)

Copyright © VTT 2013

JULKAISIJA – UTGIVARE – PUBLISHER

VTT  
PL 1000 (Tekniikantie 4 A, Espoo)  
02044 VTT  
Puh. 020 722 111, faksi 020 722 7001

VTT  
PB 1000 (Teknikvägen 4 A, Esbo)  
FI-02044 VTT  
Tfn. +358 20 722 111, telefax +358 20 722 7001

VTT Technical Research Centre of Finland  
P.O. Box 1000 (Tekniikantie 4 A, Espoo)  
FI-02044 VTT, Finland  
Tel. +358 20 722 111, fax +358 20 722 7001

# Numerical methods for nuclear fuel burnup calculations

**Maria Pusa.** Espoo 2013. VTT Science 32. 86 p. + app. 78 p.

## Abstract

The material composition of nuclear fuel changes constantly due to nuclides transforming to other nuclides via neutron-induced transmutation reactions and spontaneous radioactive decay. The objective of burnup calculations is to simulate these changes over time. This thesis considers two essential topics of burnup calculations: the numerical solution of burnup equations based on computing the burnup matrix exponential, and the uncertainty analysis of neutron transport criticality equation based on perturbation theory.

The burnup equations govern the changes in nuclide concentrations over time. They form a system of first order differential equations that can be formally solved by computing the matrix exponential of the burnup matrix. Due to the dramatic variation in the half-lives of different nuclides, the system is extremely stiff and the problem is complicated by vast variations in the time steps used in burnup calculations. In this thesis, the mathematical properties of burnup matrices are studied. It is deduced that their eigenvalues are generally confined to a region near the negative real axis. Rational approximations that are accurate near the negative real axis, and the Chebyshev rational approximation method (CRAM) in particular, are proposed as a novel method for solving the burnup equations. The results suggest that the proposed approach is capable of providing a robust and accurate solution to the burnup equations with a very short computation time.

When a mathematical model contains uncertain parameters, this uncertainty is propagated to responses dependent on the model. This thesis studies the propagation of neutron interaction data uncertainty through the criticality equation on a fuel assembly level. The considered approach is based on perturbation theory, which allows computing the sensitivity profiles of a response with respect to any number of parameters in an efficient manner by solving an adjoint system in addition to the original forward problem. The uncertainty related to these parameters can then be propagated deterministically to the response by linearizing the response.

**Keywords** burnup equations, Chebyshev rational approximation, CRAM, matrix exponential, sensitivity analysis, uncertainty analysis

## Academic dissertation

Supervisor	Prof. Olavi Nevanlinna Department of Mathematics and Systems Analysis Aalto University, Finland
Instructor	Dr. Jaakko Leppänen Nuclear Energy VTT Technical Research Centre of Finland
Preliminary examiners	Dr. Ivan Kodeli Jožef Stefan Institute, Slovenia  Prof. Jukka Tuomela Department of Mathematics University of Eastern Finland
Opponent	Prof. Antonella Zanna Munthe-Kaas Department of Mathematics University of Bergen, Norway

# Contents

<b>Acknowledgments</b>	<b>7</b>
<b>List of publications</b>	<b>8</b>
<b>Author's contribution</b>	<b>9</b>
<b>1 Introduction</b>	<b>11</b>
1.1 Background . . . . .	11
1.2 Research objectives . . . . .	12
1.2.1 Numerical solution of burnup equations . . . . .	12
1.2.2 Propagation of uncertainty through criticality equation . . . . .	13
<b>2 Burnup calculations</b>	<b>15</b>
2.1 Neutron transport and criticality equation . . . . .	15
2.2 Burnup equations . . . . .	19
<b>3 Matrix exponential solution of burnup equations</b>	<b>23</b>
3.1 Mathematical properties of burnup matrices . . . . .	23
3.1.1 Graph-theoretical approach . . . . .	27
3.1.2 Spectrum . . . . .	28
3.2 Matrix exponential . . . . .	35
3.2.1 Definitions of matrix functions . . . . .	35
3.2.2 Application to burnup matrices . . . . .	37
3.2.3 Numerical computation . . . . .	39
3.3 Solution based on rational approximations near the negative real axis . . . . .	42
3.3.1 Partial fraction decomposition form . . . . .	43
3.3.2 Chebyshev rational approximation method (CRAM) . . . . .	43
3.3.3 Rational approximations from contour integrals . . . . .	54
<b>4 Perturbation theory based sensitivity and uncertainty analysis applied to criticality equation</b>	<b>61</b>
4.1 Background for sensitivity and uncertainty analysis . . . . .	62
4.2 Perturbation theory . . . . .	65

4.2.1	Numerical computation . . . . .	66
4.3	Application to CASMO-4 . . . . .	68
<b>5</b>	<b>Summary of the publications</b>	<b>73</b>
5.1	Publication I: Computing the matrix exponential in burnup calculations	73
5.2	Publication II: Rational approximations to the matrix exponential in burnup calculations . . . . .	74
5.3	Publication III: Correction to partial fraction decomposition coefficients for Chebyshev rational approximation on the negative real axis . . . . .	75
5.4	Publication IV: Solving linear systems with sparse Gaussian elimination in the Chebyshev rational approximation method (CRAM) . . . . .	75
5.5	Publication V: Incorporating sensitivity and uncertainty analysis to a lattice physics code with application to CASMO-4 . . . . .	76
5.6	Publication VI: Perturbation-theory-based sensitivity and uncertainty analysis with CASMO-4 . . . . .	77
<b>6</b>	<b>Conclusions</b>	<b>79</b>
	<b>Bibliography</b>	<b>82</b>
	<b>Appendices</b>	
	Publications I–VI	

## Acknowledgments

I wish to express my sincere gratitude to my instructor at VTT, Dr. Jaakko Leppänen, for his support and insight during this entire process and especially for the unique opportunity to be a part of developing Serpent. Working together has been a lot of fun during these years.

I am obliged to our Group Manager, Dr. Petri Kotiluoto, and our Technology Manager, Dr. Timo Vanttola, for their support and for giving me the freedom in my research work. I'd also like to thank my colleagues at VTT, especially my team members and everyone in our office.

I'm grateful to Prof. Olavi Nevanlinna of the Department of Mathematics and Systems Analysis, Aalto University, for acting as my supervisor and for his mathematical insight and ideas that helped me to improve this dissertation, and to Prof. Antonella Zanna Munthe-Kaas of the Department of Mathematics, University of Bergen, Norway, for acting as my opponent in the defense of this thesis. I wish to thank the preliminary examiners of my dissertation, Dr. Ivan Kodeli of Jožef Stefan Institute, Slovenia and Prof. Jukka Tuomela of University of Eastern Finland, for their careful work. In addition, I'm grateful to Dr. Kodeli for his kind help over the years related to the UAM benchmark.

Above all, I want to thank my dear husband Mikko, not only for his constant love and support, but also for his practical help in every aspect of the process.

This work has been funded through the Finnish Research Programme on Nuclear Power Plant Safety SAFIR and the Academy of Finland research programmes NETNUC and NUMPS.

## List of publications

This thesis consists of the present article and the following six publications.

- I M. PUSA and J. LEPPÄNEN, “Computing the matrix exponential in burnup calculations”, *Nucl. Sci. Eng.*, **164**, 2, 140–150 (2010).
- II M. PUSA, “Rational approximations to the matrix exponential in burnup calculations”, *Nucl. Sci. Eng.*, **169**, 2, 155–167 (2011).
- III M. PUSA, “Correction to partial fraction decomposition coefficients for Chebyshev rational approximation on the negative real axis”, [arXiv:1206.2880v1](https://arxiv.org/abs/1206.2880v1) [[math.NA](https://arxiv.org/abs/1206.2880v1)] (2012).
- IV M. PUSA and J. LEPPÄNEN, “Solving linear systems with sparse Gaussian elimination in the Chebyshev rational approximation method (CRAM)”, accepted for publication in *Nucl. Sci. Eng.* (Nov 2013).
- V M. PUSA, “Incorporating sensitivity and uncertainty analysis to a lattice physics code with application to CASMO-4”, *Ann. Nucl. Energy*, **40**, 1, 153–162 (2012).
- VI M. PUSA, “Perturbation-theory-based sensitivity and uncertainty analysis with CASMO-4”, *Sci. Technol. Nucl. Install.*, **2012**, 157029 (2012).

## **Author's contribution**

Publications II, III, V, VI and the present article, which contains also new considerations, were written solely by the author. The author had a major role in Publications I and IV. A detailed description on the author's contribution in these two publications is given below.

### **Publication I: Computing the matrix exponential in burnup calculations**

The author was responsible for the theoretical considerations, selecting the matrix exponential methods to be studied, implementing the Krylov-based matrix exponential method and the Chebyshev rational approximation method, and performing the computations. The article was written by the author, apart from the introduction section, which was written in collaboration by the two authors.

The second author designed the interface for the matrix exponential solver and added the implemented CRAM solution method to the reactor physics code Serpent. The second author also chose the test cases to be studied, calculated the burnup matrices with Serpent, and performed the calculation that compared the efficiency of the matrix exponential solution against the TTA method in a full assembly burnup calculation with Serpent.

### **Publication IV: Solving linear systems with sparse Gaussian elimination in the Chebyshev rational approximation method (CRAM)**

The author was responsible for the theoretical considerations, selecting the solution method and implementing it to the reactor physics code Serpent, performing the computations and writing the article.

The second author selected the test case to be studied and provided the input file for Serpent.



# 1. Introduction

## 1.1 Background

In an operating nuclear reactor, the material composition of a nuclear fuel changes constantly. In nuclear fission, the original nucleus splits into lighter nuclides, releasing secondary particles and energy. In addition, nuclides transform to other nuclides through other neutron-induced transmutation reactions and spontaneous radioactive decay. The radioactive decay process continues even when nuclear fuel is removed from the reactor.

In many applications, it is essential to be able to predict the changes in the nuclear fuel composition. For example, the safety and economy of a reactor core loading depend heavily on the changes in nuclide concentrations and how these changes are compensated for. This is relevant when designing new reactor concepts and when optimizing the reactor core loading of existing reactors alike. Also, it is important to assess the material decomposition of spent fuel after removing it from the reactor and at any time afterwards. Final disposition applications necessitate predicting the nuclide concentrations at time steps of the order of thousands of years.

In practice, the changes in nuclear fuel material composition are evaluated by dedicated burnup calculation codes. Unfortunately, it is extremely difficult to simulate the problem in the true time-dependent form, due to the coupling between nuclide concentrations and neutron density distribution—the transmutation rates of neutron-induced reactions depend on the neutron density distribution in the system, and the neutron density distribution, on the other hand, is strongly dependent on the isotopic compositions of the fissile material.

*Burnup calculations* are based upon the assumption that nuclide concentrations can be assumed constant when solving the neutron density distribution. They are formulated around two central equations in reactor physics, which are the *neutron transport equation* and the *burnup equations*. The neutron transport equation is essentially a balance equation for the neutron density. In burnup calculations, it is modeled as a time-independent eigenvalue problem, called the *criticality equation*, in which case the solution comprises of neutron density distribution and the multiplication factor, which characterizes the time dependence of the system. Based on the neutron density distribution solution, it is possible to compute the rates at which

nuclides transform to other nuclides. These reaction rates can be used to form the burnup equations, which govern the changes in nuclide concentrations over time. Burnup calculations form a cyclic process, where the system is modeled forward in time by solving the criticality equation and the burnup equations in a sequential manner.

### 1.2 Research objectives

Due to the special demands related to the target of application, it is crucial that the computational methods related to burnup calculations are constantly developed and refined, and that their accuracy and efficiency are improved. In addition, uncertainty analysis methods are needed for evaluating the reliability of the calculation results.

#### 1.2.1 Numerical solution of burnup equations

There are generally various numerical methods for solving the neutron transport equation. However, notably little interest and research effort has been previously shown towards the solution of burnup equations. The burnup equations form a system of first order differential equations, which can be formally solved by computing the matrix exponential of the burnup matrix. Since the half-lives of different nuclides vary dramatically, the system is extremely stiff. It is also difficult that the time steps used in burnup calculations generally vary from less than a day at the beginning of the irradiation cycle to a few hundred days at the end. For these reasons, the computation of the matrix exponential has been previously considered impossible for the full burnup system. Instead, simplified burnup chains have been used, or the most short-lived nuclides have been treated separately when computing a matrix exponential solution.

The focus of this thesis was to examine if it is possible to solve a detailed burnup system containing over a thousand nuclides by a single matrix exponential method. The motivation for this was the development of the burnup calculation routines in the Serpent Monte Carlo reactor physics code developed at VTT.<sup>1</sup>

In this thesis, the mathematical properties of burnup matrices are studied systematically for the first time. It turns out that the eigenvalues of burnup matrices are confined to a region near the negative real axis and that they are connected with the class of  $M$ -matrices. These properties can be utilized in solving the burnup equations by employing rational approximations that are accurate near the negative real axis. The Chebyshev rational approximation method (CRAM), defined as the best rational approximation on the negative real axis, is proposed as a novel method for solving the burnup equations. In addition, rational approximation based on quadrature formulas derived from complex contour integrals is proposed. The proposed methods are compared to established numerical methods and highly accurate reference solutions.

---

<sup>1</sup>A complete and up-to-date description of the Serpent code is found at the project website. (<http://montecarlo.vtt.fi>)

### **1.2.2 Propagation of uncertainty through criticality equation**

In addition to numerical error, the reliability of calculation results is affected by uncertain parameter values utilized in the computations. In particular, reactor physics calculations employ large nuclear data libraries containing the interaction data between neutrons and nuclei. These nuclear data libraries are believed to be one of the most significant sources of uncertainty in all reactor physics calculations, including burnup calculations. In order to evaluate the reliability of the calculation results, this parameter uncertainty needs to be propagated through the calculations. Since the libraries typically contain at least tens of thousands of uncertain parameters, calculation times often inhibit the use of statistical approaches in practical applications.

In this thesis, uncertainty analysis is applied to the criticality equation, which is one of the two equations that are solved sequentially during burnup calculations. The considered uncertainty analysis method is based on perturbation theory, which allows efficiently propagating the uncertainty related to a nuclear data library to the response of interest by solving an adjoint system in addition to the original forward problem. The described work was done in a context other than burnup calculations, but it forms a theoretical background for propagating nuclear data uncertainty through the criticality equation to parameters needed in burnup equations.



## 2. Burnup calculations

The objective of burnup calculations is to simulate the long-term time behavior of a nuclear reactor. The neutronic properties of nuclear fuel depend strongly on the isotopic composition of the fissile materials. In an operating reactor, these material compositions change constantly due to neutron-induced reactions and spontaneous radioactive decay. The rates of the former reactions depend on the neutron density distribution in the system. Unfortunately, it is not possible to solve the coupled problem for neutron density distribution and nuclide concentrations in a truly time-dependent form, and approximations are required.

Burnup calculations are based on the assumption that the neutron density distribution and the changes in the nuclide concentrations can be solved sequentially in a cyclic manner by alternating the two computation steps, and using results from the previous step. During the first step, the neutron density distribution is computed assuming that the nuclide concentrations are fixed. This requires solving the *neutron transport equation*, which is essentially a balance equation for neutrons. Based on the neutron density distribution, the rates of the neutron-induced reactions can be computed. During the second step, the changes in the nuclide concentrations are solved from the *burnup equations* assuming constant reaction rates. This calculational strategy can be further refined by means of predictor–corrector methods, which aim at predicting the most representative averages for the reaction rates approximated as constants during the solution of burnup equations.<sup>2</sup> The following subsections introduce the two basic equations—the criticality equation and the burnup equations—on which burnup calculations are based.

### 2.1 Neutron transport and criticality equation

The neutron transport equation is a balance equation for the neutron density distribution  $N(\mathbf{r}, \boldsymbol{\Omega}, E, t)$ , defined in a six-dimensional phase space as the expected number of neutrons in a volume  $dV$  about the point  $\mathbf{r}$ , traveling in the cone of directions  $d\boldsymbol{\Omega}$  about the direction  $\boldsymbol{\Omega}$ , with energies in the interval  $[E, E + dE]$  at the time instant  $t$ . In nuclear reactors, neutron–neutron interactions can be neglected, and the neutron

---

<sup>2</sup>The use of predictor–corrector methods does not affect the solution of the criticality equation nor the burnup equations.

## 2. Burnup calculations

---

density distribution depends solely on the interactions between neutrons and matter.

The interaction probabilities between neutrons and matter are described by quantities called *neutron cross-sections*. These probabilities depend on the target nucleus, the type of the interaction, and the energy of the neutron. The microscopic cross-section  $\sigma_{i,x}(E)$  characterizes the probability that a neutron with energy  $E$  interacts with nuclide  $i$  through reaction  $x$ . It has the dimensions of area and it can be interpreted as the effective cross-sectional area per nucleus seen by a neutron. The macroscopic cross-section is defined as the microscopic cross-section multiplied by nuclide density. In a medium consisting of several nuclides, the macroscopic cross-section for reaction  $x$  may be written

$$\Sigma_x(\mathbf{r}, E) = \sum_{i=1}^n n_i(\mathbf{r}) \sigma_{i,x}(E), \quad (2.1)$$

where  $n_i$  denotes the concentration of nuclide  $i$ . A macroscopic cross-section can be interpreted physically as the interaction probability per path length traversed by a neutron.

There are various reactions through which neutrons and nuclides may interact. These reactions can be divided into fission, capture and scattering reactions. Capture reactions include all of the reactions, where no secondary neutrons are emitted. It is customary to include both fission and capture reactions in absorption. The total cross-section  $\Sigma_t(\mathbf{r}, E)$  corresponds to the probability of any type of reaction.

In scattering reactions, it is necessary to specify the probability distributions for the energy and direction of the scattered neutron. The differential scattering cross-section

$$\Sigma_s(\mathbf{r}, E \rightarrow E', \boldsymbol{\Omega} \cdot \boldsymbol{\Omega}')$$

corresponds to the probability that the scattered neutron will have the direction  $\boldsymbol{\Omega}'$  and energy  $E'$ . Scattering collisions can be divided into elastic and inelastic reactions. The latter may result in the emission of multiple secondary neutrons.

In fission, it can be approximated that secondary neutrons are produced isotropically and that their energy spectrum is independent of the energy of the neutron causing the fission. Therefore, only two additional quantities need to be specified in addition to the fission cross-section  $\Sigma_f(\mathbf{r}, E)$ . These quantities are the mean number of fission neutrons produced in a fission caused by a neutron with energy  $E$ , denoted by  $\nu(E)$ , and the fission neutron energy spectrum, denoted by  $\chi(E)$ .

Neutron transport problems are most often formulated in terms of the *neutron flux*  $\Phi$ , which is defined

$$\Phi(\mathbf{r}, \boldsymbol{\Omega}, E, t) = v N(\mathbf{r}, \boldsymbol{\Omega}, E, t),$$

where  $v$  is the neutron velocity. The *scalar flux* is obtained by integrating the angular flux  $\Phi$  over all directions:

$$\phi(\mathbf{r}, E) = \int d\boldsymbol{\Omega} \Phi(\mathbf{r}, \boldsymbol{\Omega}, E). \quad (2.2)$$

The time-dependent transport equation for the neutron flux can now be written

$$\frac{1}{v} \frac{\partial \Phi}{\partial t} + \boldsymbol{\Omega} \cdot \nabla_r \Phi + \Sigma_t \Phi = \int dE' \int d\boldsymbol{\Omega}' \Sigma'_s \Phi' + \frac{\chi(E)}{4\pi} \int dE' \nu(E') \Sigma'_f \Phi', \quad (2.3)$$

where

- $\Phi = \Phi(\mathbf{r}, \boldsymbol{\Omega}, E, t)$
- $\Phi' = \Phi(\mathbf{r}, \boldsymbol{\Omega}', E', t)$
- $\phi' = \phi(\mathbf{r}, E')$
- $\Sigma_t = \Sigma_t(\mathbf{r}, E)$
- $\Sigma'_s = \Sigma_s(\mathbf{r}, E' \rightarrow E, \boldsymbol{\Omega}' \cdot \boldsymbol{\Omega})$
- $\Sigma'_f = \Sigma_f(\mathbf{r}, E')$

Equation (2.3) can be written in operator form as

$$\frac{1}{v} \frac{\partial \Phi}{\partial t} + A\Phi = B\Phi, \quad (2.4)$$

where  $A\Phi$  includes all terms, except for the time derivative and the fission source term  $B\Phi$ .

In most cases the time-dependence of the neutron transport equation is not treated explicitly, but the problem is solved as a criticality eigenvalue problem. Physically it is clear that by adjusting the number of fission neutrons emitted, it is possible to obtain a system in which the rate of neutron production is equal to the losses by absorption and leakage. Therefore, Eq. (2.3) can be written as an eigenvalue problem called the *criticality equation*

$$A\Phi = \frac{1}{k} B\Phi, \quad (2.5)$$

to which a non-negative solution is guaranteed to exist, corresponding to the largest eigenvalue  $k$ . This eigenvalue is called the multiplication factor and it characterizes the time behavior of the system. If  $k > 1$ , the neutron flux will increase with time, and the system is called supercritical. The case  $k = 1$  corresponds to a truly time-independent solution, in which case the system is called critical. Finally, if  $k < 1$ , the neutron flux will decrease with time, and the system is called subcritical. Since Eq. (2.5) is homogeneous, it allows an arbitrary normalization of the solution. In burnup calculations the flux solution is typically normalized to coincide with the power of the system.

There exists a variety of computational methods for solving the criticality equation and they can be divided into deterministic methods and Monte Carlo simulation. Traditionally, burnup calculations have been performed in two dimensions using deterministic methods. A review of the different methods falls outside the scope of this thesis, but practically all deterministic methods use similar strategies for dealing with the energy and angular dependence of the criticality equation, and these techniques are explained briefly in the following.

The angular dependence of the scattering source in Eq. (2.5) is most often handled by expanding it as a truncated series of spherical harmonics. In this case, the truncation order zero corresponds to isotropic scattering. After this, there are two

## 2. Burnup calculations

---

established practices to deal with the angular dependence of the neutron flux. In the discrete ordinates method, the criticality equation is evaluated and solved in discrete angular directions  $\{\boldsymbol{\Omega}_j\}_{j=1}^N$ . In the spherical harmonics method, on the other hand, the angular flux is expanded as a truncated series of spherical harmonics.

The energy discretization procedure is virtually always based on the *multi-group approximation*. In this approach, the considered energy interval  $[E_{\min}, E_{\max}]$  is divided into groups,  $[E_g, E_{g-1}]$ ,  $g = 1, \dots, G$ , with  $E_0 = E_{\max}$  and  $E_G = E_{\min}$ . After expanding the scattering source in the base of spherical harmonics, the multi-group criticality equation for group  $g$  may be obtained by integrating Eq. (2.5) over the interval  $[E_g, E_{g-1}]$ . Assuming isotropic scattering, this leads to a system of the form

$$\begin{aligned} & \boldsymbol{\Omega} \cdot \nabla \Phi^g(\mathbf{r}, \boldsymbol{\Omega}) + \Sigma^g \Phi^g(\mathbf{r}, \boldsymbol{\Omega}) \\ &= \frac{1}{4\pi} \sum_{h=1}^G \Sigma_s^{h \rightarrow g} \phi^h(\mathbf{r}) + \frac{\chi_g}{4\pi k} \sum_{h=1}^G \bar{\nu} \Sigma_f^h \phi^h(\mathbf{r}), \quad g = 1, \dots, G, \end{aligned} \quad (2.6)$$

where the multi-group quantities are defined as

$$\Sigma^g(\mathbf{r}) = \frac{\int_g \Sigma(\mathbf{r}, E) \phi(\mathbf{r}, E) dE}{\int_g \phi(\mathbf{r}, E) dE}, \quad (2.7)$$

$$\Sigma_s^{g' \rightarrow g}(\mathbf{r}) = \frac{\int_{g'} \int_g \Sigma_s(\mathbf{r}, E' \rightarrow E) \phi(\mathbf{r}, E') dE' dE}{\int_{g'} \phi(\mathbf{r}, E') dE'}, \quad (2.8)$$

$$\chi^g = \int_g \chi(E) dE, \quad (2.9)$$

and the multi-group flux as

$$\Phi^g(\mathbf{r}, \boldsymbol{\Omega}) = \int_g \Phi(\mathbf{r}, \boldsymbol{\Omega}, E) dE. \quad (2.10)$$

Of course, solving the multi-group flux from Eq. (2.6) requires that the multi-group cross-sections are known. In practice, this requires computing the multi-group cross-sections approximatively before the actual transport calculation in the true geometry has been carried out. Depending on the number of energy groups used in the transport calculation, this may require a series of calculations based on different computational strategies.

The Monte Carlo method is a stochastic solution scheme, in which the random walk of individual neutrons is simulated by drawing samples from probability distributions. In a simple Monte Carlo simulation, neutrons are tracked through geometries by sampling their free path lengths. If the sampled free path length does not cross material boundaries, it determines the next collision site for the neutron. In this case, also the interaction nuclide and type are sampled from appropriate probability distributions. The interaction between the neutron and the nuclide can either be an absorption or a scattering reaction. If the neutron is absorbed, its history is terminated. In case of a scattering reaction, the energy and direction of the scattered neutron are sampled from appropriate distributions. When a material boundary is crossed, the simulation proceeds by sampling a new free path length in the entered material,

starting from the boundary. The history of a neutron consists of these tracks from the initial emission to the final absorption or escape from the system. The simulation results can then be used to compute statistical estimates for reaction rates and other quantities of interest, without the need to explicitly solve the flux distribution. The main advantage of the Monte Carlo approach is that it can easily deal with complex three dimensional geometries. It is also useful that the latest available knowledge on neutron interactions can readily be utilized in Monte Carlo calculations. The drawback of the method, on the other hand, is the high computational cost, which often becomes a practical limitation.

## 2.2 Burnup equations

Burnup equations describe the changes in the concentrations of the nuclides considered in a burnup calculation. They form a system of first order linear differential equations that can be written

$$n'_i(t) = -r_i n_i(t) + \sum_{j \neq i} r_{j \rightarrow i} n_j(t), \quad n_i(0) = n_0^i, \quad i = 1 \dots, n, \quad (2.11)$$

where  $r_i$  is the total rate density at which nuclide  $i$  is transformed to other nuclides,  $r_{j \rightarrow i}$  is the rate density at which nuclide  $j \neq i$  is transformed to nuclide  $i$ , and  $n_0^i$  is the initial concentration of nuclide  $i$ . Equation (2.11) can be written in matrix form as

$$\mathbf{n}' = \mathbf{A} \mathbf{n}, \quad \mathbf{n}(0) = \mathbf{n}_0, \quad (2.12)$$

where  $\mathbf{A} \in \mathbb{R}^{n \times n}$  is called the *burnup matrix* and  $\mathbf{n} \in \mathbb{R}^n$  is the nuclide concentration vector. The diagonal elements  $a_{ii} = -r_i$  of the burnup matrix correspond to the total loss rates, and the off-diagonal elements  $a_{ij} = r_{j \rightarrow i}$  to the production rates.

Nuclides can transform to other nuclides through neutron-induced reactions and spontaneous radioactive decay. As previously explained, burnup equations are formed based on the assumption that the reaction rates of the neutron-induced reactions can be approximated as fixed constants. After solving the neutron flux, the rate for a particular neutron reaction can be computed by integrating the flux multiplied by the corresponding microscopic cross-section over space and energy.

Let us first consider reactions other than fission, and let  $\sigma_{ji}$  denote the microscopic cross-section for the neutron reactions that transform nuclide  $j$  to nuclide  $i$ . The corresponding average transmutation rate density can be computed as

$$V^{-1} \int_{E_{\min}}^{E_{\max}} dE \int_V dV \sigma_{ji}(E) \phi(\mathbf{r}, E) = \bar{\sigma}_{ji} \bar{\phi}, \quad (2.13)$$

where

$$\bar{\sigma}_{ji} = \frac{\int_{E_{\min}}^{E_{\max}} dE \int_V dV \sigma_{ji}(E) \phi(\mathbf{r}, E)}{\int_{E_{\min}}^{E_{\max}} dE \int_V dV \phi(\mathbf{r}, E)} \quad (2.14)$$

and

$$\bar{\phi} = V^{-1} \int_{E_{\min}}^{E_{\max}} dE \int_V dV \phi(\mathbf{r}, E) \quad (2.15)$$

## 2. Burnup calculations

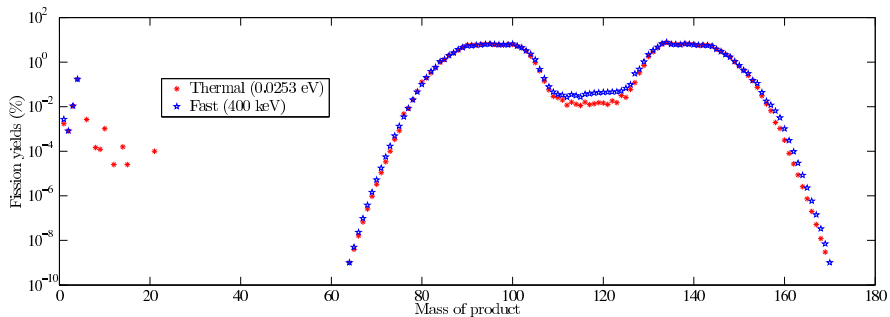


**Figure 2.1.** Independent fission product yields for  $^{235}\text{U}$ .

is the energy and region averaged flux, normalized to coincide with the power of the system.

In the case of fission, the transmutation rate  $j \rightarrow i$  can be written

$$V^{-1} \int_{E_{\min}}^{E_{\max}} dE \int_V dV \gamma_{ji}(E) \sigma_{j,t}(\mathbf{r}, E) \phi(\mathbf{r}, E) = \gamma_{ji} \bar{\sigma}_{j,t} \bar{\phi}, \quad (2.16)$$

where  $\gamma_{ji}$  is the yield of the fission product nuclide  $i$ .

In addition to neutron reactions, nuclides can transform to other nuclides via spontaneous radioactive decay. Let  $\lambda_{ji}$  denote the decay constant corresponding to radioactive decay  $j \rightarrow i$ . The total rate at which nuclide  $j$  is transformed to nuclide  $i$  can now be written

$$r_{j \rightarrow i} = \bar{\sigma}_{ji} \bar{\phi} + \gamma_{ji} \bar{\sigma}_{j,t} \bar{\phi} + \lambda_{ji}, \quad (2.17)$$

and the total loss rate correspondingly

$$r_j = \sum_{k \neq j} \bar{\sigma}_{jk} + \bar{\sigma}_{j,t} + \sum_{k \neq j} \lambda_{jk}. \quad (2.18)$$

Let  $Z$  denote the atomic number and  $A$  the mass number of a nuclide. Table 2.1 lists the most relevant decay and neutron-induced reactions in burnup calculations. Figure 2.1 shows a plot of the fission product yields for  $^{235}\text{U}$ .

When forming the burnup equations, it is possible to take into account the production of by-product nuclides. In this case, for example, the reaction rate for each  $(n, p)$  reaction contributes to the production rate of  $^1\text{H}$ . Traditionally, the production of nuclides as by-products has been ignored [1, 2]. Therefore, the term *augmented burnup matrix* will be used to refer to the case, where the production of by-product nuclides has been taken into account when constructing the burnup matrix.

**Definition 2.2.1** (Augmented burnup matrix). *A burnup matrix  $\mathbf{A} \in \mathbb{R}^{n \times n}$  is called augmented, when it has been constructed such that the reactions, in which by-products are emitted, also contribute to the production rates of the by-product nuclides.*

In the absence of neutron irradiation, nuclides transform only through radioactive decay, and the burnup equations reduce to decay equations. In this case, the burnup matrix is called a *decay matrix*.

**Table 2.1.** The most relevant decay and neutron-induced reactions in burnup calculations for a nuclide with atomic number  $Z$  and mass number  $A$ .

Mode of decay	Daughter nuclide	By-product nuclide
$\alpha$ decay	$(Z - 2, A - 4)$	${}^4\text{He}$
Proton emission	$(Z - 1, A - 1)$	${}^1\text{H}$
Neutron emission	$(Z, A - 1)$	-
$\beta^-$ decay	$(Z + 1, A)$	-
$\beta^+$ decay	$(Z - 1, A)$	-
$(n, 2n)$	$(Z, A - 1)$	-
$(n, 3n)$	$(Z, A - 2)$	-
$(n, 4n)$	$(Z, A - 3)$	-
$(n, \gamma)$	$(Z, A + 1)$	-
$(n, p)$	$(Z - 1, A)$	${}^1\text{H}$
$(n, d)$	$(Z - 1, A - 1)$	${}^2\text{H}$
$(n, t)$	$(Z - 1, A - 2)$	${}^3\text{H}$
$(n, {}^3\text{He})$	$(Z - 2, A - 2)$	${}^3\text{He}$
$(n, \alpha)$	$(Z - 2, A - 3)$	${}^4\text{He}$
Fission	fission product nuclides	-



### 3. Matrix exponential solution of burnup equations

The burnup equations according to Eq. (2.12) can be formally solved by the matrix exponential method yielding the simple solution

$$\mathbf{n}(t) = e^{\mathbf{A}t} \mathbf{n}_0 , \quad (3.1)$$

where the exponential of the matrix  $\mathbf{A}t$  can be defined as the power series expression

$$e^{\mathbf{A}t} = \sum_{k=0}^{\infty} \frac{1}{k!} (\mathbf{A}t)^k , \quad (3.2)$$

with the additional definition  $\mathbf{A}^0 = \mathbf{I}$ . There are generally various numerical methods for computing the matrix exponential. However, the suitability of a particular method depends substantially on the characteristics of the problem at hand. The mathematical properties of (augmented) burnup matrices are studied systematically in Section 3.1. The characteristics and numerical computation of the burnup matrix exponential are then considered in Section 3.2. Rational approximations accurate near the negative real axis are proposed as a novel method for solving the burnup equations and this framework is considered in Section 3.3.

#### 3.1 Mathematical properties of burnup matrices

In order to select a well-suited method for computing the matrix exponential solution, it is necessary to consider the mathematical characteristics of burnup matrices.

First of all, burnup matrices are relatively large and sparse. The total number of nuclides depends both on the employed nuclear data library and the criterion for selecting the nuclides. The evaluated nuclear data library JEFF-3.1 [3], for example, contains neutron interaction data for 381 nuclides and decay data for 3852 nuclides. The nuclides to be considered in a burnup calculation are chosen based on the transmutation chains originating from the initial nuclides, possibly accompanied with a probabilistic criterion, the resulting total number of nuclides typically being between 1200 and 1700.

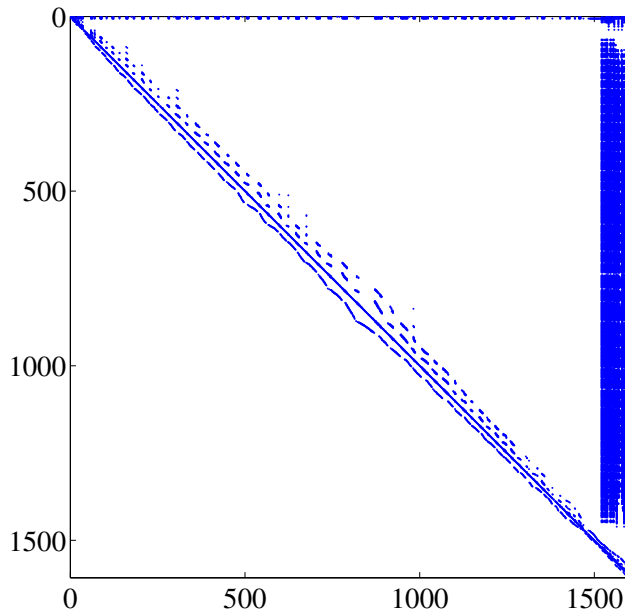


**Figure 3.1.** Sparsity pattern of an augmented burnup matrix corresponding to a system with 1606 nuclides.

When constructing the burnup matrix, the nuclides can be indexed arbitrarily. The burnup matrix becomes nearly upper triangular if the nuclides are indexed in an ascending order with respect to their ZAI index, defined as  $ZAI = 10\,000Z + 10A + I$ , where  $Z$  is the atomic number,  $A$  is the mass number of the nuclide and  $I$  is the isomeric state number. In this case, the non-zero elements are concentrated around the diagonal, and fission product distributions on the right hand side. The matrix elements below the diagonal correspond to reactions where the ZAI index increases, the only considered reactions being  $\beta^-$  decay and the  $(n, \gamma)$  reaction. Figure 3.1 shows the sparsity pattern of a typical burnup matrix for a system with 1606 nuclides. The matrix elements on the first subdiagonal correspond to the  $(n, \gamma)$  reaction, in which the mass number of the nuclide increases by one. The non-zeros below the first subdiagonal, on the other hand, correspond to  $\beta^-$  decay with each arc corresponding to the isotopes of a single element. The sparsity pattern follows from that  $\beta^-$  decay generally occurs in neutron-rich nuclides only. Empty columns in the matrix correspond to nuclides which are stable and do not elicit any neutron reactions.

As explained in Section 2.2, the diagonal elements of the burnup matrix are non-positive, and the element  $-a_{ii}$  characterizes the total rate at which nuclide  $i$  is transformed to other nuclides. The off-diagonal elements, on the other hand, are non-negative, and the element  $a_{ij}$  describes the rate by which nuclide  $j$  is transformed to nuclide  $i$ . This simple sign pattern connects the burnup matrices with the class of *Z-matrices*.

**Definition 3.1.1.** A matrix  $\mathbf{Z} \in \mathbb{R}^{n \times n}$  is called a *Z-matrix* if its off-diagonal elements are non-positive, i.e.  $z_{ij} \leq 0$  for  $i \neq j$ . The class of Z-matrices is denoted by

$$\mathbf{Z}_n = \{ \mathbf{Z} \in \mathbb{R}^n \mid z_{ij} \leq 0, \quad i \neq j \}. \quad (3.3)$$

Based on this definition, it is evident that the negatives of burnup matrices belong to Z-matrices. This observation is interesting, because it suggests connections with the theory of non-negative matrices. Especially, every  $\mathbf{Z} \in \mathbf{Z}_n$  can be expressed in the form

$$\mathbf{Z} = s\mathbf{I} - \mathbf{B}, \quad s > 0, \quad \mathbf{B} \geq 0, \quad (3.4)$$

where  $\mathbf{B} \geq 0$  denotes  $B_{ij} \geq 0$  for  $i, j = 1, \dots, n$ . This is further discussed in Section 3.1.2, where the spectral properties of burnup matrices are considered.

Nuclides may transform to other nuclides through spontaneous radioactive decay and neutron-induced reactions. The measured nuclide half-lives corresponding to radioactive decay can vary from  $10^{-24}$  seconds to billions of years, which introduces elements of both extremely small and large magnitude to the burnup matrix, making the system numerically extremely stiff. The highly unstable nuclides, whose decay constants can be of the order of  $10^{21} \text{ s}^{-1}$ , are numerically the most difficult. An example of such nuclide is the boron isotope  ${}^7\text{B}$ , which decays to the beryllium isotope  ${}^6\text{Be}$  by proton emission with a half-life of the order of  $10^{-22} \text{ s}$ . Since

$$\|\mathbf{A}\|_1 \geq \max_{i,j} |a_{ij}|,$$

this reaction alone increases the burnup matrix norm to be at least of the order of  $10^{21}$ .

The magnitudes of neutron-induced reaction rates vary significantly less. In accordance with Eqs. (2.13) and (2.16), their values are bounded by the maximum values of the cross-sections and the normalization of the neutron flux by power. One of the largest known cross-sections is the capture cross-section of  ${}^{135}\text{Xe}$ , whose maximum value is of the order of  $10^{-16} \text{ cm}^2$ . The highest ever measured neutron fluxes are of the order  $\sim 10^{16}/(\text{cm}^2 \text{ s})$ , the record being  $\sim 3 \times 10^{16}$  neutrons/ $(\text{cm}^2 \text{ s})$  achieved in the High Flux Isotope Reactor at Oak Ridge National Laboratory. Therefore, the magnitudes of neutron-induced reactions can be conservatively bounded from above by unity in reactor conditions.

To illustrate the extensive variations in the decay and transmutation rates, Fig. 3.2 shows a plot of the absolute values of a  $1606 \times 1606$  augmented burnup matrix. Figure 3.3 is a close-up from Fig. 3.2, showing  $\mathbf{A}(1 : 36, 1 : 30)$  and corresponding to the 36 lightest nuclides, ranging from the hydrogen isotope  ${}^1\text{H}$  to the oxygen isotope  ${}^{18}\text{O}$ .

### 3. Matrix exponential solution of burnup equations

---

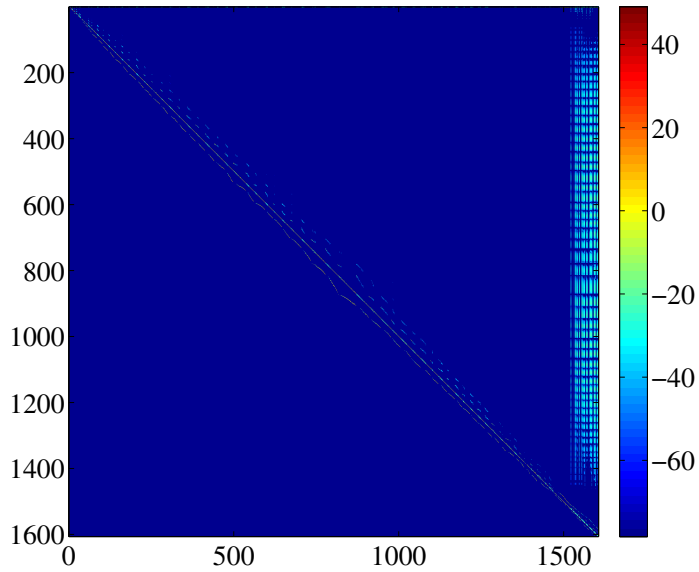


**Figure 3.2.** A plot illustrating the (10-base) logarithmic variations in the absolute values of burnup matrix elements for a test case with 1606 nuclides.

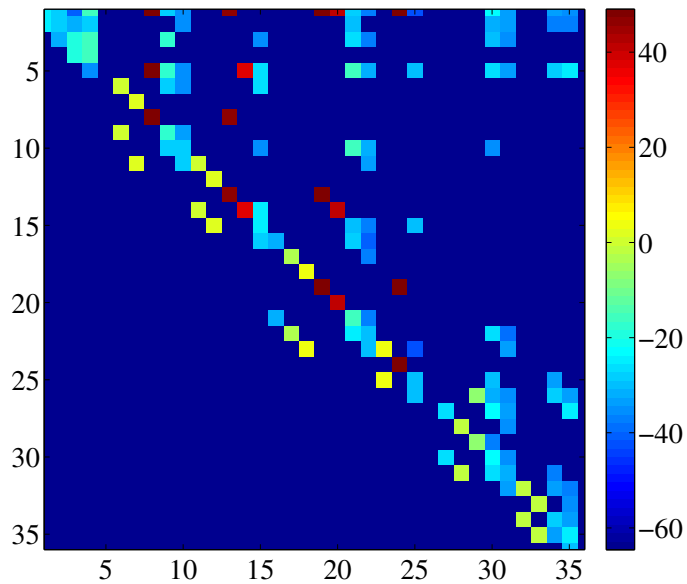


**Figure 3.3.** A close-up of the matrix in Fig. 3.2 corresponding to the 36 lightest nuclides ranging from  $^1\text{H}$  to  $^{18}\text{O}$ .

### 3.1.1 Graph-theoretical approach

Some insight into the numerical properties of burnup matrices can be gained by considering their graphs. In this context, the column and row indices of  $\mathbf{A}$  are referred to as vertices. When  $a_{ij} \neq 0$ , there exists an *edge* from vertex  $i$  to vertex  $j$ , and the notation  $i \rightarrow j$  is used. A *path* of length  $m$  from node  $i$  to node  $k$  is defined as a sequence of non-zero vertices  $[i = i_1, i_2, i_3, \dots, i_m, i_{m+1} = k]$ , such that  $i_n \rightarrow i_{n+1}$  for  $n = 1, \dots, m+1$ . The physical interpretation for this is that there exists a transmutation path of length  $m$  from nuclide  $k$  to nuclide  $i$ .

A graph is called acyclic, if the paths related to it do not form closed cycles. In this case, the vertices can be ordered topologically, meaning that if  $i \rightarrow j$ , the vertex  $i$  appears before  $j$  in the ordering. An acyclic graph corresponds to a matrix that can be permuted to lower triangular form. When a graph is not acyclic, it can be divided into *strongly connected components* (SCCs). A strongly connected component is defined as a set of vertices, for which there exists a path from each vertex to every other vertex. After dividing a graph into strongly connected components, these components can be ordered topologically in the same manner as the vertices of an acyclic graph, after which the corresponding systems of differential equations can be solved independently in this order. This corresponds to permuting the matrix to lower block triangular form with irreducible diagonal blocks.

In the case of a burnup matrix, a strongly connected component corresponds to a set of nuclides for which there exists a transmutation path from every nuclide to every other nuclide. In this context, it should be noted that measured nuclear data does not exist for all reactions that are unlikely but possible in theory. The considerations in this section are based on evaluated nuclear data libraries and the library JEFF-3.1 [3] in particular. Some general conclusions can be drawn from studying the transmutation paths of nuclides. First of all, the only reactions increasing the ZAI index are the  $(n, \gamma)$  reaction and  $\beta^-$  decay. Therefore, a closed cycle must necessarily contain at least one of these reactions. Nuclides that do not undergo either of these reactions, form SCCs whose size is one. It can also be deduced that fissile nuclides and fission product nuclides belong to different SCCs, since transmutation paths from fission products to fissile nuclides are extremely unlikely under reactor conditions.<sup>3</sup>

Interestingly, the nuclides produced as by-products, i.e.  $^1\text{H}$ ,  $^2\text{H}$ ,  $^3\text{H}$ ,  $^3\text{He}$  and  $^4\text{He}$ , always form a *sink* in the augmented burnup matrix, meaning that there is no out-bound edge from this set of vertices. This is due to the fact that these nuclides do not elicit any reactions that would produce nuclides outside this group. The nuclide  $^4\text{He}$  is stable and elicits no neutron reactions corresponding to a zero column in the burnup matrix, whereas the rest of the by-product nuclides form a single SCC.

Let us again consider the augmented burnup matrix plotted in Figures 3.1 and 3.2. This matrix corresponds to a burnup system with 1606 nuclides, ranging from

<sup>3</sup>Interestingly, these paths are theoretically possible if data based on nuclear models rather than measurements is considered. For example, the nuclear data library TENDL-2011 [4] produced with the nuclear reaction program Talys [4] contains data that enables paths from fission products to fissile nuclides. However, since these transmutation paths are extremely unlikely, they are not further considered here.

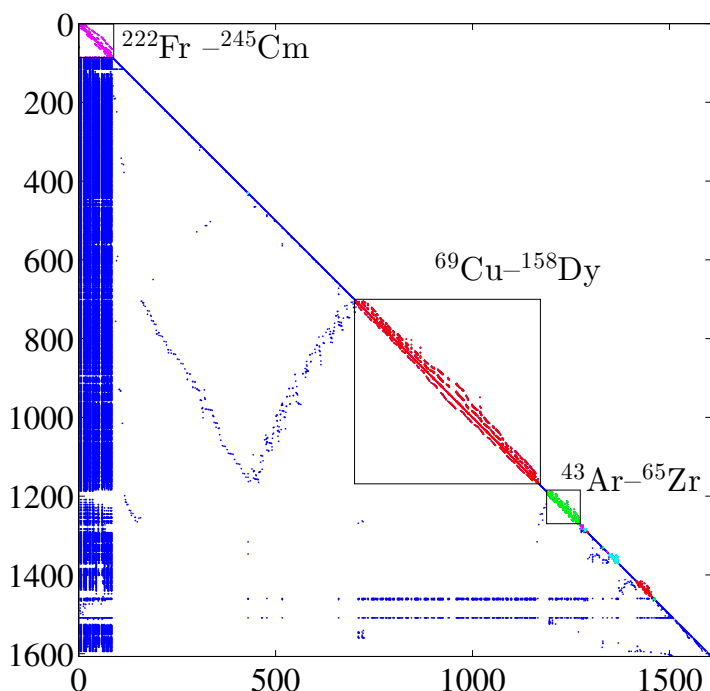


**Figure 3.4.** Burnup matrix permuted to lower block triangular form. The diagonal blocks with size greater than one have been plotted with magenta, red, green or cyan. For the three largest blocks, the nuclides with the smallest and the greatest ZAI indices in the SCC have been indicated.

$^1\text{H}$  to  $^{245}\text{Cm}$  when ordered according to their ZAI index. For this matrix, the number of SCCs is 896. However, only twelve of these components include more than a single nuclide. The *source* SCC, i.e. a SCC without any inbound edges, consists 83 nuclides ranging from  $^{222}\text{Fr}$  to  $^{245}\text{Cm}$ . The largest SCC comprises 463 nuclides ranging from  $^{69}\text{Cu}$  to  $^{159}\text{Dy}$ . Figure 3.4 depicts the SCCs of the test case burnup matrix by showing a plot of the matrix permuted to block lower triangular form.

#### 3.1.2 Spectrum

##### Real parts of eigenvalues

When considering the spectral properties of burnup matrices, it is important to distinguish between classically defined and augmented burnup matrices. In the case of conventional burnup matrices, the number of nuclides does not increase in all reactions except fission. As explained in Section 3.1.1, there are generally no transmutation chains from fission product nuclides to fissile nuclides. Therefore, the con-

**Table 3.1.** Possible decay and neutron reactions for the by-product nuclides.

Nuclide	Possible reactions
$^1\text{H}$	$(n,\gamma)$
$^2\text{H}$	$(n,\gamma)$ $(n,2n)$
$^3\text{H}$	$\beta^-$ $(n,2n)$
$^3\text{He}$	$(n,p)$ $(n,d)$ $(n,t)$
$^4\text{He}$	

centrations of all nuclides must remain bounded at all times [1]. In this case, the following theorem ([5], p. 165) gives a useful characterization of the real parts of the burnup matrix eigenvalues.

**Theorem 3.1.2.** *Every solution  $\mathbf{n}$  of system (2.12) remains bounded as  $t \rightarrow \infty$  if and only if the following holds*

(i)  $\text{Re}(\lambda) \leq 0 \quad \forall \lambda \in \Lambda(\mathbf{A})$

(ii) *Every  $\lambda \in \Lambda(\mathbf{A})$  with  $\text{Re}(\lambda) = 0$  is a semisimple eigenvalue, i.e. the geometric and algebraic multiplicities agree.*

Here  $\Lambda(\mathbf{A})$  denotes the set of the eigenvalues of  $\mathbf{A}$ .

However, the situation changes slightly for the augmented burnup matrix. In this case, the number of nuclides increases in all reactions that produce a by-product nuclide in addition to the daughter nuclide. In this context, it is not evident that all nuclide concentrations remain bounded as  $t \rightarrow \infty$ . This follows from that neutrons are not assumed to be part of the burnup system but they are supposed to be added constantly to the system. However, as discussed in Section 3.1.1, the only nuclides produced as by-products are  $^1\text{H}$ ,  $^2\text{H}$ ,  $^3\text{H}$ ,  $^3\text{He}$  and  $^4\text{He}$ . The vertices corresponding to these nuclides always form a sink in the burnup matrix graph. It follows that no nuclides are produced from these nuclides, and that *the concentrations of all nuclides except for these by-product nuclides must remain bounded at all times.*

Fortunately, the eigenvalues related to the by-product nuclides can be separated from the rest of the eigenvalues of the augmented burnup matrix, remembering that the spectrum of a block triangular matrix is the union of the spectra of the diagonal blocks, i.e.

$$\Lambda(\mathbf{A}) = \bigcup_I \Lambda(\mathbf{A}_{ij}), \tag{3.5}$$

where  $\mathbf{A}_{ij}$  are the irreducible diagonal blocks. Here each diagonal block corresponds to the set of nuclides forming a SCC. Therefore, it can be concluded that Theorem 3.1.2 applies to all eigenvalues of an augmented burnup matrix except for the ones related to the diagonal block corresponding to the nuclides  $^1\text{H}$ ,  $^2\text{H}$ ,  $^3\text{H}$  and  $^3\text{He}$ . This submatrix, denoted by  $\tilde{\mathbf{A}} \in \mathbb{R}^{4 \times 4}$ , and its spectrum are considered in the following.

Table 3.1 lists the reactions that are possible for the by-product nuclides. From the perspective of eigenvalues, it is noteworthy that  $^3\text{He}$  elicits  $(n, p)$ ,  $(n, d)$ , and  $(n, t)$

### 3. Matrix exponential solution of burnup equations

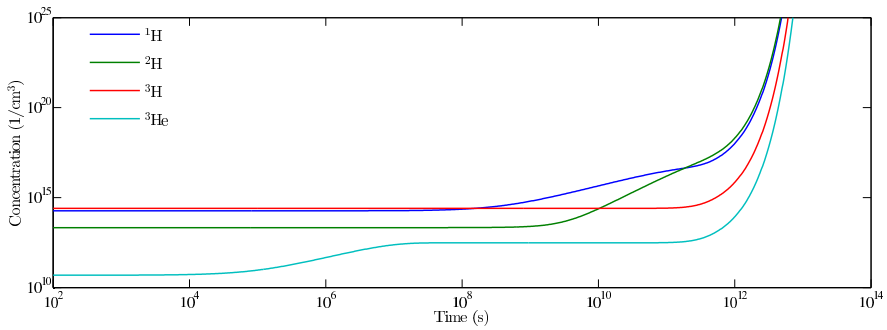


**Figure 3.5.** Nuclide concentrations corresponding the solution of  $\mathbf{x}' = \tilde{\mathbf{A}}\mathbf{x}$ .

reactions (in this case, (n, p) and (n, t) are actually the same reaction) producing either one  $^3\text{H}$  and one  $^1\text{H}$  nuclide or two  $^2\text{H}$  nuclides. Therefore, the number of nuclides increases in both of these reactions. As can be seen from Table 3.1, there are transmutation paths from  $^1\text{H}$ ,  $^2\text{H}$  and  $^3\text{H}$  to  $^3\text{He}$ , meaning that also the number of  $^3\text{He}$  nuclides increases as a function of time. Considering this, it is evident that the nuclide concentrations of the by-product nuclides grow unboundedly when  $t \rightarrow \infty$ . This clearly unphysical behavior stems from the assumption of constant rates for the neutron-induced reactions during the burnup step. According to this assumption, neutrons are added to the system constantly and, in the  $\beta^-$  decay of  $^3\text{H}$  to  $^3\text{He}$ , neutrons are converted to protons, increasing the amount of matter as a function of time. Therefore, the eigenvalues related to  $\tilde{\mathbf{A}}$  can have positive real parts.

In reality, of course, all nuclide concentrations remain bounded at all times. Therefore, the dynamical behavior of the subsystem  $\mathbf{x}' = \tilde{\mathbf{A}}\mathbf{x}$  reflects the validity of the assumption of constant reaction rates during the burnup step. Therefore,  $\lambda t \gg 1$  for any  $\lambda \in \Lambda(\tilde{\mathbf{A}})$  would indicate the invalidity of this assumption for the time step  $t$ . Figure 3.5 shows the nuclide concentrations as a function of time for a PWR pin-cell test problem. In this test case,  $\tilde{\mathbf{A}}$  has a single positive eigenvalue which is of the order of  $10^{-12}$ . It can be seen from this figure that the nuclide concentrations begin to increase unrealistically when  $\lambda t \rightarrow 1$ . It should also be noted that although the rate for the  $\beta^-$  decay is constant, the magnitudes of the neutron reactions are ultimately determined by the normalization of the neutron flux by power. Increasing the power by a factor of 10 000, for example, increases the sole positive eigenvalue from the order of  $10^{-12}$  only to the order of  $10^{-10}$ . This extreme example illustrates that the theoretical mathematical instability of this subsystem does not pose a problem in practice.

#### Imaginary parts of eigenvalues

The characterization of the imaginary parts of the burnup eigenvalues is more difficult. It is again useful to consider the SCCs separately. It is evident, that the eigenvalues corresponding to SCCs consisting of a single vertex coincide with the respective

diagonal elements of the matrix.

From a physical standpoint, the imaginary part  $\omega$  of an eigenvalue corresponds to an oscillation with period  $T = 2\pi/\omega$ . Some insight on the interactions' underlying oscillatory behavior can be gained by considering a small system that can be solved analytically. First of all, it is easy to show that a system consisting of two nuclides cannot have non-real eigenvalues. Therefore, the following closed-cycle system consisting of three nuclides can be regarded as a model problem in this context:

$$\begin{bmatrix} n'_1 \\ n'_2 \\ n'_3 \end{bmatrix} = \begin{bmatrix} -\mu_1 & 0 & \mu_3 \\ \mu_1 & -\mu_2 & 0 \\ 0 & \mu_2 & -\mu_3 \end{bmatrix} \begin{bmatrix} n_1 \\ n_2 \\ n_3 \end{bmatrix}. \quad (3.6)$$

For this system, a necessary condition for the existence of a non-real eigenvalue is that the constants  $\mu_i$  satisfy

$$\sqrt{\mu_1} - \sqrt{\mu_2} < \sqrt{\mu_3} < \sqrt{\mu_1} + \sqrt{\mu_2}. \quad (3.7)$$

Furthermore, the absolute value of the imaginary part  $\omega$  attains its maximum value

$$\omega_{\max} = \sqrt{\mu_1 \mu_2} \quad (3.8)$$

when  $\mu_3 = \mu_1 + \mu_2$ . When  $\mu_1 \gg \mu_2$ , the left-hand and right-hand sides of the inequality (3.7) approach  $\sqrt{\mu_1}$ , and  $\mu_3$  must be arbitrarily close to  $\mu_1$  in order to induce a complex eigenvalue. Assuming, for example,  $\mu_1 \sim 10^{-2}$  and  $\mu_2 \sim 10^{-8}$ , the first 4 decimals of  $\mu_1$  and  $\mu_3$  must coincide in order for this system to have non-real eigenvalues.

The principles related to this model problem can be generalized to more complex closed-cycle systems. Non-real eigenvalues are most likely to occur, when the rates of the reactions forming a closed cycle are of the same magnitude. When some of the reactions are significantly more likely than others, they can be considered instant. Physically, it is intuitive that the imaginary parts must be of the same order as the rates for the least likely reactions in the cycle.

As discussed in the beginning of Section 3.1, the values of the decay constants vary extensively, whereas the rates for neutron reactions are relatively slow. In a thermal reactor operating at full power, most of the transmutation coefficients are of order  $\leq 10^{-8} \text{ s}^{-1}$ . In a fast reactor, the flux is higher but most of the neutron reactions are less likely, which results in most of the reaction rates being even smaller than in a thermal reactor. Based on computing the eigenvalues for a wide range of burnup matrices, it seems that they are generally confined to a region near the negative real axis. For every burnup matrix that we have considered, this has also been the case. When the power level is decreased, the transmutation coefficients become smaller. In this case the absolute values of the imaginary parts of the eigenvalues decrease as well. It seems that the oscillations are most likely to occur for reduced power cases where the greatest transmutation coefficients are of order  $\leq 10^{-12}$ . In

### 3. Matrix exponential solution of burnup equations

---

general, the eigenvalues of the burnup matrix appear to remain bounded near the negative real axis in all conceivable burnup calculation cases with imaginary parts at the most of the order of  $10^{-8}$ .

It was stated previously that the negatives of burnup matrices belong to  $Z$ -matrices. This property can be exploited in deriving a wedge condition for the burnup matrix eigenvalues. Let  $\mathbf{Z} \in \mathbb{Z}_n$ , in which case we can write  $\mathbf{Z} = s\mathbf{I} - \mathbf{B}$  with  $s > 0$  and  $\mathbf{B} \geq 0$ . Since  $\mathbf{B} \geq 0$ , it follows from the Perron–Frobenius theorem that  $\mathbf{B}$  has a real eigenvalue  $\lambda \geq 0$  such that  $|\mu| \leq \lambda \forall \mu \in \Lambda(\mathbf{B})$ . Therefore,  $\lambda$  corresponds to the spectral radius of  $\mathbf{B}$ , denoted by  $\rho(\mathbf{B})$ .

**Definition 3.1.3** (*M-matrix*). Let  $\mathbf{Z} \in \mathbb{Z}_n$  so that it can be written in the form  $\mathbf{Z} = s\mathbf{I} - \mathbf{B}$  with  $s > 0$  and  $\mathbf{B} \geq 0$ . If  $s \geq \rho(\mathbf{B})$ ,  $\mathbf{Z}$  is called an *M-matrix*. If  $s = \rho(\mathbf{B})$ , the *M-matrix* is singular, and if  $s > \rho(\mathbf{B})$ , it is non-singular.

*M*-matrices can be characterized by various equivalent properties (see Theorem 2.3 in [6]), of which the following three are of special interest:

**Theorem 3.1.4.** Let  $\mathbf{A} \in \mathbb{Z}_n$  Then the following properties are equivalent

1.  $\mathbf{A}$  is an *M-matrix*
2.  $\mathbf{A} + \varepsilon\mathbf{I}$  is a non-singular *M-matrix* for any  $\varepsilon > 0$
3. Every eigenvalue of the matrix  $\mathbf{A}$  has a non-negative real part

From the third property we directly obtain the following theorem.

**Theorem 3.1.5.** The negatives of (conventional) burnup matrices belong to the class of *M-matrices*.

The connection between burnup matrices and *M*-matrices is interesting because it gives a wedge condition to the non-real eigenvalues of burnup matrices.

**Theorem 3.1.6** (Eigenvalues of singular *M-matrix*). Let  $\mathbf{M} \in \mathbb{R}^{n \times n}$  be a singular *M-matrix* with  $n \geq 2$ . Then its eigenvalues are confined to the closed wedge

$$\overline{W}_n = \left\{ z = re^{i\theta} \mid r > 0, |\theta| \leq \frac{\pi}{2} - \frac{\pi}{n} \right\}. \quad (3.9)$$

*Proof.* It has been proven that the eigenvalues of non-singular *M*-matrices belong to the open wedge

$$W_n = \left\{ z = re^{i\theta} \mid r > 0, |\theta| < \frac{\pi}{2} - \frac{\pi}{n} \right\} \quad (3.10)$$

if  $n > 2$  and in  $(0, \infty)$  if  $n = 2$  [7]. Based on property 2 in Theorem 3.1.4, for any  $\varepsilon > 0$ , the matrix  $\mathbf{M} + \varepsilon\mathbf{I}$  is a non-singular *M-matrix* whose eigenvalues are confined to the region  $W_n$ . However, since the eigenvalues of a matrix depend continuously on the matrix, it follows that the eigenvalues of the singular matrix  $\mathbf{M}$  must be confined to the wedge  $\overline{W}_n$ .  $\square$

Notice that Theorem 3.1.6 can also be applied to the irreducible diagonal blocks corresponding to the SCCs of a burnup matrix. In this case, the wedge  $W_n$  can be narrowed to correspond to the size of the largest SCC of the matrix. When considering augmented burnup matrices, it is evident that all diagonal blocks—apart from the one corresponding to the by-product nuclides—are  $M$ -matrices to which these wedge conditions can be applied. The block matrix  $\tilde{\mathbf{A}} \in \mathbb{R}^{4 \times 4}$  corresponding to the by-product nuclides may have eigenvalues with a positive real part. However, any of its  $2 \times 2$  principal submatrix is an  $M$ -matrix. This can be attributed to the fact that removing any two nuclides from the respective burnup chain cuts off the feedback mechanism necessary for the nuclide concentrations to increase as a function of time. Therefore, we can identify  $\tilde{\mathbf{A}}$  with the following class of matrices [8]:

**Definition 3.1.7.**  $\mathbf{A} \in L_0^k$  if and only if  $\mathbf{A}$  is a  $Z$ -matrix and each  $k \times k$  principal sub-matrix of  $\mathbf{A}$  is an  $M$ -matrix, but there is at least one  $(k + 1) \times (k + 1)$  principal sub-matrix that is not an  $M$ -matrix.

Based on this definition,  $-\tilde{\mathbf{A}} \in L_0^{n-2} = L_0^2$ . From [8] we now obtain the following characterization:  $\tilde{\mathbf{A}}$  has exactly one eigenvalue on the positive real axis with all the other eigenvalues having non-positive real parts.

We can now summarize the estimates obtained for the eigenvalues of augmented burnup matrices:

**Theorem 3.1.8.** (*Eigenvalues of augmented burnup matrices*) Let  $\mathbf{A} \in \mathbb{R}^{n \times n}$  be an augmented burnup matrix. If  $n = 2$ ,

$$\Lambda(\mathbf{A}) \subset (-\infty, 0].$$

Otherwise, if the nuclides  $^1H$ ,  $^2H$ ,  $^3H$ , and  $^3He$  are included to the burnup system,  $\mathbf{A}$  has four eigenvalues corresponding to them. Exactly one of these eigenvalues is real-valued and positive, while the other three eigenvalues have non-positive real parts. The remaining eigenvalues of  $\mathbf{A}$  are confined to the wedge

$$W_n = \left\{ z = re^{i\theta} \mid r > 0, |\theta| \geq \frac{\pi}{2} + \frac{\pi}{n} \right\} \quad (3.11)$$

around the negative real axis.

Figure 3.6 shows an example of the spectrum of an augmented burnup matrix for a system with 1606 nuclides. This is the same matrix that was plotted in Figures 3.1 and 3.2. Figure 3.7 shows a close-up from Figure 3.6 together with the wedge estimate from Theorem 3.1.8.

### Eigenvalue decomposition

A matrix  $\mathbf{A} \in \mathbb{R}^{n \times n}$  is called diagonalizable, if it has the eigenvalue decomposition

$$\mathbf{A} = \mathbf{T} \mathbf{\Lambda} \mathbf{T}^{-1}, \quad (3.12)$$

where  $\mathbf{\Lambda}$  is a diagonal matrix containing the eigenvalues of  $\mathbf{A}$ , and  $\mathbf{T}$  is an invertible matrix containing the respective eigenvectors. Therefore, in order for the matrix  $\mathbf{A}$

### 3. Matrix exponential solution of burnup equations

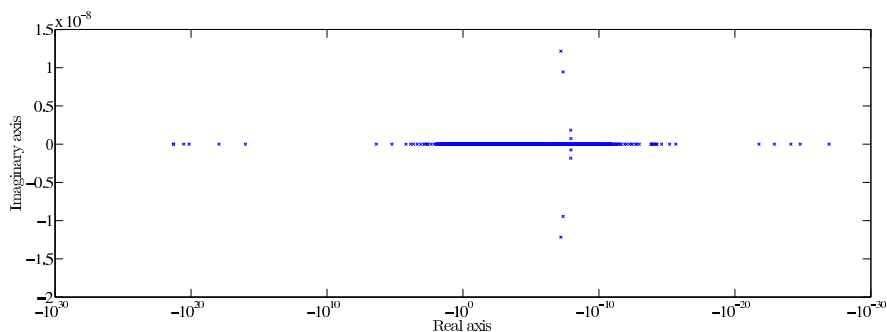


**Figure 3.6.** Plot of the eigenvalues  $z \in \{z \in \mathbb{C} \mid z \in \Lambda(\mathbf{A}), \operatorname{Re} z < 0\}$  of an augmented burnup matrix  $\mathbf{A}$  for a system with 1606 nuclides. In addition, the matrix has a single positive eigenvalue  $z_+ \approx 4.15 \times 10^{-12}$  and zero as a 29-fold eigenvalue.

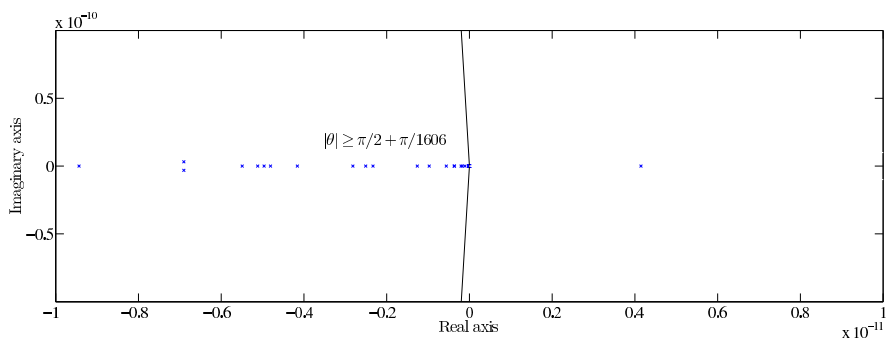


**Figure 3.7.** Close-up of the eigenvalues plotted in Fig. 3.6 near the origin, together with the wedge estimate from Theorem 3.1.8.

to be diagonalizable, it must have  $n$  linearly independent eigenvectors that span the space  $\mathbb{C}^n$ . This happens especially if the matrix has  $n$  distinct eigenvalues.

If a nuclide is stable and does not elicit any neutron reactions, it always induces a zero eigenvalue to the burnup matrix. For this reason, burnup matrices are nearly always singular with zero as a multiple eigenvalue. However, according to Theorem 3.1.2, the eigenvalue zero is semi-simple meaning that its geometric and algebraic multiplicities agree. Therefore, in order for a burnup matrix to be defective, it should have a non-zero eigenvalue, whose geometric multiplicity is smaller than its algebraic multiplicity.

For a single nuclide forming a SCC of unit size, the respective eigenvalue coincides with its removal rate. When considering a SCC consisting of several nuclides, an eigenvalue can no longer be connected with a particular nuclide but they all represent the set of nuclides and their effective removal rates taking the feedback mechanisms (i.e. closed cycles) into consideration. Since the decay and transmutation constants of different nuclides are never *precisely* equal, a repeated non-zero eigenvalue is

theoretically extremely unlikely. Therefore, burnup matrices should ideally be diagonalizable with zero as the only multiple eigenvalue. Nonetheless, as recently noted in [9], the half-lives of some short-lived nuclides have not been measured accurately, which results in identical estimates for some of them.<sup>4</sup> This imprecision of the decay data may cause a burnup matrix to have multiple eigenvalues in practise. In addition to these multiple eigenvalues resulting from inaccurate decay data, burnup matrices typically have many nearly confluent eigenvalues, which complicates their numerical computation.<sup>5</sup>

In some cases, the condition of an eigenvalue problem may be a sign of that the eigenvalues are not meaningful, and the pseudospectra of the matrix should be studied instead [10]. The  $\varepsilon$ -pseudospectrum  $\sigma_\varepsilon(\mathbf{A})$  of  $\mathbf{A}$  is defined as the set  $z \in \mathbb{C}$  such that

$$\|(z\mathbf{I} - \mathbf{A})^{-1}\| > 1/\varepsilon, \quad (3.13)$$

where the matrix  $(z\mathbf{I} - \mathbf{A})^{-1}$  is called the *resolvent* of  $\mathbf{A}$  at  $z$ . In the previous definition, it is assumed that  $\|(z\mathbf{I} - \mathbf{A})^{-1}\| = \infty$  when  $z \in \Lambda(\mathbf{A})$  so that the spectrum of  $\mathbf{A}$  is contained in the  $\varepsilon$ -pseudospectrum for every  $\varepsilon > 0$ . It can be shown that when matrix  $\mathbf{A}$  is perturbed by a matrix  $\mathbf{E}$  such that  $\|\mathbf{E}\| < \varepsilon$ , the eigenvalues of  $\mathbf{A} + \mathbf{E}$  are confined to  $\sigma_\varepsilon(\mathbf{A})$  [10]. Therefore, the  $\varepsilon$ -pseudospectrum characterizes the sensitivity of the eigenvalue problem to perturbations.

When computing the eigenvalues of a burnup matrix, problems are typically faced due to the algorithm not being able to distinguish between the nearly confluent eigenvalues. Also, round-off errors may induce small positive eigenvalues, which are clearly nonphysical. From a practical point of view, these errors are not acceptable since they change the character of the problem. However, the absolute magnitudes of the errors are generally of the order of the arithmetic precision used in the computation, suggesting that the eigenvalue problem is not especially sensitive to perturbations. The study of the pseudospectra of burnup matrices supports this conclusion. Figure 3.8 shows the boundaries of the 2-norm  $\varepsilon$ -pseudospectra for a burnup matrix that was formed by selecting only the most important actinides and fission products, totalling in 219 nuclides. The norm of the respective burnup matrix is of the order of  $10^{-4}$ . It can be seen from Fig. 3.8 that at distance  $\delta$  from the eigenvalues, the norm  $\|(z\mathbf{I} - \mathbf{A})^{-1}\|$  is of the order of  $\delta^{-1}$ .

## 3.2 Matrix exponential

### 3.2.1 Definitions of matrix functions

There are many equivalent ways to define the matrix exponential  $e^{\mathbf{A}t}$  in addition to the power series definition of Eq. (3.2). In this context, it is useful to consider definitions for general matrix functions first. Two definitions of particular interest are presented

<sup>4</sup>It should be noted that in [9] the focus is on the identical eigenvalues resulting from linearizing the closed cycles in the burnup chain rather than identical eigenvalues of burnup matrices.

<sup>5</sup>The computation of the eigenvalues becomes significantly better-conditioned if the SCCs of the matrix are formed first and the eigenvalues are then computed for each diagonal block corresponding a SCC.

### 3. Matrix exponential solution of burnup equations

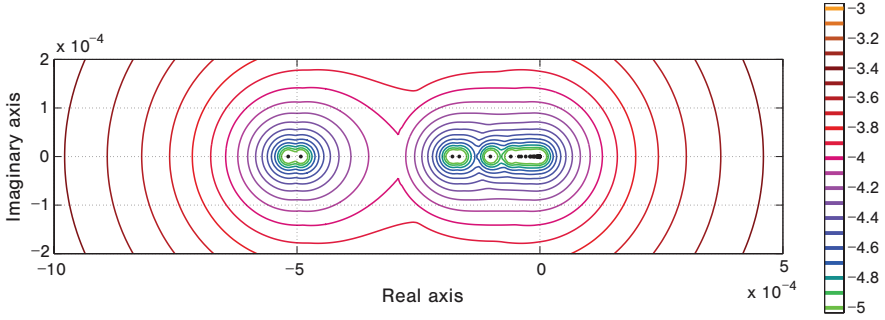


**Figure 3.8.** Pseudospectra of a small burnup matrix corresponding to a system with 219 nuclides. The outer boundaries of  $\sigma_\varepsilon(\mathbf{A})$  are plotted for selected values between  $\varepsilon = 10^{-5}$  and  $\varepsilon = 10^{-3}$ . The eigenvalues of the matrix are marked with black dots. The plot was computed with the Eigtool package for MATLAB [11].

here—the definition based on Jordan canonical form, and the definition based on the Cauchy integral formula.

It is well-known that any matrix  $\mathbf{A} \in \mathbb{C}^{n \times n}$  can be written in the Jordan canonical form

$$\mathbf{A} = \mathbf{T} \mathbf{J} \mathbf{T}^{-1}, \quad (3.14)$$

where  $\mathbf{J}$  is a diagonal block matrix

$$\mathbf{J} = \text{diag} [\mathbf{J}_{m_1}(\lambda_1), \dots, \mathbf{J}_{m_p}(\lambda_p)]$$

and  $\lambda_1, \dots, \lambda_p$  are eigenvalues of  $\mathbf{A}$ . The matrix  $\mathbf{J}$  is unique up to the order of the diagonal blocks, whereas the transformation matrix  $\mathbf{T}$  is in general not unique. The diagonal blocks are of the form

$$\mathbf{J}_{m_j}(\lambda_j) = \begin{bmatrix} \lambda_j & 1 & 0 & \cdots & 0 \\ & \lambda_j & 1 & \ddots & \vdots \\ & & \lambda_j & \ddots & 0 \\ \mathbf{0} & & & \ddots & 1 \\ & & & & \lambda_j \end{bmatrix} = \lambda_j \mathbf{I} + \mathbf{S}_{m_j} \in \mathbb{C}^{m_j \times m_j} \quad (3.15)$$

with  $\sum_{j=1}^p m_j = n$ . The number of Jordan blocks corresponding to  $\lambda_j$  is equal to the number of linearly independent eigenvectors related to that eigenvalue. Let  $l_j$  denote the *index* of  $\lambda_j$ , defined as the size of the largest Jordan block corresponding to  $\lambda_j$ . In order to define the matrix function  $f(\mathbf{A}t)$  based on Jordan canonical form, we need the following definition [12].

**Definition 3.2.1.** A function  $f$  is defined on the spectrum of  $\mathbf{A}t$  if the values

$$f^{(i)}(t\lambda_j), \quad i = 0 \dots, l_j - 1, \quad j = 1, \dots, s \quad (3.16)$$

exist. Here  $\{\lambda_1, \dots, \lambda_s\}$  are the distinct eigenvalues of  $\mathbf{A}$ .

We can now formulate the following definition for the matrix function  $f(\mathbf{A}t)$ .

**Definition 3.2.2.** Let the function  $f$  be defined on the spectrum of  $\mathbf{A}t \in \mathbb{C}^{n \times n}$  and let  $\mathbf{A} = \mathbf{T} \mathbf{J} \mathbf{T}^{-1}$  denote the Jordan decomposition of  $\mathbf{A}$ . Then

$$f(\mathbf{A}t) = \mathbf{T} \operatorname{diag} [f(\mathbf{J}_{m_1}(t\lambda_1)), \dots, f(\mathbf{J}_{m_p}(t\lambda_p))] \mathbf{T}^{-1}, \quad (3.17)$$

where

$$f(\mathbf{J}_{m_j}(t\lambda_j)) = \sum_{\nu=0}^{m_j-1} \frac{f^{(\nu)}(t\lambda_j)}{\nu!} \mathbf{S}_{m_j}^{\nu}. \quad (3.18)$$

Notice that when the matrix  $\mathbf{A}$  is diagonalizable, the Jordan decomposition reduces to the eigenvalue decomposition and  $f(\mathbf{A}t)$  can be computed simply as

$$f(\mathbf{A}t) = \mathbf{T} f(\mathbf{\Lambda}t) \mathbf{T}^{-1}. \quad (3.19)$$

Definition 3.2.2 and Eq. (3.19) are useful because they directly show the connection between the eigenvalues and the exponential of a matrix. It should be noticed that since the exponential function is analytic everywhere in the complex plane, the matrix function  $e^{\mathbf{A}t}$  is defined for all  $\mathbf{A}t \in \mathbb{C}^{n \times n}$ .

Another interesting definition for the matrix function  $f(\mathbf{A}t)$  is based on a generalization of the Cauchy integral theorem.

**Definition 3.2.3.** Let  $\mathbf{A} \in \mathbb{C}^{n \times n}$  and let  $f$  be analytic inside the closed contour  $\Gamma$  that winds once around the spectrum of  $\mathbf{A}t$ . Then

$$f(\mathbf{A}t) = \frac{1}{2\pi i} \int_{\Gamma} f(z) (z\mathbf{I} - \mathbf{A}t)^{-1} dz. \quad (3.20)$$

In the previous definition, the resolvent of  $\mathbf{A}t$  can be written in the form

$$(z\mathbf{I} - \mathbf{A}t)^{-1} = \frac{\mathbf{B}(z)}{\det(z\mathbf{I} - \mathbf{A}t)}, \quad (3.21)$$

where

$$\mathbf{B}(z) = z^{n-1} \mathbf{B}_0 + z^{n-2} \mathbf{B}_1 + \dots + z \mathbf{B}_{n-2} + \mathbf{B}_{n-1} \quad (3.22)$$

with  $\mathbf{B}_0, \mathbf{B}_1, \dots, \mathbf{B}_{n-1}$  matrices with constant elements [13].

### 3.2.2 Application to burnup matrices

Some interesting properties of the burnup matrix exponential  $\mathbf{E}(t) = e^{\mathbf{A}t}$  can be deduced based on physical considerations. First of all, for each value of  $t$ , the element  $E_{ij}(t)$  characterizes the contribution from nuclide  $j$  to nuclide  $i$  during time step  $t$ . Therefore, it is clear that all elements of  $\mathbf{E}(t)$  must be non-negative at all times. Interestingly, this same conclusion follows directly from the fact that the negatives of (augmented) burnup matrices are  $Z$ -matrices. The following theorem is from [12]:

**Theorem 3.2.4.**  $e^{\mathbf{A}t} \geq 0$  for all  $t \geq 0$  if and only if  $-\mathbf{A}$  is a  $Z$ -matrix.

### 3. Matrix exponential solution of burnup equations

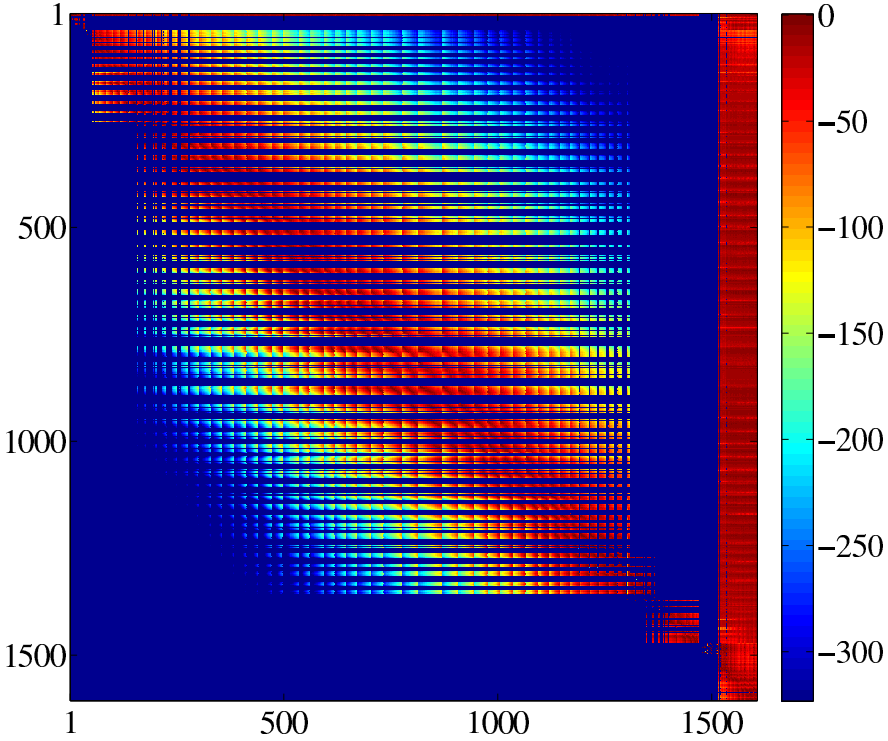


**Figure 3.9.** Plot of the matrix elements  $\mathbf{E} = e^{\mathbf{A}t}$  with  $t \approx 8.64 \times 10^5$  s on a logarithmic scale. The matrix  $\mathbf{E}$  was computed with MATLAB's Symbolic toolbox using high-precision arithmetics.

Due to the previous theorem, the negatives of  $Z$ -matrices are sometimes called *essentially non-negative*. Figure 3.9 shows a plot of the matrix exponential for an augmented burnup system with 1606 nuclides. Notice that a zero element  $E_{ij} = 0$  in the figure means that there is no transmutation path from nuclide  $j$  to nuclide  $i$ . Especially, the rows 2, ..., 6 corresponding to the by-product nuclides have zero elements, since no nuclides are produced from these nuclides. It can also be seen from the figure that the elements with the greatest magnitude are gathered around the diagonal. This is in accordance with the reasoning that the longer and more complex a particular transmutation path, the less likely it is to contribute to the respective nuclide concentration.

In some cases, it is useful to consider the norm  $\|e^{\mathbf{A}t}\|$  as a function of time. For non-normal matrices, it is possible that the transient behavior of the system differs from the behavior at  $t \rightarrow \infty$ . The following theorem from [10] gives a useful relationship between  $e^{\mathbf{A}t}$  and the resolvent  $(z\mathbf{I} - \mathbf{A})^{-1}$ .

**Theorem 3.2.5.** Let  $\mathbf{A} \in \mathbb{C}^{n \times n}$  and let  $\omega \in \mathbb{R}$  and  $M \geq 1$  be such that

$$\|e^{\mathbf{A}t}\| \leq M e^{\omega t} \quad \forall t \geq 0. \quad (3.23)$$

For any  $z \in \mathbb{C}$  with  $\text{Re } z > \omega$  in the resolvent set of  $\mathbf{A}$  it holds

$$(z\mathbf{I} - \mathbf{A})^{-1} = \int_0^{\infty} e^{-zs} e^{s\mathbf{A}} ds, \quad (3.24)$$

and

$$\|(z\mathbf{I} - \mathbf{A})^{-1}\| \leq \frac{M}{\text{Re } z - \omega}. \quad (3.25)$$

In the case of conventional burnup matrices, the number of nuclides increases only through fission. As explained in Section 3.1.1, there are generally no transmutation paths from fission product nuclides back to fissionable nuclides. Therefore, the total number of nuclides in the system is bounded. The element  $E_{ij}(t)$  of  $\mathbf{E}(t) = e^{\mathbf{A}t}$  is equal to the concentration of nuclide  $i$  at time  $t$ , assuming nuclide  $j$  is the only nuclide with a non-zero initial concentration and that this concentration is equal to unity. The column sum,  $\sum_{i=1}^n E_{ij}(t)$ , on the other hand, corresponds to the total number of nuclides in the system at time  $t$ , assuming an initial condition consisting of a single nuclide  $j$ . The norm  $\|e^{\mathbf{A}t}\|_1$  is defined as the maximum absolute column sum of the matrix. Therefore, we can state that

$$\|e^{\mathbf{A}t}\|_1 \leq C, \quad (3.26)$$

where  $C$  is a constant equal to the maximum number of nuclides that can result from an initial state consisting of a single nuclide. In practise, there are always reactions competing with fission, for which reason the previous inequality holds for  $C$  smaller than the maximum number of fission product nuclides. However,  $C$  can always be chosen as the maximum number of nuclides produced in a fission.

Based on Theorem 3.2.5, we now obtain the following bound for the resolvent in 1-norm:

**Theorem 3.2.6.** *Let  $\mathbf{A} \in \mathbb{R}^{n \times n}$  be a (conventional) burnup matrix. Then for any  $\text{Re } z > 0$*

$$\|(z\mathbf{I} - \mathbf{A})^{-1}\|_1 \leq \frac{C}{\text{Re } z}. \quad (3.27)$$

### 3.2.3 Numerical computation

In general, there are various numerical methods for computing the matrix exponential. However, the suitability of a particular method depends on the characteristics of the problem under consideration. When considering the efficiency of a particular method, there are a few cases that should be distinguished. First of all, computing  $e^{\mathbf{A}t}$  for a single value of  $t$  is different from computing it for several values of  $t$ . Also, the case where the full matrix  $e^{\mathbf{A}t}$  is required differs from the case where only the action of the matrix exponential on a vector is needed, i.e.  $e^{\mathbf{A}t} \mathbf{y}$  for some  $\mathbf{y} \in \mathbb{R}^n$ .

In burnup calculations, the objective is generally to compute the nuclide concentrations at time step  $t$ , i.e. the product  $e^{\mathbf{A}t} \mathbf{n}_0$  for a single value of  $t$  and a single nuclide initial concentration vector  $\mathbf{n}_0$ . The full matrix exponential is occasionally needed in special applications, where it is important to know the contributions from individual

### 3. Matrix exponential solution of burnup equations

---

nuclides. As mentioned previously, the time steps used in burnup calculations typically vary from a few days at the beginning of the irradiation cycle to a few hundred days at the end. When considering nuclear fuel outside the reactor, the burnup equations reduce to equations describing radio-active decay, and the time steps can in principle extend to thousands of years.

Due to the extensive variations in the magnitudes of the burnup matrix elements, the computation of matrix exponential has previously been considered infeasible for entire burnup systems. Instead, simplified burnup chains have been used, or the most short-lived nuclides have been treated separately when computing a matrix exponential solution. For example, in the ORIGEN [14] code, the matrix exponential is computed with the truncated Taylor series method with scaling and squaring, after excluding short-lived nuclides from the burnup matrix to be treated separately. In the AEGIS code, a Krylov subspace method is applied to a simplified burnup chain with 221 nuclides, in which case the burnup matrix norm is of the order of  $10^{-2}$  [15]. These frameworks are considered briefly in the following.

Truncated Taylor series is perhaps the most obvious numerical method for computing the matrix exponential. The main limitation of this approach is related to round-off errors. In some cases, even increasing the number of terms does not improve accuracy due to the accuracy limitations in the computer arithmetics. The applicability range of the method can be extended by the method of *scaling and squaring*, which is based on the identity

$$e^{\mathbf{A}t} = \left( e^{\mathbf{A}t/m} \right)^m, \quad (3.28)$$

where  $m$  can be taken as a power of two,  $m = 2^k$ , so that the norm  $\|\mathbf{A}/m\|$  becomes sufficiently small. In this context it should be pointed out that the method of scaling and squaring is only applicable to computing the full matrix  $e^{\mathbf{A}t}$  and it cannot be applied, when only the vector  $e^{\mathbf{A}t}\mathbf{y}$  is desired.<sup>6</sup> Unfortunately, the squaring phase of the scaling and squaring method may lead to a loss of accuracy due to round-off errors in the canceling of large elements [16]. In ORIGEN [14], the fastest transitions are removed from the burnup system in order for the matrix norm to meet the criterion

$$\min \{ \|\mathbf{A}t\|_1, \|\mathbf{A}t\|_\infty \} < -2 \log(0.001) \approx 13.8155$$

before the computation of the matrix exponential. This corresponds to removing nuclides  $i$  for which  $e^{a_{ii}t} < 0.001$  [14].

In Krylov methods, the computation of the product  $e^{\mathbf{A}t}\mathbf{n}_0$  is made more affordable by projecting the matrix  $\mathbf{A}$  to a lower-dimensional Krylov subspace. The projection can be carried out with the Arnoldi iteration, which results in  $m$  iteration steps to the partial Hessenberg reduction

$$\mathbf{A} \mathbf{Q}_m = \mathbf{Q}_m \mathbf{H}_m + h_{m+1,m} \mathbf{q}_{m+1} \mathbf{e}_m^T, \quad (3.29)$$

---

<sup>6</sup>When computing  $e^{\mathbf{A}t}\mathbf{y}$ , the norm of  $\mathbf{A}t$  can only be reduced by dividing the time step  $t$  into smaller sub-steps and by repeating the computation for each sub-step.

where  $\mathbf{Q}_m \in \mathbb{R}^{n \times m}$  is orthogonal,  $\mathbf{H}_m \in \mathbb{R}^{m \times m}$  is a Hessenberg matrix, and  $m < n$ . The matrix exponential solution can then be approximated as

$$e^{\mathbf{A}t} \mathbf{n}_0 \approx \|\mathbf{n}_0\| \mathbf{Q}_m e^{\mathbf{H}_m t} \mathbf{e}_1, \quad (3.30)$$

where the product  $e^{\mathbf{H}_m t} \mathbf{e}_1$  for the small and dense matrix  $\mathbf{H}_m$  can be computed by any suitable algorithm. The eigenvalues of  $\mathbf{H}_m$ , called the Ritz values, are typically close to the eigenvalues of  $\mathbf{A}$  near the edge of the spectrum. The accuracy of the Krylov approximation may be compromised if these extreme eigenvalues are not representative of the original problem, which clearly is the case with burnup matrices. Besides, Krylov subspace methods are generally motivated by the original problem being too large to be solved directly, the typical applications including matrices arising from the discretization of a differential equation. In this context, burnup matrices can be regarded relatively small considering that polynomial or rational approximations can easily be applied directly to them. Therefore, the solution of burnup equations falls out of the scope of the application area of Krylov subspace methods.

The methods described above have been previously used for solving the burnup equations. In addition to these, another method worth mentioning is the rational Padé approximation of the exponential function. Padé approximation with scaling and squaring can be considered the most established matrix exponential method, and it is the method implemented in MATLAB's matrix exponential function `expm` [17]. The  $(k, m)$  Padé approximant of the exponential function is defined as the rational function  $r_{km}(x) = p_{km}(x)/q_{km}(x)$  such that

$$p_{km} = \sum_{j=0}^k \frac{(k+m-j)! k!}{(k+m)! (k-j)!} \frac{x^j}{j!} \quad (3.31)$$

and

$$q_{km} = \sum_{j=0}^m \frac{(k+m-j)! m!}{(k+m)! (m-j)!} \frac{(-x)^j}{j!}. \quad (3.32)$$

This approximation can be shown to fit the exponential function  $e^x$  to the order  $(m+n)$  at the origin, i.e.

$$\left( \frac{d^j r_{km}(x)}{dx^j} \right)_{x=0} = 1, \quad j = 0, 1, \dots, m+n. \quad (3.33)$$

The accuracy of the approximant is restricted near the origin, and for this reason it is generally applied together with the method of scaling and squaring. When the matrix  $\mathbf{A}$  is not diagonalizable and the matrix exponential is defined based on the Jordan decomposition according to Eq. (3.2.2), it is advantageous that the accuracy of the Padé approximation extends to the derivatives in the vicinity of the origin. However, without scaling and squaring the method yields poor results for matrices with eigenvalues far from the origin, and therefore this approach is not well-suited for solving the burnup equations, where the matrix norm is large and only the vector  $e^{\mathbf{A}t} \mathbf{n}_0$  is desired.

### 3.3 Solution based on rational approximations near the negative real axis

The matrix exponential can be computed based on a rational function  $r(z)$  that is known to be a good approximation to the function  $e^z$  in some region in the complex plane  $\mathbb{C}$ . According to Definition 3.2.3, the matrix exponential can be defined as a contour integral, with the integration path winding around the spectrum of the matrix. Therefore, calculating  $e^{\mathbf{A}t}$  is essentially equivalent to evaluating contour integrals of the form

$$(e^{\mathbf{A}t})_{kl} = \frac{1}{2\pi i} \int_{\Gamma} e^z R_{kl}(z) dz, \quad (3.34)$$

where  $\mathbf{R} = (z\mathbf{I} - \mathbf{A}t)^{-1}$ ,  $R_{kl} = o(1)$  when  $z \rightarrow -\infty$ , and the singularities of  $R_{kl}$  are the eigenvalues of  $\mathbf{A}t$ . Since the eigenvalues of (augmented) burnup matrices are confined to a region near the negative real axis, the integration contour can be extended to a parabolic or hyperbolic shape in the left complex plane. Because the integrand will decrease exponentially, these contour integrals can be approximated efficiently using quadrature formulas [18]. Interestingly, the quadrature formulas can be associated with rational functions, whose poles and residues are the nodes and weights of the numerical integration formula, respectively [18]. In addition, every rational function can be correspondingly interpreted as a quadrature formula applied to a contour integral in the left complex plane. This interpretation gives the following expression for the approximation error [18]:

$$I - I_N = \frac{1}{2\pi i} \int_{\Gamma'} (e^z - r(z)) R_{kl}(z) dz, \quad (3.35)$$

where  $\Gamma'$  is a contour that extends from  $-\infty$  towards the origin, encircles the origin while remaining to the left of the poles of  $r$ , and then extends back to  $-\infty$  without crossing the negative real axis at any point.

In Eq. (3.35),  $I_N$  denotes the integral of Eq. (3.34) approximated by some quadrature rule with  $N$  points. When deriving Eq. (3.35), the integration contour  $\Gamma$  is assumed to encircle the eigenvalues of  $\mathbf{A}t$ . Therefore, the accuracy of the rational approximation may suffer a break-down if the eigenvalues of  $\mathbf{A}t$  fall outside the contour defined by the poles of the rational function. Interestingly, this phenomenon is not visible when only Definition 3.2.2 is considered.

The framework based on Cauchy integral formula has been considered in detail in the context of burnup equations [I, II]. This has drawn attention to the non-real eigenvalues of burnup matrices. Especially, the accuracy of a rational approximation optimal on the negative real axis is expected to be affected by the magnitudes of the eigenvalues' imaginary parts. Also, the method may suffer a break-down if some of the eigenvalues fall outside the integration contour implicitly defined by the rational approximation.

### 3.3.1 Partial fraction decomposition form

When approximating the matrix exponential, it is usually advantageous to employ the partial fraction decomposition (PFD) form of the rational function. Let  $\pi_{k,l}$  denote the set of rational functions  $r_{k,l}(x) = p_k(x)/q_l(x)$ , where  $p_k$  is a polynomial of order  $k$  and  $q_k$  is a polynomial of order  $l$ . For a rational function  $r_{k,k}$  with simple poles, the partial fraction decomposition is of the form

$$r_{k,k}(z) = \alpha_0 + \sum_{j=1}^k \frac{\alpha_j}{z - \theta_j}, \quad (3.36)$$

where  $\alpha_0$  is the limit of the function  $r_{k,k}$  at infinity, and  $\alpha_j$  are the residues at the poles  $\theta_j$ :

$$\alpha_j = \frac{p_k(\theta_j)}{q_k'(\theta_j)}. \quad (3.37)$$

Also, rational functions in  $\pi_{k-1,k}$  that have simple poles can be written in this form with  $\alpha_0 = 0$ .

When the coefficients of  $r_{k,k}$  are real, its poles form conjugate pairs, so that the computational cost can be reduced to half for a real variable  $x$ :

$$r_{k,k}(x) = \alpha_0 + 2 \operatorname{Re} \left( \sum_{j=1}^{k/2} \frac{\alpha_j}{x - \theta_j} \right) \quad (3.38)$$

and for a real matrix  $\mathbf{A} \in \mathbb{R}^{n \times n}$ , the rational function may be computed as

$$r_{k,k}(\mathbf{A}t)\mathbf{n}_0 = \alpha_0\mathbf{n}_0 + 2 \operatorname{Re} \left( \sum_{j=1}^{k/2} \alpha_j (\mathbf{A}t - \theta_j \mathbf{I})^{-1} \mathbf{n}_0 \right). \quad (3.39)$$

It can be seen from Eq. (3.39) that computing a rational approximation  $r_{k,k}(\mathbf{A}t)$  requires solving  $k/2$  linear systems.

When no nuclides are excluded from the burnup computation, the dimensions of the burnup matrix are generally between 1200 and 1700, making the linear systems relatively large. The numerical characteristics of burnup matrices, discussed in Section 3.1, may compromise the accuracy of widely used iterative solvers, many of which are based on Krylov subspace techniques whose convergence is ultimately related to the spectral properties of the matrix at hand. Luckily, the nearly upper triangular sparsity pattern of burnup matrices, depicted in Fig. 3.1 for example, can be utilized by employing a direct method. A method based on sparse Gaussian elimination has been implemented to the reactor physics code Serpent. The suitability and characteristics of this method in the context of burnup equations are analyzed in detail in [IV].

### 3.3.2 Chebyshev rational approximation method (CRAM)

In Chebyshev Rational Approximation Method (CRAM), the rational function  $\hat{r}(z)$  is chosen as the best rational approximation of the exponential function on the negative

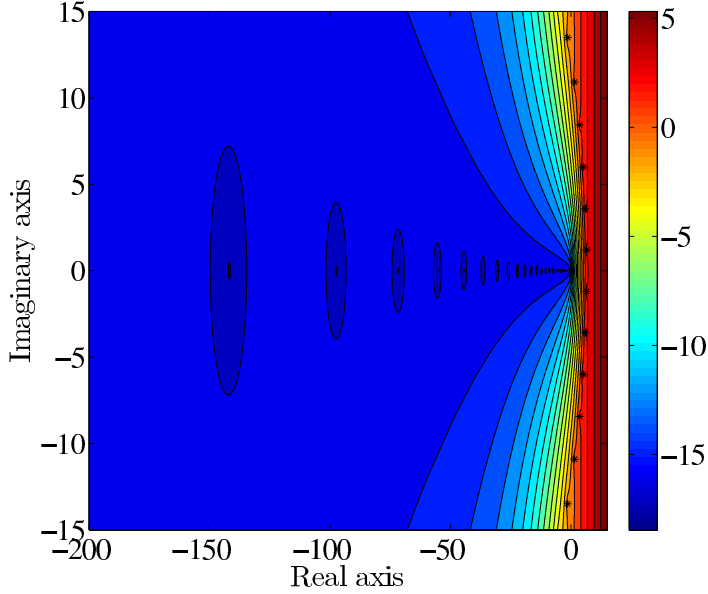


**Figure 3.10.** Plot of  $\log_{10} |e^z - \hat{r}_{16,16}(z)|$  illustrating the accuracy of CRAM of order 16 in the complex plane. The poles of  $\hat{r}_{16,16}$  have been marked with black asterisks.

real axis  $\mathbb{R}_-$ . Let  $\pi$  denote the set of rational functions  $r_{k,k}(x) = p_k(x)/q_k(x)$ , where  $p_k$  and  $q_k$  are polynomials of order  $k$ . The CRAM approximation of order  $k$  is defined as the unique rational function  $\hat{r}_{k,k} = \hat{p}_k(x)/\hat{q}_k(x)$  satisfying

$$\hat{\varepsilon}_{k,k} \equiv \sup_{x \in \mathbb{R}_-} |\hat{r}_{k,k}(x) - e^x| = \inf_{r_{k,k} \in \pi_{k,k}} \left\{ \sup_{x \in \mathbb{R}_-} |r_{k,k}(x) - e^x| \right\}. \quad (3.40)$$

The asymptotic convergence of this approximation on the negative real axis is remarkably fast, with the convergence rate  $\mathcal{O}(H^{-k})$ , where  $H = 9.289\,025\,49\dots$  is called the Halphen constant [19]. It was recently discovered by Stahl and Schmelzer [20] that this convergence extends to compact subsets on the complex plane and also to Hankel contours in  $\mathbb{C} \setminus \mathbb{R}_-$ , i.e. to contours that extend from  $-\infty$  around the origin clockwise back to  $-\infty$  without crossing the negative real axis. Figure 3.10 illustrates the accuracy of CRAM of order 16 in the left complex plane. It should be noticed that the accuracy of the approximation is not confined merely to the negative real axis, but extends to a wide region near it. Also, the function is relatively flat in the direction of the imaginary axis.

On the negative real axis, the deviation between the approximation  $\hat{r}_{k,k}$  and the exponential function equioscillates between  $-\hat{\varepsilon}_{k,k}$  and  $\hat{\varepsilon}_{k,k}$ . As  $x \rightarrow -\infty$ , the exponential function tends to zero, whereas CRAM of order  $k$  stabilizes to  $\hat{\varepsilon}_{k,k}$ . This is illustrated in Figure 3.11 which shows a plot of  $\hat{r}_{16,16}$  on the negative real axis. Therefore, as  $x \rightarrow -\infty$ , the *relative* accuracy of  $\hat{r}_{k,k}$  deteriorates. This is illustrated in Figure 3.12, which shows the relative error of CRAM of order 16 on the negative

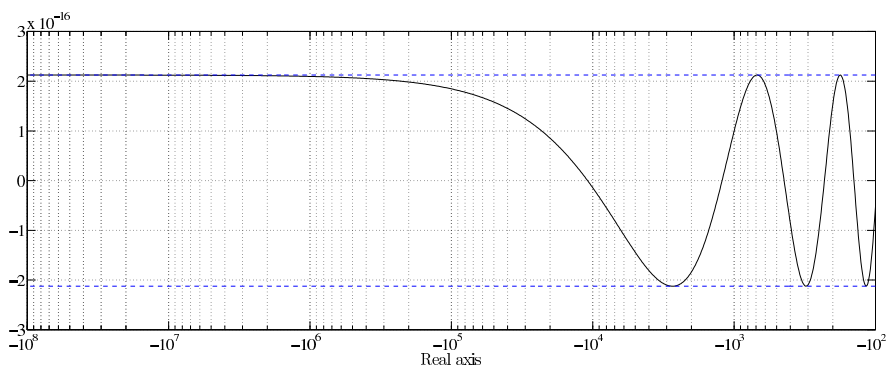


Figure 3.11. Plot of  $\hat{r}_{16,16}(x)$  on the negative real axis.

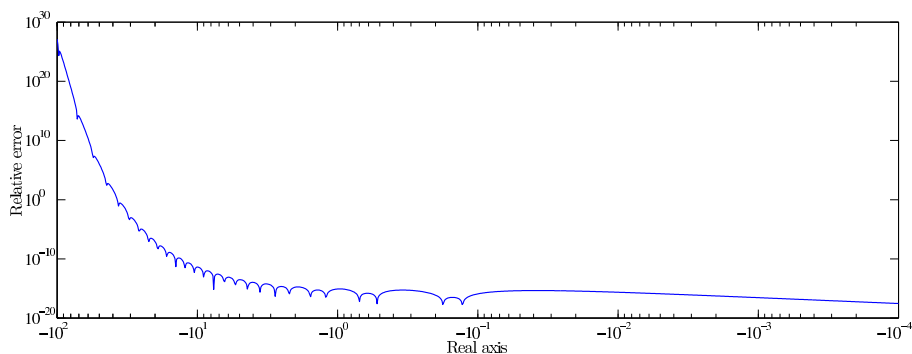


Figure 3.12. Plot of  $|e^x - \hat{r}_{16,16}(x)| e^{-x}$  illustrating the relative accuracy of CRAM of order 16 on the negative real axis.

real axis. In this context, it should be mentioned that it is generally impossible to derive best approximations with respect to relative error.

The main difficulty in using CRAM is determining the coefficients of the rational function for a given  $k$ . In principle, the polynomial coefficients of  $\hat{p}_k$  and  $\hat{q}_k$  can be computed with Remez-type methods, but this requires delicate algorithms combined with high-precision arithmetics. Fortunately, these coefficients have been computed to a high accuracy by Carpenter et al. for approximation orders  $k = 0, 1, \dots, 30$ , and they are provided in [21]. Although the PFD coefficients can in principle be computed from the polynomial coefficients, the computation of the polynomial roots may be ill-conditioned and requires great care. The PFD coefficients for approximation orders 10 and 14 have been provided in [22], and the given coefficients for  $k = 14$  have been used in several applications, including the matrix exponential computing package EXPOKIT [23]. However, it was recently observed that the coefficients reported in [22] contain errors and do not correspond to the true best approximation [11]. After discovering the erroneous behavior induced by the coefficients from [22], partial fraction coefficients for approximation orders  $k = 14$  and  $k = 16$  were computed from

the polynomial coefficients provided in [21] and subsequently reported in [II] and [III].

The application of CRAM to computing the matrix exponential was originally made famous by Cody, Meinardus, and Varga in 1969 in the context of rational approximation of  $e^{-x}$  on  $[0, \infty)$ , and it was recently resurfaced by Trefethen, Weideman, and Schmelzer [18]. The application of CRAM to burnup equations was first considered in [I] and [II] and it was later compared to other depletion algorithms in [24]. The main conclusions are briefly summarized here. Overall, CRAM has been shown to give a robust and accurate solution to burnup equations with high computational efficiency. In contrast to other matrix exponential methods considered previously, CRAM can be applied to large burnup problems containing over thousand nuclides and with the matrix norm being of the order of  $10^{21}$ . In this context, CRAM has been demonstrated to allow time steps of the order of  $10^7$  s, which can be considered to be the maximum feasible time step in burnup calculations. The convergence rate of CRAM, when applied to burnup equations, has been close to the asymptotic convergence rate on the negative real axis. [II]

It has been observed that the accuracy of CRAM depends relatively little on the characteristics of the problem at hand, such as the nuclear fuel or the neutron spectrum in the system [24]. However, it has been noticed that CRAM gives less accurate results for fresh fuel cases compared to depleted fuel cases [24]. It has been suggested that the reduced relative accuracy is related to the longer and more complex burnup chains being computed less accurately with CRAM [24]. When the fuel is fresh, only a few elements of  $\mathbf{n}_0$  are nonzero, and all the nuclides are produced solely from these initial nuclides. For a large part of nuclides, this means both long and complex transmutation chains being emphasized in the result. This reasoning was later supported based on computing the full matrix  $\hat{r}_{16,16}(\mathbf{A}t)$  explicitly [II].

As discussed in Section 3.1.2, burnup matrices are generally diagonalizable, although the imprecision of decay data may compromise this property in some cases. It is nonetheless fruitful to study the approximation error of CRAM from this perspective. Assuming a diagonal decomposition according to Eq. (3.19), we obtain the following expression for the approximation error of CRAM of order  $k$ , when applied to burnup equations:

$$\varepsilon_{k,k}(t) = \mathbf{T} \left( e^{\mathbf{A}t} - \hat{r}_{k,k}(\mathbf{A}t) \right) \beta, \quad (3.41)$$

where  $\beta = \mathbf{T}^{-1} \mathbf{n}_0$ . Let us consider this error as a function of time. When the eigenvalues of  $\mathbf{A}$  are located strictly on the negative real axis, the elements of  $\varepsilon_{k,k}$  are expected to oscillate until  $\hat{r}_{k,k}(\lambda_j t)$  has stabilized to  $\hat{\varepsilon}_{k,k}$  for all the eigenvalues  $\lambda_j$ . Otherwise, as  $t$  increases, the non-real eigenvalues of  $\mathbf{A}t$  shift along lines, whose slopes are determined by the ratio of their real and imaginary parts. In theory, the error according to Eq. (3.41) may increase as a function of time if the eigenvalues shift to a region where the accuracy of the approximation  $\hat{r}_{k,k}$  is notably worse than on the negative real axis. In particular, in accordance with Definition 3.2.3, the approximation error increases significantly when the contour implicitly defined by the rational approximation is crossed. However, based on discussion in Section 3.1.2, this scenario seems highly unlikely. Therefore, it can be deduced that the absolute error related to a CRAM solution to burnup equations is not expected to increase as

a function of time.

If the burnup matrix is not diagonalizable due to a multiple eigenvalue  $\tilde{\lambda}$  with index  $l$ , the error related to this eigenvalue can be traced back to the deviation between the exponential function and the derivatives  $\hat{r}_{k,k}(\tilde{\lambda}), \hat{r}'_{k,k}(\tilde{\lambda}), \dots, \hat{r}^{(l-1)}_{k,k}(\tilde{\lambda})$ . However, the previous reasoning still applies in the sense that the absolute approximation error is not expected to increase as a function of time.

We are usually interested in the *relative* accuracy of the solution, i.e. we want to know how many of its digits are correct. Based on previous discussion, the absolute error of the solution is not expected to increase, but oscillate as a function of time. Therefore, the time behavior of the relative error depends mainly on the nuclide concentration  $n_i(t)$ . It is clear that if a nuclide concentration diminishes significantly during the time step considered, the relative accuracy of the CRAM solution may be compromised.

To further study the accuracy of CRAM in the context of burnup equations, CRAM of order 16 was applied to two test cases, which are considered in the following. The first test case considers a small burnup system, which allows the approximation error to be analyzed in more detail. The second test case considers a decay system, i.e. burnup equations in the absence of neutron irradiation.

#### Application to a small test problem

In this section CRAM is applied to a small burnup system, which was formed by selecting the 36 lightest nuclides (from  $^1\text{H}$  to  $^{18}\text{O}$ ) from the burnup chain of 1606 nuclides corresponding to a PWR pin-cell with fuel irradiated to 0.1 MWd/kgU burnup. The corresponding burnup matrix is shown in Fig. 3.3. For this test case, the burnup matrix norm is of the order of  $10^{21}$ , the shortest transition being the decay of  $^7\text{B}$  whose half-life is of the order of  $10^{-24}$  seconds.

The spectrum of this small test case matrix captures well the relevant properties of burnup matrices. The matrix has a single positive eigenvalue,  $z_+ \approx 4.15 \times 10^{-12}$ , and zero as a threefold eigenvalue. The rest of the eigenvalues are plotted in Figure 3.13. The two eigenvalues with non-zero imaginary parts are related to the sub-matrix  $\tilde{\mathbf{A}} \in \mathbb{R}^{4 \times 4}$  corresponding to the by-product nuclides  $^1\text{H}$ ,  $^2\text{H}$ ,  $^3\text{H}$ , and  $^3\text{He}$ . In accordance with Theorem 3.1.8, the eigenvalue zero is semisimple and the matrix is diagonalizable.

The exponential of the burnup matrix is depicted in Fig. 3.14, and the relative error of CRAM of order 16 applied to the same matrix is shown in Fig. 3.15 on a logarithmic scale. It can be seen from Fig. 3.15 that the approximation is very accurate for almost all matrix elements. The three greatest errors, ( $D_{23,23} \approx 2.44 \times 10^{-1}$ ,  $D_{18,18} \approx 4.11 \times 10^{-2}$  and  $D_{23,18} \approx 3.76 \times 10^{-4}$ ), plotted in red, correspond to nuclides  $^{12}\text{Be}$  (index 23) and  $^{12}\text{B}$  (index 18) that are both short-lived, with half-lives of the order of milliseconds.

In this test case, the nuclide  $^{12}\text{B}$  is not formed from any other nuclide and it forms its own strongly connected component. The relative accuracy of the matrix element  $\hat{E}_{18,18}$  is determined solely by the relative accuracy of  $\hat{r}_{16,16}$  at the corresponding

### 3. Matrix exponential solution of burnup equations

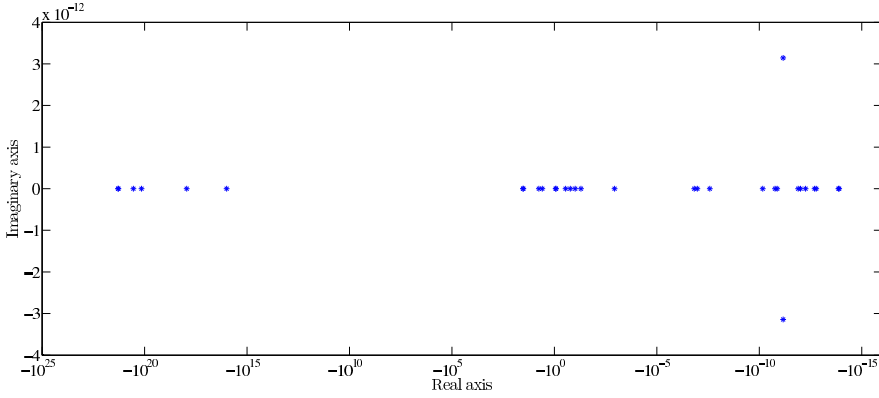


**Figure 3.13.** A plot of the eigenvalues  $z \in \{z \in \mathbb{C} \mid z \in \Lambda(\mathbf{A}), \operatorname{Re} z < 0\}$  for the test case with 36 nuclides. In addition, the matrix has a single positive eigenvalue,  $z_+ \approx 4.15 \times 10^{-12}$ , and zero as a threefold eigenvalue.

eigenvalue  $z_1 = A_{18,18} \approx -32.5$ . The nuclide  $^{12}\text{Be}$  forms a SCC with 6 other nuclides, and the matrix element  $E_{23,18}$  is a linear combination of eight different modes, 7 of them corresponding to the SCC, and one to the decay of  $^{12}\text{B}$  to  $^{12}\text{Be}$ . When considering the element  $E_{23,18}$ , the eigenvalues corresponding to the transition  $^{12}\text{B} \rightarrow ^{12}\text{Be}$  and the effective removal rate of the nuclide are the most important. Therefore, the accuracy of the  $\hat{E}_{23,18}$  is dominated by the relative accuracy of  $\hat{r}_{16,16}$  at these two eigenvalues  $z_1 \approx -32.5$  and  $z_2 \approx -34.3$ . The same reasoning applies to the element  $\hat{E}_{23,23}$ , for which the most significant mode corresponds to the eigenvalue  $z_2 \approx -34.3$ .

As can be seen from Figs. 3.14 and 3.15, there is a clear trend in that the relative errors tend to be greater for the matrix elements with smaller values. However, even arbitrarily small matrix elements can be captured with amazing accuracy by CRAM, if the relative accuracy of the approximation is good at the eigenvalues corresponding to the relevant modes. For example, the matrix element  $E_{17,23} \approx 1.73 \times 10^{-69}$  is computed to 8 correct digits with CRAM of order 16. The index 17 corresponds to the nuclide  $^{10}\text{Be}$  which belongs to the same SCC as  $^{12}\text{Be}$ . For this matrix element, the most significant modes correspond to eigenvalues  $z \in [-10^{-13}, -10^{-14}]$ .

Figure 3.16 shows the test case nuclide concentrations and Fig. 3.17 the respective approximation error of  $\hat{r}_{16,16}$  as a function of time between 10 s and  $10^{12}$  s  $\approx 32\,000$  years. The reference solutions were computed with MATLAB's Symbolic Toolbox using high-precision arithmetics. As can be seen from the the figure, for  $t \in [10, 10^{10}]$  s, the approximation error is the greatest for nuclides, whose concentrations diminish the most rapidly. The trend that these errors begin to diminish for time steps greater than  $10^6$  s is explained by the fact that after this time the respective nuclide concentrations begin to increase as a function of time. It should be pointed out that the concentration of  $^{12}\text{Be}$  falls to zero so rapidly that its concentration and the respective approximation error were not included in the plots. It is interesting that

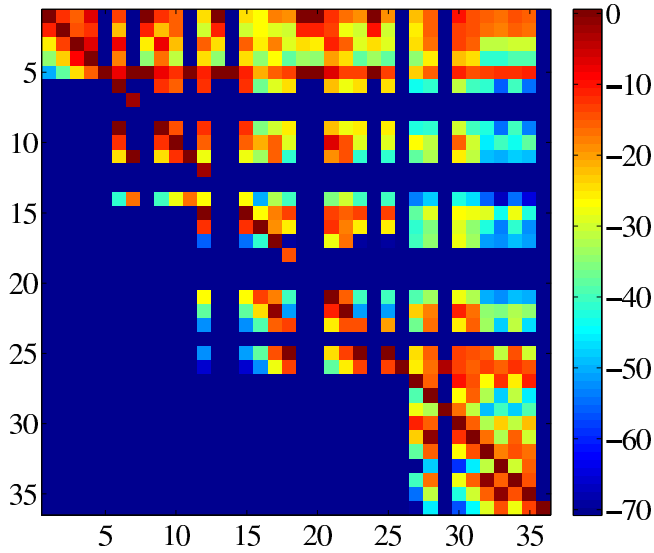


**Figure 3.14.** Plot of the matrix elements  $\mathbf{E} = e^{\mathbf{A}}$  on a logarithmic scale. The matrix  $\mathbf{E}$  was computed with MATLAB's Symbolic Toolbox with high-precision arithmetics.

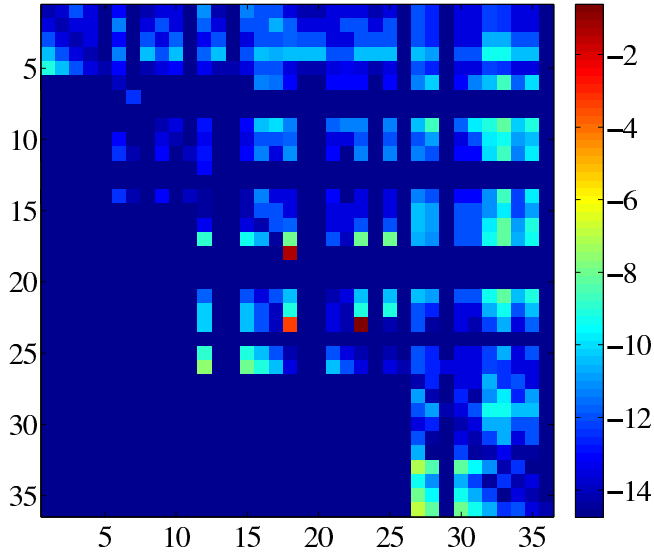


**Figure 3.15.** Relative error of CRAM of order 16 when applied to the burnup matrix corresponding to the test case with 36 nuclides, i.e. plot of matrix  $\mathbf{D}$  defined as  $D_{ij} = \log_{10} \left( \frac{E_{ij}(1) - \hat{E}_{ij}(1)}{E_{ij}(1)} \right)$ , where  $\hat{\mathbf{E}} = \hat{r}_{16,16}(\mathbf{A})$ .

### 3. Matrix exponential solution of burnup equations

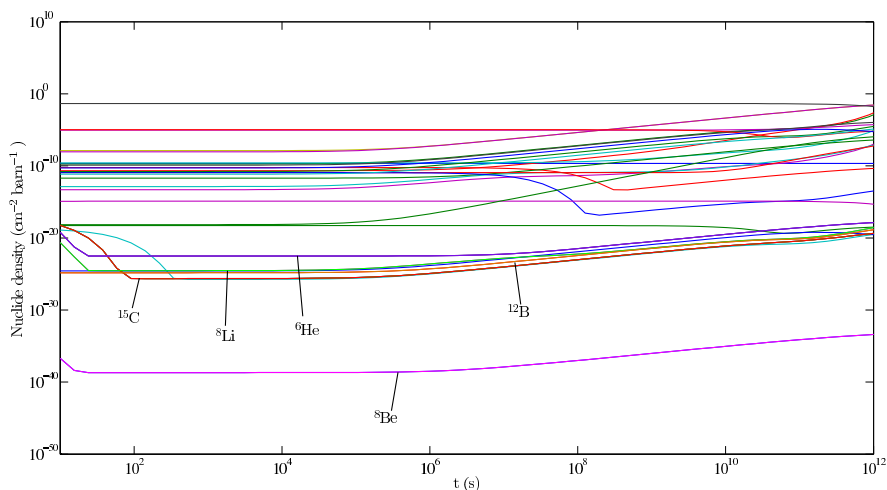


**Figure 3.16.** Nuclide concentrations corresponding the small test case with 36 nuclides.

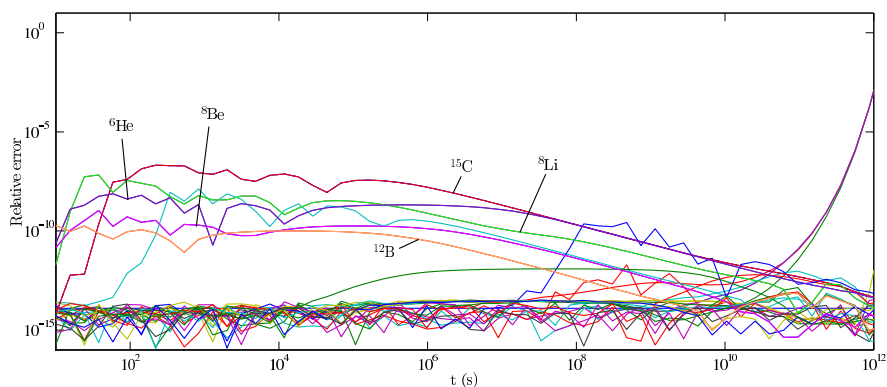


**Figure 3.17.** The relative errors of CRAM solution of order 16 for the nuclide concentrations corresponding to the small test case with 36 nuclides.

although the approximation error is comparatively large for the matrix element  $\hat{E}_{18,23}$ , corresponding the transition  $^{12}\text{Be} \rightarrow ^{12}\text{B}$ , the error is much smaller for the concentration of  $^{12}\text{B}$ . This is due to the accuracy of the solution being dominated by the matrix elements corresponding to the greatest initial nuclide densities. When  $t \rightarrow 10^{12}$  s,  $z_+ t \rightarrow 1$ , and the accuracy of the approximation begins to deteriorate for the by-product nuclides  $^1\text{H}$ ,  $^2\text{H}$ ,  $^3\text{H}$ , and  $^3\text{He}$  corresponding to the positive eigenvalue  $z_+$ . This results from the accuracy of  $\hat{r}_{16,16}$  quickly deteriorating on the positive real axis.

The test case nuclide concentrations and the approximation error of CRAM of order 16 for time steps between  $t = 10^{12}$  s  $\approx 32\,000$  years and  $t = 10^{20}$  s  $\approx 3.2 \times 10^{12}$  years

are shown in Figures 3.20 and 3.21. Time steps of this magnitude are clearly not feasible in burnup calculations, but they are considered here to further study the characteristics of the approximation. As can be seen from Figure 3.20, the concentrations of the by-product nuclides begin to increase very rapidly for time steps greater than  $10^{12}$  s. This increase is not captured by the CRAM approximation that virtually breaks down on the positive real axis. Therefore, the relative error of the by-product nuclide concentrations quickly stabilizes to unity. For time steps greater than  $10^{14}$  s, these concentrations are rounded off to infinity in computer arithmetics, after which the respective relative errors are no longer well-defined. Large oscillations in the error curves after  $t = 10^{15}$  s  $\approx 7.6 \times 10^8$  years are explained by the oscillation of  $\hat{r}_{16,16}$  around the negative real axis. The stabilized nuclide concentrations, plotted in green and blue, correspond to  $^{12}\text{C}$  and  $^{18}\text{O}$ , which do not elicit any neutron nor decay reactions based on the data used in the test case.

#### Application to a decay system

In the absence of neutron irradiation, nuclides transform to other nuclides merely through radioactive decay and the burnup equations reduce to decay equations. The decay paths do not form closed cycles and therefore the decay matrix can be permuted to upper triangular form. It follows that the eigenvalues of decay matrices are known to be strictly confined to the negative real axis. The lack of closed loops causes a great part of the nuclide concentrations to diminish rapidly in comparison to burnup cases. Based on the previous discussion, this is expected to affect the relative accuracy of the CRAM solution.

In this section, CRAM is applied to a decay system consisting of 1531 nuclides. Compared to the burnup cases considered previously, the decay matrix is significantly sparser. Figure 3.20 shows the nuclide concentrations of the test case actinides as a function of time. The reference solutions were computed with MATLAB's Symbolic Toolbox using high-precision arithmetics. As can be seen from the figure, several of the nuclide concentrations fall quickly to zero after the time step  $t \sim 10^4$  s, and this trend becomes stronger as  $t$  increases. Figure 3.21 shows the relative error of CRAM of order 16 for the respective nuclide concentrations. By comparing these figures, it is evident that the relative accuracy of the CRAM solution deteriorates as the nuclide concentrations diminish.

Let us consider the approximation error of CRAM as a function of time assuming the diagonalizability of the decay matrix in which case the error satisfies Eq. (3.41). As explained previously, the CRAM approximation of order  $k$  approaches  $\hat{\epsilon}_{k,k}$  as  $x \rightarrow -\infty$ , whereas the exponential function falls to zero. If a nuclide concentration  $n_i(t)$  diminishes drastically during the time step  $t$ , it can be anticipated that  $-\lambda_j t \gg 1$  for all the relevant eigenvalues. In this case, it can be approximated  $e^{\lambda_j t} - \hat{r}_{16,16}(\lambda_j t) \approx \hat{\epsilon}_{k,k}$  for all these eigenvalues (see also Figure 3.12), and the following estimate can be

### 3. Matrix exponential solution of burnup equations

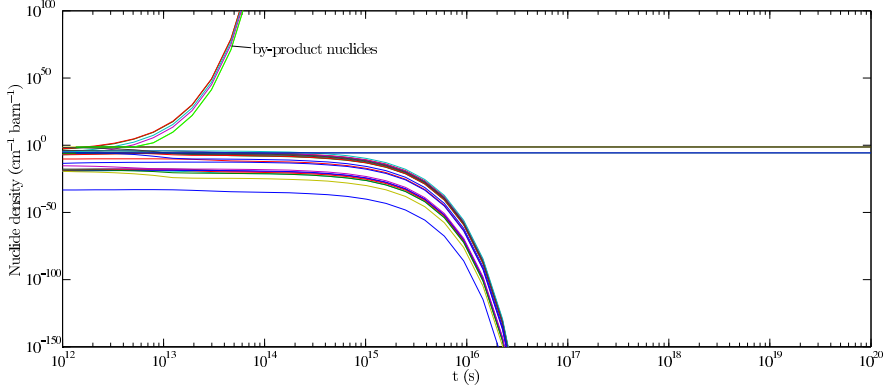


**Figure 3.18.** Nuclide concentrations corresponding the small test case with 36 nuclides for time steps greater than  $t = 10^{12}$  s.

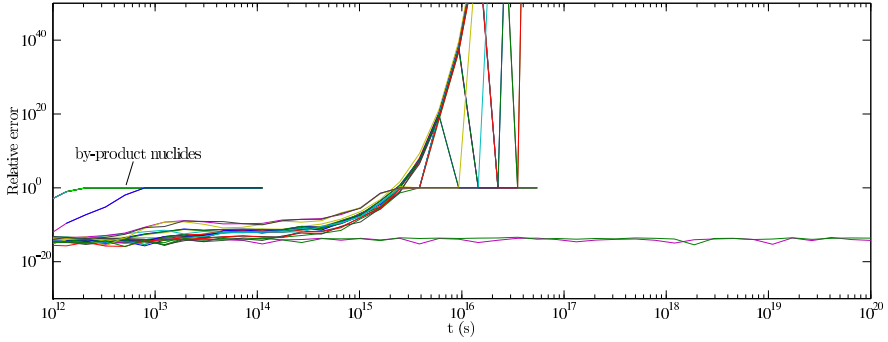


**Figure 3.19.** The relative errors of CRAM solution of order 16 for the nuclide concentrations corresponding to the small test case with 36 nuclides for time steps greater than  $t = 10^{12}$  s.

derived for the approximation error:

$$\begin{aligned}
 \frac{\varepsilon_i(t)}{n_i(t)} &= \frac{|\sum_{j=1}^n T_{ij} (e^{\lambda_j t} - \hat{r}_{k,k}(\lambda_j t)) \beta_j|}{n_i(t)} \\
 &= \frac{|\sum_{j=1}^n \sum_{m=1}^n T_{ij} (e^{\lambda_j t} - \hat{r}_{k,k}(\lambda_j t)) T_{jm}^{-1} n_m(0)|}{n_i(t)} \\
 &\approx \frac{|-\hat{\varepsilon}_{k,k} \sum_{m=1}^n \sum_{j=1}^n T_{ij} T_{jm}^{-1} n_m(0)|}{n_i(t)} = \hat{\varepsilon}_{k,k} \frac{n_i(0)}{n_i(t)}. \quad (3.42)
 \end{aligned}$$

Equation (3.42) suggests that the relative accuracy of the CRAM solution deteriorates significantly if  $n_i(t)$  becomes smaller than  $\hat{\varepsilon}_{k,k} n_i(0)$ . In other words, the value  $\hat{\varepsilon}_{k,k}$  implicitly defines a numerical cut-off for the results. Therefore, concentrations  $\hat{n}_i(t)$  smaller than  $\hat{\varepsilon}_{k,k} n_i(0)$  (as given by CRAM of order  $k$ ) should be treated as zero. How-

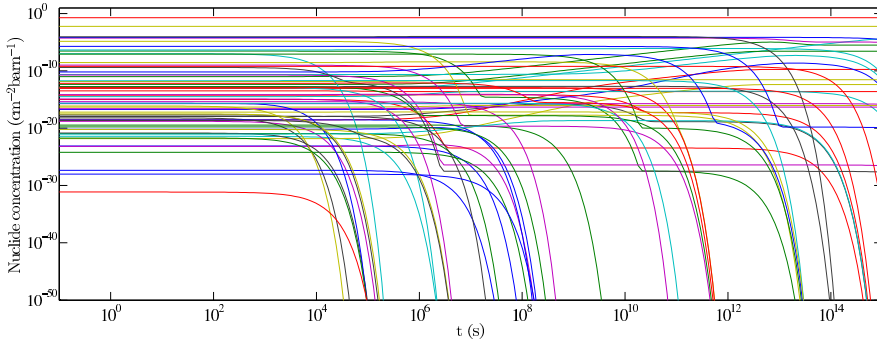


**Figure 3.20.** Concentrations of the actinides corresponding the decay system test case with 1531 nuclides.

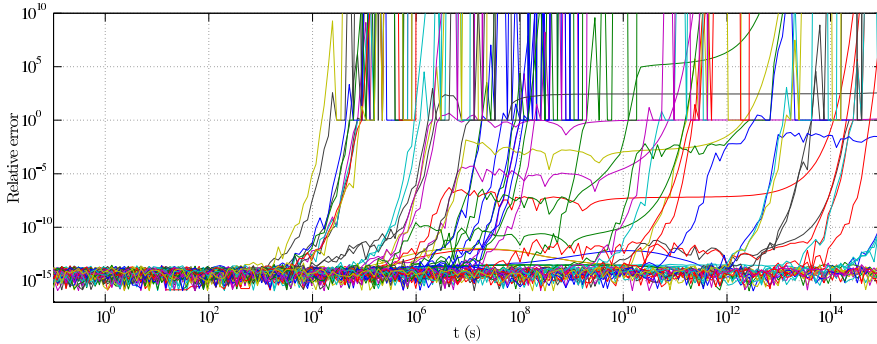


**Figure 3.21.** Relative error of the CRAM of order 16 solution for the actinides corresponding the decay system test case with 1531 nuclides.

ever, it should be emphasized that CRAM may also yield a reduced relative accuracy for the solution in other situations. Nonetheless, it is clear that nuclide concentrations smaller than  $\hat{\epsilon}_{k,k} n_j(0)$  have a poor relative accuracy when computed with CRAM of order  $k$ .

Figure 3.22 shows the nuclide concentrations for the time step  $t = 10^7$  s  $\approx$  116 days, together with the concentrations given by CRAM of order 16. At this time, 1007 of the 1531 nuclides have concentrations smaller than  $\hat{\epsilon}_{16,16}$  times their initial concentrations. Let  $\hat{n}$  denote the solution given by CRAM of order 16. It can be clearly seen from the figure that the values of  $\hat{n}_j$  saturate to  $\hat{\epsilon}_{16,16} n_j(0)$  when the reference solution  $n_j$  becomes smaller than this value.

Compared to the burnup cases considered previously in [I, II] and in [24], CRAM yields significantly less accurate results for this decay system. This clearly results from the nuclide concentrations diminishing faster than in burnup cases, where the nuclide chains contain more closed cycles. This supports the conclusion that the non-real eigenvalues of burnup matrices are not as relevant to the accuracy of CRAM

### 3. Matrix exponential solution of burnup equations

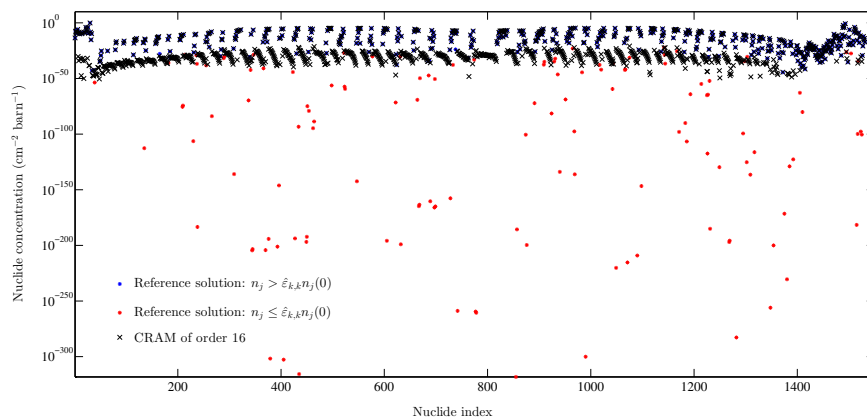


**Figure 3.22.** Test case nuclide concentrations for the time step  $t = 10^7$  s given by a highly accurate reference solution and CRAM of order 16.

after all. Furthermore, CRAM should be used with caution in conjunction with decay systems. It should also be noted that the decay equations can be solved analytically by the linear chain method [25, 26]. In the development version of Serpent 2, the analytical method is used by default in the absence of neutron irradiation. Of course, problems can be encountered in reduced power cases, where an analytical solution cannot be found, but the nuclide concentrations diminish rather rapidly due to the neutron reactions being unlikely. In these applications, the length of the time step should be kept sufficiently small in order to guarantee the accuracy of the solution.

#### 3.3.3 Rational approximations from contour integrals

As explained previously, the burnup matrix exponential can be defined as an integral along a contour with, for example, a parabolic or hyperbolic shape in the left complex plane. Because the integrand will decrease exponentially, these contour integrals can be approximated efficiently using quadrature formulas. These quadrature formulas can furthermore be interpreted as rational approximations that can be used to approximate the matrix exponential, the poles and residues of the function being the nodes and weights of the numerical integration formula [18]. This approach was first applied to the solution of burnup equations in [11].

As discussed previously, the application of these numerical integration schemes requires that the singularities of the integrand lie inside the contour. Therefore, the respective rational approximation is expected to give poorer results when the eigenvalues of  $\mathbf{A}t$  fall outside the contour. This phenomenon is studied more closely in the context of burnup equations in the following subsection.

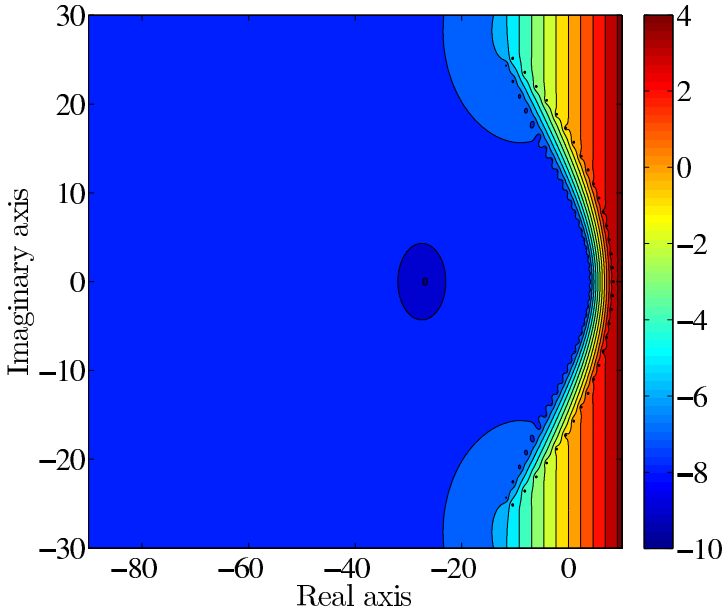


**Figure 3.23.** A plot of  $\log_{10} |r_{31,32}(z) - e^z|$  in the complex plane. The 32 quadrature points (i.e. poles of  $r_{31,32}$ ) have been marked with black dots in the plot.

#### Application to a test problem with 219 nuclides

In this section, a quadrature-based rational approximation is applied to a small burnup test case formed by selecting only the most important actinides and fission products, totalling in 219 nuclides. The test case represents a PWR pin-cell lattice in which the fuel has been irradiated to 25 MWd/kgU burnup. The chosen rational approximation is based on the following contour, suggested by Weideman [27] and later considered in [II]:

$$\phi : \mathbb{R} \rightarrow \mathbb{C}, \quad \phi(x) = N(0.1309 - 0.1149x^2 + i0.2500x). \quad (3.43)$$

This contour is asymptotically optimal with the convergence rate of  $\mathcal{O}(2.85^{-N})$ , when singularities are located on the negative real axis. In this study,  $N = 32$  quadrature points were chosen, which resulted in the rational function  $r_{31,32} \in \pi_{31,32}$ . The approximation error related to this rational function is shown in Figure 3.23.

The spectrum of the (conventional) burnup matrix corresponding to this test case is plotted in Figure 3.24. The burnup matrix has four pairs of eigenvalues with non-zero imaginary parts, the smallest of them being of the order of  $10^{-13}$  and the largest of the order of  $10^{-8}$ . As  $t$  increases, the eigenvalues of  $\mathbf{A}t$  shift along lines, whose slopes are determined by the ratio of their real and imaginary parts. This is illustrated in Figure 3.25, which shows the lines corresponding to the four complex eigenvalues of  $\mathbf{A}$  together with the parabolic contour for  $N = 32$ . As can be seen from the figure,

### 3. Matrix exponential solution of burnup equations

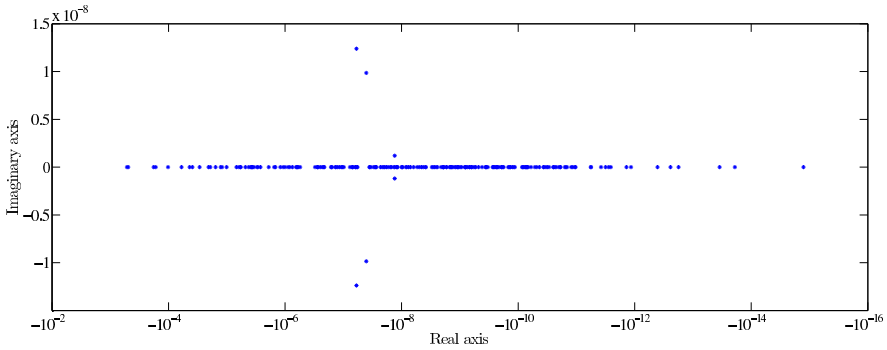


**Figure 3.24.** A plot of the eigenvalues  $z \in \{z \in \mathbb{C} \mid z \in \Lambda(\mathbf{A}), \operatorname{Re} z < 0\}$  for the test case with 219 nuclides. In addition, the matrix has zero as a twofold eigenvalue.

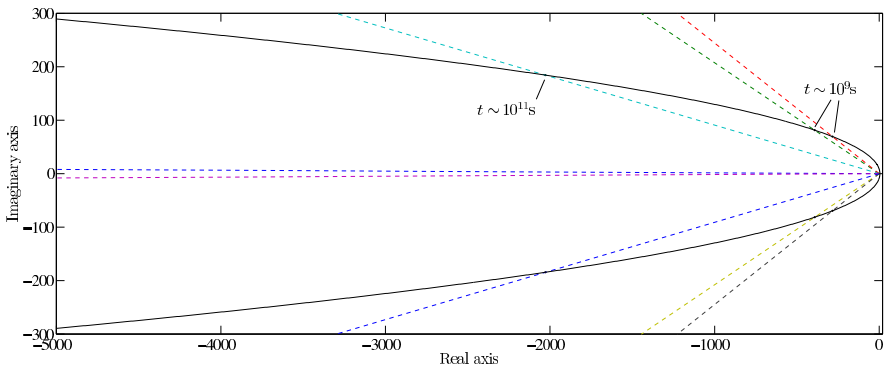


**Figure 3.25.** A plot of the lines  $z = \lambda t$  (dashed line) for the four complex eigenvalues  $\lambda \in \Lambda(\mathbf{A})$  and the parabolic contour of Eq. (3.43) (solid line) for  $N = 32$ .

two of the eigenvalues cross the contour when  $t$  is of the order of  $10^9 \text{ s} \approx 32 \text{ years}$  and one when  $t$  is of the order of  $10^{11} \text{ s} \approx 3200 \text{ years}$ . The eigenvalue with the smallest imaginary part crosses the contour when  $t \sim 10^{13} \text{ s} \approx 0.32 \text{ million years}$ .

Figure 3.26 shows the matrix exponential  $e^{\mathbf{A}t}$  and the relative error related to  $r_{31,32}(\mathbf{A}t)$  for  $t = 10^8 \text{ s} \approx 3.2 \text{ years}$ , and Figure 3.27 the mean and maximum relative errors of the nuclide concentrations as a function of time. The error begins to increase notably when  $t \rightarrow 10^{11} \text{ s}$ . Figure 3.28 shows the relative errors plotted against the reference nuclide concentrations for the values  $t \sim 10^8 \text{ s}$  and  $t \sim 10^{11} \text{ s}$ . Based on this figure, it appears that the increase in the relative error is again due to some of the nuclide concentrations tending to zero when  $t \rightarrow \infty$ . The impact of the eigenvalues shifting over the integration contour could not be detected by studying the error related to the elements of the matrix  $r_{31,32}(\mathbf{A}t)$  at different time steps.

The fact that the complex eigenvalues are not manifested in the accuracy of the solution can be explained by investigating the rational approximation more closely.

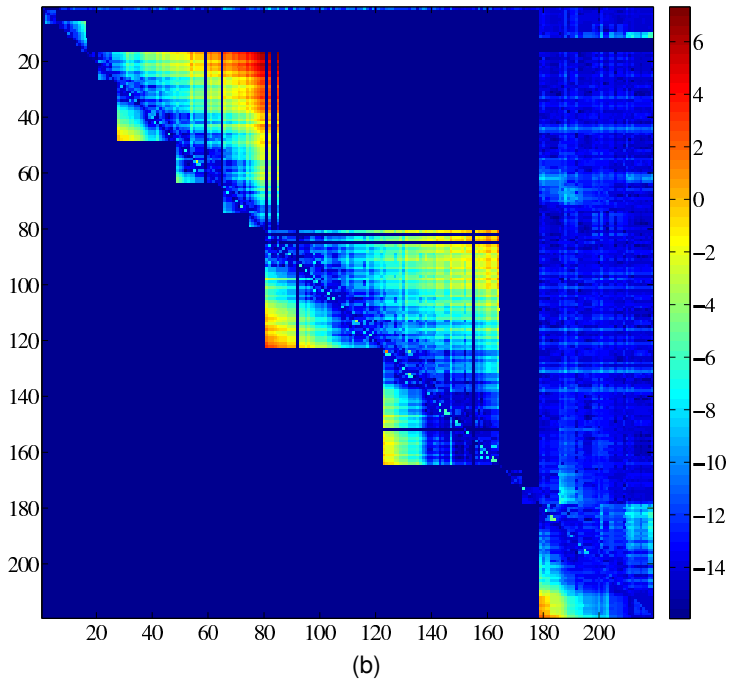
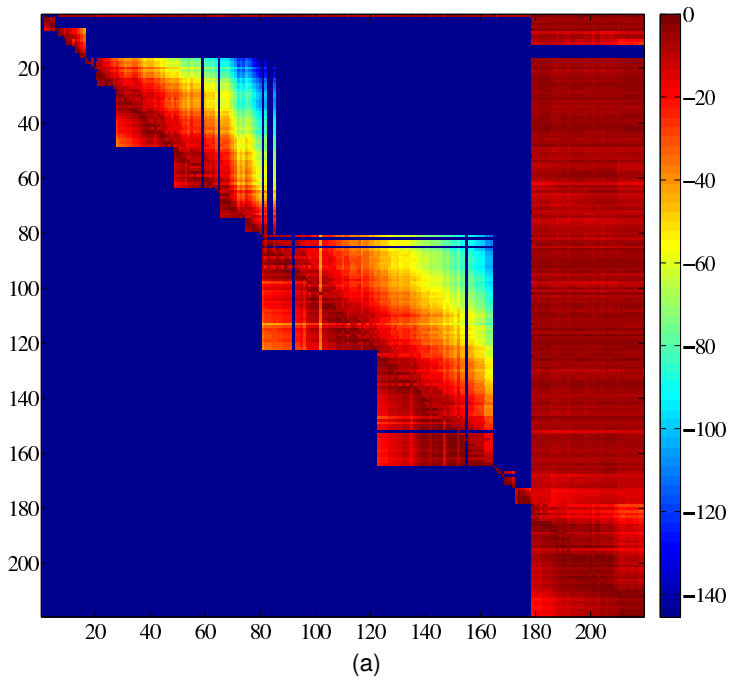


**Figure 3.26.** Plot of (a) the matrix elements  $\mathbf{E} = e^{\mathbf{A}t}$ , and (b) the relative error related to  $r_{32,31}(\mathbf{A}t)$  for  $t = 10^8$  s  $\approx 3.2$  years on a logarithmic scale.

### 3. Matrix exponential solution of burnup equations

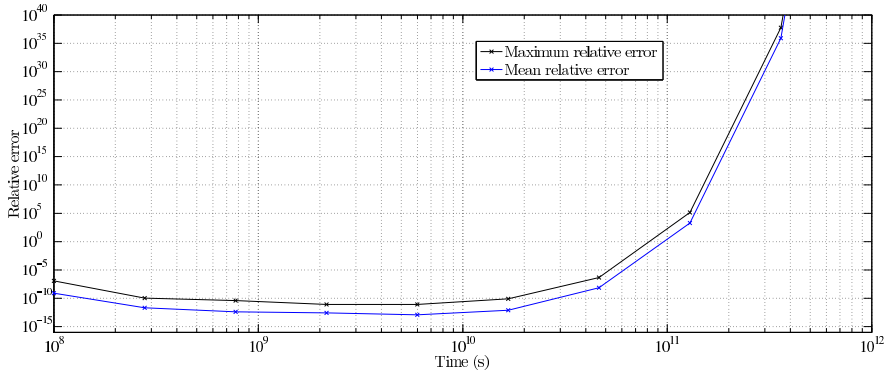


**Figure 3.27.** Mean and maximum relative errors of the quadrature-based solution as a function of time for the small test case with 219 nuclides.

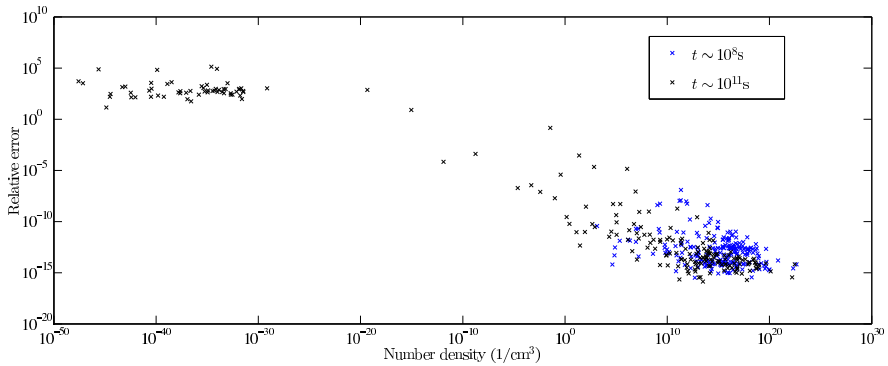


**Figure 3.28.** Plot of the relative error of the quadrature-based solution for time steps  $t \approx 10^8$  s and  $t \approx 10^{11}$  s for the small test case with 219 nuclides.

In accordance with Definition 3.2.3, it is clear that the integral along the contour of Eq. (3.43) no longer represents the matrix exponential, if some of the eigenvalues are located outside the contour. However, after applying the quadrature rule, the part of the contour extending beyond the quadrature points becomes irrelevant. Therefore, if the eigenvalues lying outside the contour are located far from the quadrature points (in the direction of the negative real axis), they are not expected to affect the accuracy of the solution. It can also be seen from Figure 3.23 that the accuracy of the approximation diminishes rapidly outside the contour near the quadrature points. However, on the left of the quadrature points the error function is basically flat. In this test case, the eigenvalues of  $\mathbf{A}t$  fall outside the contour of Eq. (3.43) so far from the quadrature points that it is clear that this is not significant to the accuracy of the solution.

When the approximation order is increased, the part of the contour spanned by the quadrature points becomes greater. However, also the contour becomes broader

according to Eq. (3.43). For this test case, there is actually no approximation order for which the eigenvalues cross the contour in the part spanned by the respective quadrature points. It follows that the quadrature-based method does not break down due to the complex eigenvalues at any time step. However, as discussed previously, the relative accuracy of the solution diminishes as  $t$  increases. The complex eigenvalues of this small burnup matrix are very representative of the spectrum of burnup matrices in general. Therefore, this study supports the previous observation of the complex eigenvalues with small imaginary parts not being relevant to the accuracy of the quadrature-based solution in the context of burnup equations [11].



## 4. Perturbation theory based sensitivity and uncertainty analysis applied to criticality equation

When uncertain parameters are utilized in computations, also the calculation results contain uncertainty. In order to estimate the reliability of these calculations, it is necessary to develop uncertainty analysis methods enabling the propagation of parameter uncertainty through the calculations.

In recent years, the interest towards sensitivity and uncertainty analysis has increased notably in the field of nuclear engineering. In 2006, the OECD/NEA expert group on Uncertainty Analysis in Modelling decided to prepare a benchmark titled *Uncertainty Analysis in Best-Estimate Modelling (UAM) for Design, Operation and Safety Analysis of LWRs* [28] to establish the current state and needs of sensitivity and uncertainty analysis. The goal of the benchmark is to propagate uncertainty through all stages of coupled neutronics/thermal hydraulics calculations. The imprecision of neutron interaction data is likely one of the most significant sources of uncertainty in these calculations, and therefore the propagation of this uncertainty is considered to be the main priority at the moment. As a first step, this requires developing sensitivity and uncertainty analysis methods for fuel assembly codes that are used to produce homogenized data for coupled neutronics/thermal-hydraulics calculations.

This chapter describes the implementation of uncertainty analysis capability to the fuel assembly burnup calculation code CASMO-4 [29] in the context of the UAM benchmark. The developed uncertainty analysis methodology is deterministic, meaning that the uncertainties are computed based on the sensitivity profiles and covariance matrices for the uncertain nuclear data parameters. Sensitivity analysis studies the changes in system responses due to perturbations in the parameters. Perturbation theory provides an efficient technique to compute sensitivity profiles by utilizing the adjoint system of the original forward problem. At the time of launching the benchmark, the generally employed reactor physics codes did not have uncertainty analysis capabilities, and the modified CASMO-4 was one of the first fuel assembly programs that enabled sensitivity and uncertainty analysis based on perturbation theory.

#### 4.1 Background for sensitivity and uncertainty analysis

Let us consider a mathematical model containing uncertain parameters. The objective of uncertainty analysis is to estimate how the uncertainty in these parameters is propagated to a response dependent on the solution of the problem under consideration. In this thesis the considered mathematical model is the neutron transport eigenvalue problem called the criticality equation, i.e. Eq. (2.5), which can be written in operator form as

$$\mathbf{A}\boldsymbol{\phi} = \frac{1}{k}\mathbf{B}\boldsymbol{\phi}, \quad (4.1)$$

where  $\boldsymbol{\phi} \in H_\phi$  is the neutron flux,  $H_\phi$  is a Hilbert space, and  $k$  is the multiplication factor. The uncertain parameters consist of neutron cross-section data and they are denoted by the vector  $\boldsymbol{\sigma} \in E_\sigma$ , where  $E_\sigma$  is a normed linear space. It should be noted that both the continuous-energy criticality equation and the various systems derived from it in numerical computations can be written in the form of Eq. (4.1). For continuous-energy criticality equation, the Hilbert space under consideration is  $L^2$ . The considered responses are the critical eigenvalue  $k$  and ratios of the form

$$R(\mathbf{e}) = \frac{\langle \boldsymbol{\phi}, \boldsymbol{\Sigma}_1 \rangle}{\langle \boldsymbol{\phi}, \boldsymbol{\Sigma}_2 \rangle}, \quad (4.2)$$

where  $\boldsymbol{\Sigma}_1, \boldsymbol{\Sigma}_2 \in H_\phi$ . Therefore, only functional responses are considered in this thesis. For example, few-group cross-sections homogenized over a geometry can be written in the form of Eq. (4.2).

The uncertainty of the parameters  $\boldsymbol{\sigma}$  should be understood in terms of the Bayesian probability interpretation [30]. In this framework, probability is defined as a subjective measure that characterizes the plausibility of various hypotheses. When estimating parameters, all knowledge about a parameter  $\sigma_j$  is assumed to be incorporated into its marginal probability distribution  $p(\sigma_j)$ . This distribution is defined so that the integral  $\int_a^b p(\sigma_j) d\sigma_j$  corresponds to the (Bayesian) probability that the value of  $\sigma_j$  belongs to the interval  $[a, b]$ . The distribution  $p(\boldsymbol{\sigma})$  can then be used to form an estimate  $\hat{\sigma}$  for the parameters and their associated uncertainties. In most cases either the mean value or the mode are chosen as  $\hat{\sigma}$ . Typically, the variance of the distribution is chosen to give a numerical value to the related uncertainty. When several parameters are considered simultaneously, the probability distribution under consideration is their joint distribution  $p(\boldsymbol{\sigma})$ , and the covariance matrix of this distribution may be chosen as the descriptive statistic for the uncertainty.

In Bayesian formalism, the outcome of the uncertainty analysis should ideally be the full posterior distribution  $p(\mathbf{R})$  for the response vector  $\mathbf{R} \in \mathbb{R}^d$ . However, determining  $p(\mathbf{R})$  analytically is usually not feasible, and therefore approximations need to be made. Uncertainty analysis methods can be divided into statistical and deterministic methods according to the chosen strategy. In statistical methods, the values of the uncertain parameters are sampled from their probability distribution, after which these values are used to compute a set of values for the responses. In this manner, the distribution  $p(\mathbf{R})$  is simulated point-wise. In deterministic uncertainty analysis, the objective is not to form the entire distribution  $p(\mathbf{R})$ , but to compute an estimate

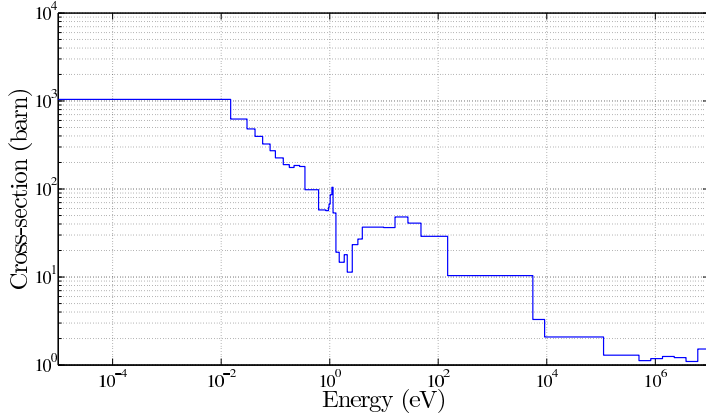


**Figure 4.1.** The self-shielded 40-group fission cross-section of  $^{235}\text{U}$  for a BWR fuel assembly test problem.

for the covariance matrix  $\text{Cov}[\mathbf{R}]$ , after which the distribution can be assumed to be Gaussian. Most often this is based on the linearization of the responses with respect to the uncertain parameters. This requires computing the *local sensitivities* of the responses at the parameters' best-estimate values.

The local sensitivity of response  $R$  is defined as the directional derivative in the direction of the perturbation  $\delta\sigma$ . When considering the continuous-energy eigenvalue problem, the cross-sections are functions of energy and location, and the appropriate derivative is the functional directional derivative called the Gâteaux-variation [31]. It follows that the sensitivity of  $R$  with respect to the perturbation  $\mathbf{h} = [\delta\boldsymbol{\phi}, \delta\boldsymbol{\sigma}] \in D = H_{\phi} \times E_{\sigma}$  at the point  $\hat{\mathbf{e}} = [\hat{\boldsymbol{\phi}}, \hat{\boldsymbol{\sigma}}] \in D$  may be defined as:

$$\delta R(\hat{\mathbf{e}}; \mathbf{h}) = \lim_{t \rightarrow 0} \frac{R(\hat{\mathbf{e}} + t\mathbf{h}) - R(\hat{\mathbf{e}})}{t}. \quad (4.3)$$

The *local relative sensitivity* is defined as  $S(\hat{\mathbf{e}}; \mathbf{h}) = \delta R(\hat{\mathbf{e}}; \mathbf{h})/R(\hat{\mathbf{e}})$ , respectively.

The objective of sensitivity analysis is to compute these derivatives with respect to all uncertain parameters in the mathematical model. When solving the criticality equation, the utilized nuclear data typically contains tens of thousands of uncertain parameters. Since neutron cross-sections are functions of energy and position, the local sensitivities need to be computed with respect to cross-section values at each energy and mesh point in the calculation. In reactor physics applications, the number of responses is typically small compared to the number of uncertain parameters. For example, the fuel assembly burnup calculation program CASMO-4 [29], utilized in this work, computes by default a few dozen responses that are passed on to subsequent codes simulating the full core. These responses include the following assembly homogenized two-group cross-sections: transport, absorption, production, fission, scattering and  $\kappa$ -fission. The two-group homogenized cross-sections can be written in the form of Eq. (4.2) and they have been considered as responses in this thesis. To illustrate the uncertainty related to nuclear data parameters, Figure 4.1

#### 4. Perturbation theory based sensitivity and uncertainty analysis applied to criticality equation

---

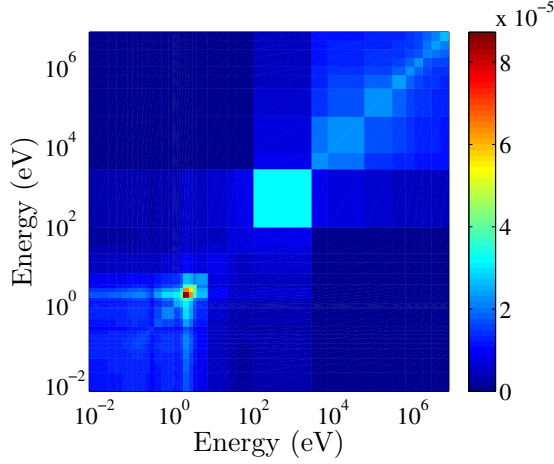


**Figure 4.2.** The relative covariance matrix of the  $^{235}\text{U}$  fission cross-section taken from the SCALE 6.1 covariance library and modified to the 40 energy group structure of CASMO-4.

shows the 40-group fission cross-section of  $^{235}\text{U}$  for a BWR fuel assembly test problem as computed with CASMO-4. The corresponding multi-group covariance matrix is shown in Figure 4.2.

The large number of uncertain parameters in reactor physics applications usually inhibits statistical uncertainty analysis in practise. Fortunately, the sensitivities can be computed deterministically in an efficient manner by exploiting the adjoint of the eigenvalue problem. This framework, referred to as *perturbation theory* in the context of reactor physics, is considered in Section 4.2.

After computing the sensitivities and linearizing the response vector,  $\mathbf{R} \approx \mathbf{R}(\hat{\sigma}) + \mathbf{S}\sigma$ , where  $\mathbf{S} \in \mathbb{R}^{J \times K}$  is the sensitivity matrix containing the derivatives with respect to all considered uncertain parameters, the covariance matrix of the response can be simply computed using the identity

$$\text{Cov}[\mathbf{R}] \approx \text{Cov}[\mathbf{R}(\hat{\sigma}) + \mathbf{S}\sigma] = \mathbf{S} \text{Cov}[\sigma] \mathbf{S}^T \quad (4.4)$$

known as the first-order uncertainty propagation formula or the *Sandwich rule*. It is noteworthy that in the case where  $\mathbf{R}$  depends linearly on the parameters and  $p(\sigma)$  is a Gaussian distribution, the Sandwich rule yields the exact posterior distribution, i.e.

$$\boldsymbol{\eta} = \mathbf{c} + \mathbf{S}\sigma \sim \mathcal{N}(\mathbf{c} + \mathbf{S}\hat{\sigma}, \mathbf{S} \text{Cov}[\sigma] \mathbf{S}^T), \quad (4.5)$$

where  $\mathbf{c} \in \mathbb{R}^K$  is a constant vector.

## 4.2 Perturbation theory

The objective of sensitivity analysis is to compute the derivatives of system responses with respect to all uncertain parameters in the mathematical model. In perturbation theory, these derivatives are computed in an efficient manner by utilizing the adjoint system of the original forward problem. This approach was first considered in reactor analysis in [32, 33].

Consider the eigenvalue system given by Eq. (4.1). When the parameters  $\sigma$  are perturbed, also the solution  $\boldsymbol{\phi}$  changes, and therefore the computation of the sensitivity  $\delta R(\hat{\mathbf{e}}; \mathbf{h})$  according to Eq. (4.3) requires that the perturbation  $\delta \boldsymbol{\phi}$  is known. In principle,  $\delta \boldsymbol{\phi}$  can be computed to first order from the following *forward sensitivity system*:

$$\begin{aligned} \delta \mathbf{A}(\hat{\mathbf{e}}; \mathbf{h}) &= -\frac{1}{k^2} \delta k(\hat{\mathbf{e}}; \mathbf{h}) \mathbf{B} \boldsymbol{\phi} + \frac{1}{k} \delta \mathbf{B}(\hat{\mathbf{e}}; \mathbf{h}) \\ \Leftrightarrow \mathbf{A}'_{\sigma}(\hat{\mathbf{e}}) \delta \sigma + \mathbf{A}(\hat{\mathbf{e}}) \delta \boldsymbol{\phi} &= -\frac{1}{k^2} \delta k(\hat{\mathbf{e}}; \mathbf{h}) \mathbf{B} \boldsymbol{\phi} + \frac{1}{k} \mathbf{B}'_{\sigma}(\hat{\mathbf{e}}) \delta \sigma + \frac{1}{k} \mathbf{B}(\hat{\mathbf{e}}) \delta \boldsymbol{\phi}, \end{aligned} \quad (4.6)$$

which can be derived by taking the Gâteaux variation of system (4.1) with respect to a perturbation  $\mathbf{h}$  on both sides. However, when computing several sensitivities, this approach would require the repetitive solving of Eq. (4.6). The adjoint system of Eq. (4.1) is defined as the system that satisfies the following relation:<sup>7</sup>

$$\left\langle \mathbf{A} \boldsymbol{\phi} - \frac{1}{k} \mathbf{B} \boldsymbol{\phi}, \boldsymbol{\psi} \right\rangle = \left\langle \boldsymbol{\phi}, \mathbf{A}^* \boldsymbol{\psi} - \frac{1}{k} \mathbf{B}^* \boldsymbol{\psi} \right\rangle, \quad (4.7)$$

where the brackets  $\langle \cdot, \cdot \rangle$  denote an inner product. When considering the continuous-energy criticality equation, it is customary to employ the  $L^2$  inner product [34, 35]. The solution to the adjoint problem

$$\left( \mathbf{A}^* - \frac{1}{k} \mathbf{B}^* \right) \boldsymbol{\psi} = 0 \quad (4.8)$$

is called the *fundamental adjoint*. Physically, the solution to this system can be interpreted to represent the average contribution, i.e. importance of a neutron to the multiplication factor. Interestingly, the adjoint system of Eq. (4.8) can be derived solely based on this physical interpretation [36].

By utilizing Eqs. (4.7) and (4.8), it is straightforward to obtain the following expression for the relative sensitivity of the multiplication factor with respect to a perturbation  $\delta \sigma$  (For derivation, see e.g. [37] or [V]):

$$\frac{\delta k(\hat{\mathbf{e}}; \mathbf{h})}{k} = -\frac{\langle (\mathbf{A}'_{\sigma}(\hat{\sigma}) \boldsymbol{\phi} - \frac{1}{k} \mathbf{B}'_{\sigma}(\hat{\sigma}) \boldsymbol{\phi}) \delta \sigma, \boldsymbol{\psi} \rangle}{\langle \frac{1}{k} \mathbf{B} \boldsymbol{\phi}, \boldsymbol{\psi} \rangle}. \quad (4.9)$$

Sensitivity analysis of the critical eigenvalue based on Eq. (4.9) is known as *classical perturbation theory* in reactor physics.

<sup>7</sup>In some cases the adjoint relation needs to be written in the form  $\langle \mathbf{A} \boldsymbol{\phi} - \frac{1}{k} \mathbf{B} \boldsymbol{\phi}, \boldsymbol{\psi} \rangle = \langle \boldsymbol{\phi}, \mathbf{A}^* \boldsymbol{\psi} - \frac{1}{k} \mathbf{B}^* \boldsymbol{\psi} \rangle + [\mathbf{P}(\boldsymbol{\psi}, \boldsymbol{\phi})]_{\mathbf{x} \in \partial \Omega}$ , where  $[\mathbf{P}(\boldsymbol{\psi}, \boldsymbol{\phi})]_{\mathbf{x} \in \partial \Omega}$  is a bilinear form associated with the system. We will only consider cases where it is straightforward to force this term to vanish.

#### 4. Perturbation theory based sensitivity and uncertainty analysis applied to criticality equation

---

For responses of the form of Eq. (4.2), the *generalized adjoint* can be defined as the solution to the following inhomogeneous system

$$\left( \mathbf{A}^* - \frac{1}{k} \mathbf{B}^* \right) \boldsymbol{\Gamma} = \frac{\nabla_{\phi} R}{R}, \quad (4.10)$$

where  $\nabla_{\phi} R$  is the Fréchet derivative of  $R$ , also called the gradient. The generalized adjoint  $\boldsymbol{\Gamma}(\mathbf{r}, \boldsymbol{\Omega}, E)$  can be physically interpreted as the average contribution of an additional neutron at the phase space point  $[\mathbf{r}, \boldsymbol{\Omega}, E]$  to the response under consideration. It is noteworthy that when considering the generalized adjoint problem, the eigenvalue  $k$  is fixed to correspond to the solution of Eq. (4.1), and the operator  $\mathbf{A}^* - \frac{1}{k} \mathbf{B}^*$  is singular. Therefore, in order for the solution  $\boldsymbol{\Gamma}$  to exist, the gradient  $\nabla_{\phi} R$  needs to be orthogonal to the forward solution

$$\langle \nabla_{\phi} R, \boldsymbol{\phi} \rangle = 0. \quad (4.11)$$

Responses satisfying Eq. (4.11) are called allowable for generalized perturbation theory [37]. It is easy to show that for responses of the form of Eq. (4.2), the relative gradient becomes

$$\frac{\nabla_{\phi} R}{R} = \frac{\boldsymbol{\Sigma}_1}{\langle \boldsymbol{\phi}, \boldsymbol{\Sigma}_1 \rangle} - \frac{\boldsymbol{\Sigma}_2}{\langle \boldsymbol{\phi}, \boldsymbol{\Sigma}_2 \rangle}. \quad (4.12)$$

and that Eq. (4.11) is satisfied. Also, when a solution  $\boldsymbol{\Gamma}_0$  to Eq. (4.10) exists, there exists an infinite amount of solutions of the form

$$\boldsymbol{\Gamma} = \boldsymbol{\Gamma}_0 + a \boldsymbol{\Psi}, \quad a \in \mathbb{R}. \quad (4.13)$$

In this case, it is possible to choose a solution orthogonal to the (forward) fission source. This particular solution can be written

$$\begin{aligned} \boldsymbol{\Gamma}_p &= \boldsymbol{\Gamma}_0 - \frac{\langle \boldsymbol{\Gamma}_0, \mathbf{B} \boldsymbol{\phi} \rangle}{\langle \boldsymbol{\Psi}, \mathbf{B} \boldsymbol{\phi} \rangle} \boldsymbol{\Psi} \\ &= \boldsymbol{\Gamma}_0 - \frac{\langle \mathbf{B}^* \boldsymbol{\Gamma}_0, \boldsymbol{\phi} \rangle}{\langle \mathbf{B}^* \boldsymbol{\Psi}, \boldsymbol{\phi} \rangle} \boldsymbol{\Psi}. \end{aligned} \quad (4.14)$$

Based on Eqs. (4.10), (4.7), (4.6) and (4.14), the following expression can be derived for the relative sensitivity of the response  $R$  with respect to a perturbation  $\delta\sigma$  [VI]:

$$\frac{\delta R(\hat{\mathbf{e}}, \mathbf{h})}{R} = \frac{R'_{\sigma}(\hat{\mathbf{e}}) \delta\sigma}{R} - \left\langle \boldsymbol{\Gamma}_p, \left( \mathbf{A}'_{\sigma}(\hat{\sigma}) \boldsymbol{\phi} - \frac{1}{k} \mathbf{B}'_{\sigma}(\hat{\sigma}) \boldsymbol{\phi} \right) \delta\sigma \right\rangle_{\phi}. \quad (4.15)$$

Sensitivity analysis based on this equation is known as *generalized perturbation theory* in reactor physics

##### 4.2.1 Numerical computation

In practice, the criticality equation and the corresponding adjoint equations are solved numerically, which introduces some complications in the perturbation theory formalism. Ideally, the discretizations should be performed in a consistent manner,

so that the respective adjoint relations are satisfied at all stages of the computation [31]. However, as discussed in more detail in [V], this is usually infeasible in reactor physics calculations and therefore it is customary to take the eigenvalue problem discretized with respect to energy and direction as the starting point for sensitivity analysis.

Assuming isotropic scattering and the discrete ordinates approximation for angular dependence, the forward problem becomes

$$\begin{aligned} & \boldsymbol{\Omega}_m \cdot \nabla \Phi^g(\mathbf{r}, \boldsymbol{\Omega}_m) + \Sigma^g \Phi^g(\mathbf{r}, \boldsymbol{\Omega}_m) \\ &= \frac{1}{4\pi} \sum_{h=1}^G \Sigma_s^{h \rightarrow g} \phi^h(\mathbf{r}) + \frac{\chi_g}{4\pi k} \sum_{h=1}^G \bar{\nu} \Sigma_f^h \phi^h(\mathbf{r}), \quad g = 1, \dots, G, \end{aligned} \quad (4.16)$$

where  $\{\boldsymbol{\Omega}_m\}_{m=1}^M$  are the considered angular directions, and the scalar flux is approximated by the quadrature formula

$$\phi^h(\mathbf{r}) = \sum_{m=1}^M \omega_m \Phi^h(\mathbf{r}, \boldsymbol{\Omega}_m). \quad (4.17)$$

Equation (4.16) follows from Eq. (2.6) after the discrete ordinates approximation. In fuel assembly calculations, the boundary conditions are usually assumed to be reflective to simulate an infinite lattice, i.e.

$$\Phi(\mathbf{r}, \boldsymbol{\Omega}_m, E) = \Phi(\mathbf{r}, \boldsymbol{\Omega}'_m, E), \quad \mathbf{r} \in \Gamma, \quad \boldsymbol{\Omega}_m \cdot \mathbf{n} < 0, \quad (4.18)$$

where  $\boldsymbol{\Omega}_m = \boldsymbol{\Omega}'_m - 2(\mathbf{n} \cdot \boldsymbol{\Omega}'_m) \mathbf{n}$  is the reflection direction.

In order to form the adjoint system of Eq. (4.16), the corresponding inner product needs to be defined. As mentioned previously, the continuous energy eigenvalue problem is typically considered in the space  $L^2$ . The inner product corresponding to the discretization employed in Eq. (4.16) can be defined in a consistent manner as

$$\langle \boldsymbol{\Phi}, \boldsymbol{\Psi} \rangle = \sum_{g=1}^G \sum_{m=1}^M \omega_m \int_D d^3\mathbf{r} \Phi^g(\mathbf{r}, \boldsymbol{\Omega}_m) \Psi^g(\mathbf{r}, \boldsymbol{\Omega}_m). \quad (4.19)$$

It is now straightforward to show that the following system

$$\begin{aligned} & -\boldsymbol{\Omega}_m \cdot \nabla \Psi^g(\mathbf{r}, \boldsymbol{\Omega}_m) + \Sigma^g \Psi^g(\mathbf{r}, \boldsymbol{\Omega}_m) \\ &= \frac{1}{4\pi} \sum_{h=1}^G \Sigma_s^{g \rightarrow h} \psi^h(\mathbf{r}) + \frac{\bar{\nu} \Sigma_f^g}{4\pi k} \sum_{h=1}^G \chi_h \psi^h(\mathbf{r}), \quad g = 1, \dots, G \end{aligned} \quad (4.20)$$

with the boundary conditions

$$\Psi(\mathbf{r}, \boldsymbol{\Omega}_m, E) = \Psi(\mathbf{r}, \boldsymbol{\Omega}'_m, E), \quad \mathbf{r} \in \Gamma, \quad \boldsymbol{\Omega}_m \cdot \mathbf{n} > 0 \quad (4.21)$$

satisfies the adjoint relation of Eq. (4.7) with respect to the inner product defined by Eq. (4.19).

#### 4. Perturbation theory based sensitivity and uncertainty analysis applied to criticality equation

---

The generalized adjoint problem for a response of the form of Eq. (4.2) can be written, respectively

$$\begin{aligned}
 -\boldsymbol{\Omega}_m \cdot \nabla \Gamma^g(\mathbf{r}, \boldsymbol{\Omega}_m) + \Sigma^g \Gamma^g(\mathbf{r}, \boldsymbol{\Omega}_m) &= \frac{1}{4\pi} \sum_{h=1}^G \Sigma_s^{g \rightarrow h} \gamma^h(\mathbf{r}) + \\
 + \frac{\bar{\nu} \Sigma_f^g}{4\pi k} \sum_{h=1}^G \chi_h \gamma^h(\mathbf{r}) + \frac{\Sigma_1^g(\mathbf{r})}{\langle \boldsymbol{\Phi}, \boldsymbol{\Sigma}_1 \rangle} - \frac{\Sigma_2^g(\mathbf{r})}{\langle \boldsymbol{\Phi}, \boldsymbol{\Sigma}_2 \rangle}, \quad g = 1, \dots, G, \quad (4.22)
 \end{aligned}$$

where the generalized adjoint scalar flux in has been denoted by  $\gamma^h(\mathbf{r})$ .

The numerical solution of the fundamental adjoint from Eq. (4.20) has been considered in [V], and the computation of the generalized adjoint functions from Eq. (4.22) in [VI]. In both cases, it is advantageous that the adjoint systems are of the same form as the forward problem, which can be utilized in numerical computations. After computing the necessary adjoint functions, the sensitivities can be computed according to Eqs. (4.9) and (4.15). In this context, it is customary to further discretize the inner product of Eq. (4.19) as

$$\langle \boldsymbol{\Phi}, \boldsymbol{\Psi} \rangle \approx \sum_{i=1}^I \sum_{g=1}^G \sum_{m=1}^M \omega_m V_i \bar{\Phi}^{g,i,m} \bar{\Psi}^{g,i,m}, \quad (4.23)$$

where  $i$  denotes the mesh index and  $\bar{\Phi}^{g,i,m}$  and  $\bar{\Psi}^{g,i,m}$  denote the average fluxes.

### 4.3 Application to CASMO-4

CASMO-4 is a two-dimensional fuel assembly burnup calculation program developed by Studsvik Scandpower [29]. It can be used for burnup calculations on boiling water reactor (BWR) and pressurized water reactor (PWR) pin cells or assemblies. The main purpose of fuel assembly transport calculations is to obtain the detailed neutron flux in the system, and to use this flux to compute homogenized parameters, which can then be passed on to the following full core computations. Because the properties of the fuel assemblies do not change sharply in the axial direction for the most part, it is generally sufficient to perform these computations in two dimensions. The boundary conditions of fuel assemblies are usually assumed to be reflective in order to represent the model as an infinite lattice.

In the 2-D transport calculation module of CASMO-4, Eq. (4.16) is solved with the method of characteristics [38]. The transport calculation is performed in the true heterogeneous geometry of the assembly, but the number of energy groups is typically reduced before the computation. The cross-section libraries of CASMO-4 contain 70 energy groups (14 fast groups, 13 resonance groups, and 43 thermal groups) and they include the following cross-sections: absorption, fission, production, scattering and total. After computing the macroscopic cross-sections based on microscopic cross-sections and the nuclide densities for the assembly under consideration, the cross-sections of the important resonance absorbers are self-shielded based on tabulated effective resonance integrals. In the following micro group calculation, the

#### 4. Perturbation theory based sensitivity and uncertainty analysis applied to criticality equation

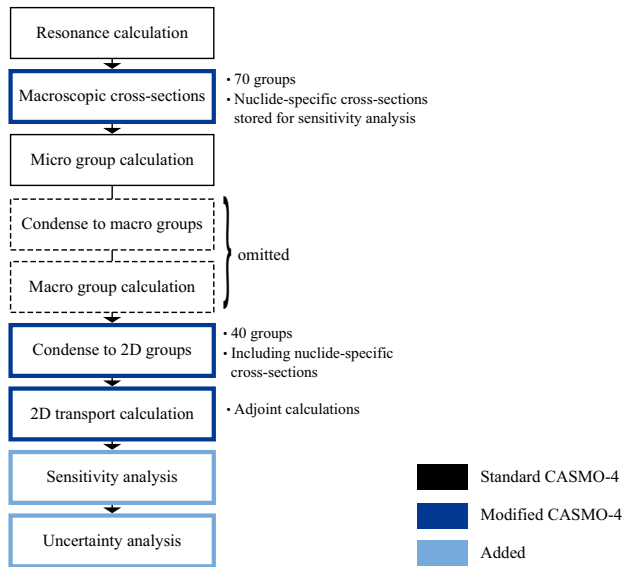


**Figure 4.3.** Outline of the CASMO-4 calculations.

detailed flux is solved for each pin cell type in the assembly by the method of collision probabilities, and the flux is used to homogenize the pin cells. These steps are followed by the macro group calculation, where the flux spectra is solved over the assembly using the homogenized pin cells and the response matrix method. The macro group calculation is performed using 40 energy groups by default. The flux spectra obtained from this computation are used to collapse the energy groups to the final group structure used in the 2-D transport calculation.

The implementation of perturbation theory according to the principles presented in Section 4.2.1 required modifications to several modules of CASMO-4. Figure 4.3 shows the flow diagram of the modified code. In order to be able to compute the sensitivities with respect to nuclide-specific cross-sections, they needed to be stored and collapsed to the energy group structure used in the 2-D transport calculation. It was decided to keep 40 energy groups in the transport calculation in order to obtain sufficiently detailed sensitivity profiles.

The solution of the fundamental adjoint and the generalized adjoint functions corresponding to the homogenized two-group cross-sections were implemented to the 2-D transport calculation module according to the guidelines presented in [V] and [VI]. After computing the necessary adjoint functions, the sensitivities of the multiplication factor and system responses are computed according to perturbation theory. The sensitivities are computed with respect to fission spectrum  $\chi$ , the average number of fission neutrons  $\bar{\nu}$ , and the multi-group cross-sections present in the nuclear data library of CASMO-4.

In order to enable uncertainty analysis, the covariance matrices from ZZ-SCALE6.0/COVA-44G [39] were processed for compatibility with CASMO-4. The

#### 4. Perturbation theory based sensitivity and uncertainty analysis applied to criticality equation

**Table 4.1.** Parameters for which there exists covariance data in the SCALE library.

Parameter	MT number
$\sigma_t$	1
$\sigma_e$	2
$\sigma_i$	4
$\sigma_{n,2n}$	16
$\sigma_f$	18
$\sigma_\gamma$	102
$\sigma_{n,p}$	103
$\sigma_{n,d}$	104
$\sigma_{n,t}$	105
$\sigma_{n,He}$	106
$\sigma_{n,\alpha}$	107
$\bar{\nu}$	456
$\chi$	1018

library is based on evaluations from various sources (including ENDF/B-VII, ENDF/B-VI, JENDL-3.1) and approximate covariance data. The covariances in the library are given in relative terms, and therefore the library is intended to be used with all cross-section libraries, including the ones that are inconsistent with the evaluations. While this is not strictly correct, it is considered to be acceptable due to the scarcity of comprehensive covariance data, among other reasons [40]. In the covariance library, the available covariance matrices are given in a 40-group structure for the parameters listed in Table 4.1. It should be emphasized that there is no covariance data for the group-to-group transfer cross-sections.

The covariance matrices from ZZ-SCALE6.0/COVA-44G were first transformed to the 40-group structure used in the 2-D transport calculation. The employed procedure, based on simple mathematical techniques, is described in detail in [V]. The use of the Sandwich rule for uncertainty analysis necessitates that the sensitivities and covariance matrices are formed with respect to the same parameters. Therefore, a problem was faced due to the covariance matrices being given for individual capture and scattering reactions, whereas the cross-section libraries of CASMO-4 only contain data for the total capture and scattering reactions. The cross-section model used in CASMO-4 is characteristic for several fuel assembly codes [41–43] and this issue affects the uncertainty analysis irrespective of the method used, whether deterministic or statistical. As a solution to this discrepancy, a technique for combining the covariance matrices of the individual subreactions was devised [V]. Since the relationships between the total and individual capture and scattering reactions are linear, the covariance matrices corresponding to the total capture and scattering reactions can be computed with the Sandwich rule without introducing any approximation. However, the sensitivity profiles with respect to the individual and the total scattering cross-sections cannot be defined in a consistent manner, and this produces some systematic differences to the results. This is explained in the following.

As mentioned previously, there is no cross-section data for the transfer cross-

#### 4. Perturbation theory based sensitivity and uncertainty analysis applied to criticality equation

---

sections  $\sigma_x^{h \rightarrow g j}$  but only for  $\sigma_x^{g j} = \sum_{h=1}^G \sigma_x^{g \rightarrow h j}$ , where  $x$  refers to a scattering reaction (e.g., elastic, inelastic) and  $j$  is the nuclide index. Therefore, in order to use the scattering covariance data, the sensitivity profiles should be computed with respect to  $\sigma_x^{g j}$ . Because of the scattering source term in Eq. (4.16), however, the derivative with respect to  $\sigma_x^{g j}$  is not mathematically well-defined without additional constraints. Typically it is assumed that the probabilities of transfers to various groups are fixed, i.e.

$$\sigma_x^{g \rightarrow h j} = \sigma_x^{g j} p_x^{g \rightarrow h j}, \quad (4.24)$$

where  $p_x^{g \rightarrow h}$  is the proportion of neutrons scattered from energy group  $g$  to energy group  $h$ , which is assumed to remain fixed, even if the scattering cross-section  $\sigma_x^{g j}$  is perturbed [44]. Based on this assumption, the scattering source in Eq. (4.16) can be written

$$S^g = \frac{1}{4\pi} \sum_{h=1}^G \Sigma_s^{h \rightarrow g} \phi^h = \frac{1}{4\pi} \sum_x \sum_j N^j \sum_{h=1}^G \sigma_x^{h j} p_x^{h \rightarrow g} \phi^h, \quad (4.25)$$

where the summations over  $x$  include all scattering reactions. After this assumption, the derivative with respect to  $\sigma_x^{g j}$  is well-defined and can be computed as usual. However, the sensitivity with respect to the total scattering cross-section  $\sigma_s^j = \sum_x \sigma_x^j$  is not well-defined, if the constraint (4.24) is enforced. In order to define this sensitivity, fixed transfer rates must be assumed for the total scattering cross-section. Since the two assumptions required to compute the individual and total scattering sensitivities are inconsistent, the chain rule of derivation does not apply to them, and, for example, although  $\sigma_s^{g j} = \sigma_e^{g j} + \sigma_i^{g j}$  holds,  $\frac{dR}{d\sigma_s^{g j}} \neq \frac{dR}{d\sigma_e^{g j}} \frac{d\sigma_s^{g j}}{d\sigma_e^{g j}}$ . Since the assumption of fixed transfer rates for the total scattering is clearly stricter than Eq. (4.24), the methodology employed in CASMO-4 typically produces smaller uncertainties, when multiple scattering reactions are present [V, VI]. However, it should be kept in mind that both of these approaches are in fact based on simplifications of the true problem, and are likely to underestimate the uncertainty related to scattering cross-sections.



## 5. Summary of the publications

This chapter summarizes the main results of the publications included in this thesis.

### 5.1 Publication I: Computing the matrix exponential in burnup calculations

Burnup equations describe the changes in the nuclide concentrations due to radioactive decay and neutron-induced transmutation reactions. They form a system of first order linear differential equations that can in principle be solved by computing the burnup matrix exponential. Due to the decay and transmutation constants of the nuclides varying extensively, the system is extremely stiff, which complicates the numerical computation of the matrix exponential solution. The short-lived nuclides are especially problematic, inducing eigenvalues of extremely large magnitude, and can lead to the burnup matrix norm being of the order of  $10^{21}$ . These difficulties have traditionally been solved by using simplified burnup chains or by treating the most short-lived nuclides separately, when computing a matrix exponential solution.

In this paper, this problem is approached for the first time by studying the spectral properties of burnup matrices. Based on physical constraints related to the problem, the eigenvalues of burnup matrices can be deduced to be generally confined to a region near the negative real axis. The established matrix exponential methods for solving the burnup equations are introduced and their suitability is discussed from this perspective. Based on the eigenvalues being located near the negative real axis, the Chebyshev rational approximation method (CRAM) is proposed as a novel method for solving the burnup equations. CRAM can be characterized as the best rational approximation on the negative real axis and it is highly accurate in the region where the burnup matrix eigenvalues are located.

The introduced matrix exponential methods are applied to two test cases representing an infinite pressurized water reactor pin-cell lattice. In addition, the test cases are solved with the semi-analytical linear chain method, in which the complicated transmutation chains are resolved into a set of linear sub-chains that can be solved analytically. The first test case was designed to be well-behaved in terms of the burnup matrix size and norm, whereas the second test case corresponds to a full burnup system with over a thousand nuclides with rather extreme numerical

characteristics. In the first test case, all matrix exponential methods gave consistent results. In the second test case, however, all other matrix exponential methods suffered a breakdown, whereas the results obtained with CRAM remained consistent with those given by the linear chain method to the same degree as in the first test case. In terms of computational efficiency, CRAM clearly outperformed all the other methods. The results suggest that CRAM is a very promising method for solving the burnup equations with a low computational cost.

### **5.2 Publication II: Rational approximations to the matrix exponential in burnup calculations**

The topic of the paper is solving the burnup equations using dedicated rational approximations accurate near the negative real axis. The burnup equations describe the changes in nuclide concentrations due to radioactive decay and neutron-induced transmutation reactions. They form a system of first order linear differential equations which is extremely stiff due to the decay constants of the nuclides varying extensively. In Publication [1], it was discovered that although the numerical properties of burnup matrices are otherwise rather difficult, their eigenvalues are generally confined to a region near the negative real axis. This observation prompted proposing the Chebyshev rational approximation method (CRAM) as a novel method for solving the burnup equations.

In this paper, two different types of rational approximation are considered for computing the exponential of a burnup matrix. The previously introduced CRAM, which can be characterized as the best rational approximation on the negative real axis, is analyzed in more detail. In addition, a method based on quadrature rules applied to a contour integral around the negative real axis is proposed. The motivation for introducing the latter method is that the computation of higher order CRAM approximations can become rather involved. In the quadrature-based approach, the approximation order can easily be adjusted to suit the needs for accuracy or efficiency. Furthermore, it was discovered that the previous literature values for coefficients of CRAM of order 14 contain errors, and result in relative accuracy two orders of magnitude poorer than expected by theory. To rectify this, new partial fraction decomposition coefficients for CRAM of order 14 and 16 were computed based on polynomial coefficients given in literature and provided in this paper.

The accuracy and convergence of both methods are studied and they are tested against highly accurate reference solutions computed with high-precision arithmetics. The sources of approximation error are analyzed and the previously observed difference in resulting accuracy for fresh and depleted fuel is explained. Based on the study, both methods appear to yield convergence rates close to the respective asymptotic convergence rates on the negative real axis when applied to burnup equations. In addition, the test cases indicate that both methods are capable of providing a very accurate and robust solution to the burnup equations.

### 5.3 Publication III: Correction to partial fraction decomposition coefficients for Chebyshev rational approximation on the negative real axis

The purpose of this note is to provide correct partial fraction decomposition (PFD) coefficients for the Chebyshev rational approximation method (CRAM) of order 14 and 16 on the negative real axis. The note was prompted by the observation that the literature values given previously for approximation order 14 by Gallopoulos and Saad in [22] are erroneous.

CRAM of order  $k$  can be characterized as the rational function yielding the smallest maximum deviation between the exponential function and any rational function of the same degree on the entire negative real axis. The asymptotic convergence rate of CRAM is remarkably fast, and it can be a viable method for computing the matrix exponential for matrices with eigenvalues in the vicinity of the negative real axis.

The main difficulty in using CRAM for computing the matrix exponential is determining the coefficients of the rational function for a given approximation order. For higher approximation orders the computation of the coefficients becomes rather involved and requires delicate algorithms combined with high-precision arithmetics. In addition, it is generally advantageous to employ the rational function in its PFD form which requires computing its poles, residues and limit at  $\text{Re } z \rightarrow -\infty$ .

The PFD coefficients for CRAM of order 14 have been previously provided in literature, and therefore they have been used in several applications. In [11], these coefficients were discovered to contain errors that resulted in  $10^2$  times poorer accuracy than expected by theory. In this note, the correct PFD coefficients are provided for approximation orders 14 and 16. The correct coefficients were computed based on literature values for the polynomial coefficients of the respective rational functions. The theory for computing the PFD coefficients from the polynomial is reviewed and the employed computational procedure is described. The approximation accuracy resulting from erroneous poles and residues is analyzed.

### 5.4 Publication IV: Solving linear systems with sparse Gaussian elimination in the Chebyshev rational approximation method (CRAM)

The topic of this paper is the solving of the linear systems arising when computing the matrix exponential solution to burnup equations with the Chebyshev rational approximation method (CRAM). The burnup matrices have difficult numerical characteristics that may compromise the accuracy of some iterative methods used for solving the linear systems. In this paper, a direct method is considered to overcome this difficulty.

The numerical properties of burnup matrices are reviewed. The proposed direct method is based on sparse Gaussian elimination in which the sparsity pattern of the resulting upper triangular matrix is determined before the numerical elimination phase. The stability of Gaussian elimination is discussed and, based on the

properties of burnup matrices, it is shown that the proposed method is well-suited for solving the linear systems. Suitable algorithms are presented for computing the symbolic factorization and numerical elimination. The accuracy and efficiency of the described technique are demonstrated by computing the CRAM approximations for a large test case with over 1600 nuclides.

### **5.5 Publication V: Incorporating sensitivity and uncertainty analysis to a lattice physics code with application to CASMO-4**

The topic of this paper is the implementation of classical perturbation theory based sensitivity and uncertainty analysis features to the fuel assembly burnup calculation program CASMO-4 in the context of the UAM benchmark [28], whose first stage aims at propagating the uncertainty related to nuclear data through fuel assembly calculations. The benchmark was prepared in 2006 to establish the current state and needs of sensitivity and uncertainty analysis, with the ultimate goal of being able to propagate uncertainty through all stages in a coupled neutronics/thermal hydraulics calculation. At that time, the generally employed reactor physics codes did not have uncertainty analysis capabilities, and the modified CASMO-4 was one of the first fuel assembly programs that enabled sensitivity and uncertainty analysis based on perturbation theory.

Classical perturbation theory studies the changes in the multiplication factor due to perturbations in system parameters. In this framework, the critical eigenvalue sensitivities to uncertain nuclear data parameters are computed efficiently by utilizing the adjoint system of the eigenvalue problem. After computing the sensitivities, the uncertainty related to these parameters can be propagated deterministically to the multiplication factor. Both the theoretical background as well as practical considerations for implementing classical perturbation theory to a reactor physics code are reviewed and discussed in detail in the paper.

In the process of modifying CASMO-4, a problem was faced due to the incompatibility of the cross-section models between the covariance libraries and the code itself. In this paper, a technique for overcoming this difficulty by combining the covariance matrices is proposed. The sensitivities can then be computed with respect to the combined reactions. The proposed technique accurately combines the capture reactions in a consistent manner, but results in systematic differences for the scattering reactions. The issue is analyzed and the difference is explained by incompatible constraints in the two calculation strategies.

Numerical results are presented for two of the benchmarks fuel pin-cell test problems representing a PWR and a GEN-III core with MOX fuel, and the results are compared against TSUNAMI-1D. The comparison supports the observations made on the developed methodology, i.e. the results are consistent except for scattering reactions, where systematic differences appear in cases with multiple scattering reactions.

## 5.6 Publication VI: Perturbation-theory-based sensitivity and uncertainty analysis with CASMO-4

This paper considers the implementation of generalized perturbation theory based sensitivity and uncertainty capability to the fuel assembly burnup calculation program CASMO-4. The motivation for the described work has been the participation in the UAM benchmark [28]. Initially, classical perturbation theory was implemented to CASMO-4, which allowed the sensitivity analysis with respect to the multiplication factor. This work was reported in [V].

Generalized perturbation theory studies the changes in responses that can be represented as reaction rate ratios. For each response, the computation of the sensitivity profiles with respect to all parameters of interest requires solving one generalized adjoint system. This is computationally efficient, when the number of parameters is large, as is the case in reactor physics applications. After computing the sensitivity profiles, the uncertainty related to nuclear data can be propagated deterministically to the response under consideration by approximating the relationship between the parameters and the response to be linear.

The mathematical background as well as the physical interpretation of the generalized adjoint solutions are reviewed in the paper, and practical guidelines are given for modifying a deterministic transport code to solve the generalized adjoint systems needed in sensitivity analysis. The theory for computing the sensitivity profiles is presented both from the perspective of function space analysis and numerical computations.

Numerical results are presented for a lattice physics test problem in the benchmark, and they are compared to the results given by the TSUNAMI-2D sequence in SCALE 6.1. Two-group homogenized cross-sections are considered as responses in the generalized perturbation theory framework. The results are in accordance with theoretical considerations. In particular, they are consistent for the thermal responses, whereas some systematic differences are observed for fast responses. These differences are explained by the incompatible constraints in defining the sensitivities, an issue which was analyzed in detail in [V].



## 6. Conclusions

The objective of burnup calculations is to simulate the changes in the composition of nuclear fuel over time. Due to safety considerations related to the target of application, it is important that the applied calculation methods are constantly improved. In addition, uncertainty analysis methods are needed for evaluating the reliability of the calculation results.

Burnup calculations are built upon solving the neutron transport criticality equation and burnup equations sequentially in a cyclic manner. This thesis focused on two areas essential for burnup calculations: the numerical solution of burnup equations based on computing the burnup matrix exponential and the uncertainty analysis of the criticality equation based on perturbation theory.

### **Matrix exponential solution of burnup equations**

The burnup equations govern the changes in nuclide concentrations over time. They form a system of first order differential equations, which can be formally solved by computing the matrix exponential of the burnup matrix. Due to the dramatic variation in the half-lives of different nuclides, the system is extremely stiff, and the problem is complicated by the vast range of time steps used in burnup calculations. Because of these characteristics, the computation of the burnup matrix exponential has been previously considered impossible for the full burnup system. Instead, simplified burnup chains have been used, or the most short-lived nuclides have been treated separately when computing a matrix exponential solution.

In Publication [1], the spectral properties of burnup matrices were studied for the first time. It was reasoned that although the magnitudes of the eigenvalues of burnup matrices vary extensively, they are generally confined to a region near the negative real axis. The observation was based on considering the physical constraints related to burnup equations and studying the strongly connected components of the burnup matrix graph.

In Chapter 3.1 of this thesis, the mathematical properties of burnup matrices were further studied. Firstly, the negatives of burnup matrices were identified to belong to the class of  $Z$ -matrices, which guarantees the non-negativity of the burnup matrix exponential, for example. To further study the eigenvalues, burnup matrices were

## 6. Conclusions

---

categorized into conventional and augmented burnup matrices based on whether the production of by-product nuclides was taken into account when constructing them. The negatives of conventional burnup matrices were then recognized as  $M$ -matrices, which gave a wedge condition to their spectrum around the negative real axis. Augmented burnup matrices, on the other hand, can be permuted to block triangular form, with the eigenvalues of the matrix comprising of the eigenvalues of the diagonal blocks. Apart from the block corresponding to the by-product nuclides, the diagonal blocks were shown to be  $M$ -matrices. The block corresponding to the by-product nuclides was identified with the matrix class  $L_0^2$ , meaning that it has a single positive eigenvalue.

The observation about the burnup matrix eigenvalues being located near the negative real axis prompted proposing rational approximations that are accurate on the negative real axis for solving the burnup equations [I, II]. In Publication [I], the Chebyshev rational approximation method (CRAM), which can also be characterized as the best rational approximation on the negative real axis, was introduced with very promising results. In contrast to other matrix exponential methods considered previously, CRAM was demonstrated to be applicable to large burnup problems containing over a thousand nuclides and with a matrix norm of the order of  $10^{21}$ . In addition, CRAM was shown to allow time steps of the order of  $10^7$  s, which can be considered the maximum feasible time step in burnup calculations. Based on these results, CRAM was implemented to the reactor physics code Serpent developed at VTT. In addition to CRAM, rational approximations based on quadrature rules applied to contour integrals around the negative real axis were suggested as an alternative solution method [II]. This approach has the advantage that the order of approximation can be easily adjusted.

The accuracy and convergence of CRAM were further studied in [II] by comparing the results against highly accurate reference solutions computed with high-precision accuracy. The results supported the assessment of CRAM being capable of providing a very accurate and robust solution to the burnup equations at a very low computational cost.

The application of CRAM requires determining the partial fraction decomposition coefficients (PFD) of the rational function for a given approximation order. Unfortunately, the computation of these coefficients is difficult and requires delicate algorithms combined with high-precision accuracy. The PFD coefficients for CRAM of order 14 have been previously provided in literature, and have therefore been used in several applications. In Publication [II], these coefficients were discovered to contain errors that resulted in  $10^2$  times poorer accuracy than expected by theory. The correct PFD coefficients for approximation order 14 and 16 were then computed based on literature values for the polynomial coefficients of the respective rational functions. These coefficients were first reported in [II] and later in [III] with a more detailed description and an analysis of the approximation accuracy deterioration resulting from the erroneous coefficients.

In practise, the application of CRAM to solving the burnup equations requires a linear solver in addition to the PFD coefficients. Due to the difficult numerical char-

acteristics of burnup matrices, the accuracy of some iterative solution methods may be compromised. In [IV] a direct method based on sparse Gaussian elimination was considered. It was demonstrated that the characteristics of burnup matrices allow using Gaussian elimination without pivoting, which enables computing the symbolic LU factorization of the matrix before starting the numerical elimination phase. Due to the sparsity pattern of burnup matrices, the linear systems arising during CRAM can be solved both efficiently and accurately with this approach [IV].

### **Uncertainty analysis of the criticality equation based on perturbation theory**

When uncertain parameters are utilized in a computation, the calculation results also contain uncertainty. The imprecision of neutron interaction data is considered to be one of the most significant sources of uncertainty in all reactor physics calculations, including burnup calculations.

In this thesis, uncertainty analysis was applied to the criticality equation on a fuel assembly level. The motivation for this work was participating in the UAM benchmark [28] whose goal is to propagate the uncertainty in the nuclear data through a coupled neutronics/thermal-hydraulics calculation. The first phase of the benchmark aims at propagating uncertainty through fuel assembly calculations, which are used to produce homogenized data for the following coupled calculations. The objective of the first phase can be considered ambitious, since the generally used fuel assembly codes did not have uncertainty analysis capabilities when the benchmark was started.

Due to vast number of uncertain nuclear data in fuel assembly calculations, perturbation theory was chosen as the framework for the uncertainty analysis. The fuel assembly burnup calculation code CASMO-4 [29] was chosen as the development platform. Perturbation theory allows computing the sensitivity profiles of a response with respect to any number of parameters in an efficient manner by solving an adjoint system in addition to the original forward problem. The uncertainty related to these parameters can then be propagated deterministically by linearizing the response.

Initially, classical perturbation theory was implemented to CASMO-4, which enabled the uncertainty analysis of the multiplication factor [V]. In the process of modifying CASMO-4, a problem was faced due to the incompatibility of the cross-section models between the covariance libraries containing the neutron interaction uncertainty data and the code itself. In publication [V], a technique for overcoming this issue by combining the covariance matrices was devised. The proposed approach accurately combines the capture reactions whereas it results in systematic differences for the scattering reactions. The issue was analyzed and the difference was explained by the incompatible constraints implicitly assumed in the two calculation strategies [V]. The uncertainty analysis methodology was later extended to responses that can be represented as reaction rate ratios [VI]. This framework is called generalized perturbation theory and it was applied to two-group homogenized cross-sections.



## Bibliography

- [1] J. LEPPÄNEN and M. PUSA, "Burnup calculation capability in the PSG2/Serpent Monte Carlo reactor physics code," In Proc. of International Conference on Mathematics, Computational Methods & Reactor Physics (M&C 2009), on CD-ROM, 1662–1673, American Nuclear Society (2009).
- [2] D. G. CACUCI, ed., *Handbook of Nuclear Engineering*, Vol. 2: Reactor Design, Springer (2010).
- [3] A. KONING, R. FORREST, M. KELLETT, R. MILLS, H. HENRIKSSON and Y. RUGAMA, "The JEFF-3.1 Nuclear Data Library", JEFF Report 21, NEA Data Bank (2006).
- [4] A. KONING, S. HILAIRE, and S. GORIELY, "TALYS-1.4, a Nuclear Reaction Program, User Manual" (2011).
- [5] H. AMANN, *Ordinary Differential Equations, An Introduction to Nonlinear Analysis*, Walter de Gruyter (1990).
- [6] A. BERMAN and R. J. PLEMMONS, *Nonnegative Matrices in the Mathematical Sciences*, SIAM (1994).
- [7] R. B. KELLOGG, "On complex eigenvalues of  $M$  and  $P$  matrices," *Numer. Math.*, **19**, 170–175 (1972).
- [8] S. M. FALLAT, C. R. JOHNSON, R. L. SMITH, and P. VAN DEN DRIESSCHE, "Eigenvalue location for nonnegative and  $Z$ -matrices," *Linear Algebra and its Applications*, **277**, 187–198 (1998).
- [9] R. DREHER, "Modified Bateman Solution for Identical Eigenvalues," *Ann. Nucl. Energy*, **53** (2013).
- [10] L. N. TREFETHEN and M. EMBREE, *Spectra and Pseudospectra*, Princeton University Press (2005).
- [11] T. G. WRIGHT, "Eigtool," <http://www.comlab.ox.ac.uk/pseudospectra/eigtool/> (accessed February 13, 2013) (2005).
- [12] N. J. HIGHAM, *Functions of Matrices, Theory and Computation*, SIAM (2008).

- [13] L. A. ZADEH and C. A. DESOER, *Linear System Theory: The State Space Approach*, McGraw-Hill Book Company, Inc. (1963).
- [14] I. C. GAULD, O. W. HERMANN, and R. M. WESTFALL, "Origen-S: Scale System Module to Calculate Fuel Depletion, Actinide Transmutation, Fission Product Buildup and Decay, and Associated Radiation Source Terms," in "SCALE: A Modular Code System for Performing Standardized Computer Analyses for Licensing Evaluation," Vol. II, Sec. F7, Oak Ridge National Library/U.S. Nuclear Regulatory Commission (Nov. 2006).
- [15] A. YAMAMOTO, M. TATSUMI, and N. SUGIMURA, "Numerical Solution of Stiff Bur-nup Equations with Short Half Lived Nuclides by the Krylov Subspace Method," *J. Nucl. Sci. Technol.*, **44**, 2, 147–154 (2007).
- [16] C. MOLER and C. VAN LOAN, "Nineteen Dubious Ways to Compute the Exponential of a Matrix, Twenty-Five Years Later," *SIAM Rev.*, **45** (2003).
- [17] N. J. HIGHAM, "The Scaling and Squaring Method for the Matrix Exponential Revisited," *SIAM J. Matrix Anal. & Appl.*, **26**, 4, 1179–1193 (2005).
- [18] L. N. TREFETHEN, J. A. C. WEIDEMAN, and T. SCHMELZER, "Talbot Quadratures and Rational Approximations," *BIT*, **46**, 3, 653–670 (2006).
- [19] A. A. GONCHAR and E. A. RAKHMANOV, "Equilibrium Distributions and Degree of Rational Approximation of Analytic Functions," *Math. USSR Sb.*, **62**, 2 (1989).
- [20] H. STAHL and T. SCHMELZER, "An Extension of the '1/9'-Problem," *Journal of Computational and Applied Mathematics*, **233**, 821–834 (2009).
- [21] A. J. CARPENTER, A. RUTTAN, and R. S. VARGA, "Extended Numerical Computations on the '1/9' Conjecture in Rational Approximation Theory," "Rational Approximation and Interpolation" in *Lecture Notes in Mathematics*, Vol. 1105, 383–411, P. R. Graves-Morris, E. B. Saff, and R. S. Varga, Eds., Springer-Verlag (1984).
- [22] E. GALLOPOULOS and Y. SAAD, "Efficient Solution of Parabolic Equations by Krylov Approximation Methods," *SIAM J. Sci. Stat. Comput.*, **13**, 5, 1236–1264 (1992).
- [23] R. B. SIDJE, "Expokit: a Software Package for Computing Matrix Exponentials," *ACM Trans. Math. Softw.*, **24**, 1, 130–156 (1998).
- [24] A. ISOTALO and P. A. AARNIO, "Comparison of depletion algorithms," *Ann. Nucl. Energy*, **38**, 2–3, 261–268 (2011).
- [25] H. BATEMAN, "Solution of a system of differential equations occurring in the theory of radioactive transformations." *Proc. Cambridge Philos. Soc.*, **15**, 423–427 (1910).

- [26] J. CETNAR, "General Solution of Bateman Equations for Nuclear Transmutations," *Ann. Nucl. Energy*, **33**, 640–645 (2006).
- [27] J. WEIDEMAN and L. N. TREFETHEN, "Parabolic and Hyperbolic Contours for Computing the Bromwich Integral," *Math. Comp.*, **76**, 259, 1341–1356 (2007).
- [28] K. IVANOV, M. AVRAMOVA, S. KAMEROW, I. KODELI, and E. SARTORI, E. IVANOV, O. CABELLOS, "Benchmark for Uncertainty Analysis in Modeling (UAM) for Design, Operation, and Safety Analysis of LWRs, Volume I: Specification and Support Data for the Neutronics Cases (Phase I)," NEA/NSC/DOC(2012)10 (2012).
- [29] J. RHODES and M. EDENIUS, "CASMO-4, A Fuel Assembly Burnup Program, User's Manual," (proprietary) Studsvik Scandpower, SSP-01/400 (2001).
- [30] E. T. JAYNES, *Probability Theory: the Logic of Science*, Cambridge University Press (2003).
- [31] D. G. CACUCI, *Sensitivity and Uncertainty Analysis*, vol. 1, Chapman & Hall/CRC (2003).
- [32] E. P. WIGNER, *Effects of Small Perturbations on Pile Period*, CP-3048, Manhattan Project Report (1945).
- [33] L. N. USACHEV, *Perturbation Theory for the Breeding Ratio and for Other Number Ratios Pertaining to Various Reactor Processes*, *J. Nucl. Energy, Parts A/B*, **18**, 571 (1964).
- [34] B. G. CARLSON and K. D. LATHROP, "Transport Theory—the Method of Discrete Ordinates," in H. GREENSPAN, C. N. KELBER, and D. OKRENT, eds., "Computing Methods in Reactor Physics," Gordon and Breach Science Publishers (1968).
- [35] E. E. LEWIS and J. W. F. MILLER, *Computational Methods of Neutron Transport*, John Wiley & Sons (1984).
- [36] J. LEWINS, *Importance: the Adjoint Function*, Pergamon Press, Oxford (1965).
- [37] M. L. WILLIAMS, "Perturbation Theory for Nuclear Reactor Analysis," in Y. RONEN, Ed., "CRC Handbook of Nuclear Reactors Calculations," , Vol. 3, CRC Press (1986).
- [38] J. R. ASKEW, "A Characteristics Formulation of the Neutron Transport Equation in Complicated Geometries," Tech. Rep. AAEW-M 1108 (1972).
- [39] ZZ-SCALE6.0/COVA-44G, a 44-group cross section covariance matrix library retrieved from the SCALE-6.0 package, NEA Data Bank code package USCD1236/03 (2011).

- [40] M. L. WILLIAMS, D. WIARDA, G. ARBANAS, and B. L. BROADHEAD, "Scale Nuclear Data Covariance Library," in "SCALE: A Modular Code System for Performing Standardized Computer Analyses for Licensing Evaluation, Version 5," ORNL/TM-2005/39, Oak Ridge National Library/U.S. Nuclear Regulatory Commission (January 2009).
- [41] "HELIOS Methods," Studsvik Scandpower (2000).
- [42] "WIMS9A, NEW FEATURES, A Guide to the New Features of WIMS Version 9A," Serco Assurance, <http://www.sercoassurance.com/answers/> (accessed February 13, 2013) (2005).
- [43] G. MARLEAU, A. HÉBERT, and R. ROY, "A User Guide For Dragon Version 4," IGE294, <http://www.polymtl.ca/nucleaire/DRAGON/> (accessed February 13, 2013) (2009).
- [44] C. R. WEISBIN and *et al*, "Application of FORSS Sensitivity and Uncertainty Methodology to Fast Reactor Benchmark Analysis," Tech. Rep. ORNL/TM-5563 (1976).

Title	<b>Numerical methods for nuclear fuel burnup calculations</b>
Author	Maria Pusa
Abstract	<p>The material composition of nuclear fuel changes constantly due to nuclides transforming to other nuclides via neutron-induced transmutation reactions and spontaneous radioactive decay. The objective of burnup calculations is to simulate these changes over time. This thesis considers two essential topics of burnup calculations: the numerical solution of burnup equations based on computing the burnup matrix exponential, and the uncertainty analysis of neutron transport criticality equation based on perturbation theory.</p> <p>The burnup equations govern the changes in nuclide concentrations over time. They form a system of first order differential equations that can be formally solved by computing the matrix exponential of the burnup matrix. Due to the dramatic variation in the half-lives of different nuclides, the system is extremely stiff and the problem is complicated by vast variations in the time steps used in burnup calculations. In this thesis, the mathematical properties of burnup matrices are studied. It is deduced that their eigenvalues are generally confined to a region near the negative real axis. Rational approximations that are accurate near the negative real axis, and the Chebyshev rational approximation method (CRAM) in particular, are proposed as a novel method for solving the burnup equations. The results suggest that the proposed approach is capable of providing a robust and accurate solution to the burnup equations with a very short computation time.</p> <p>When a mathematical model contains uncertain parameters, this uncertainty is propagated to responses dependent on the model. This thesis studies the propagation of neutron interaction data uncertainty through the criticality equation on a fuel assembly level. The considered approach is based on perturbation theory, which allows computing the sensitivity profiles of a response with respect to any number of parameters in an efficient manner by solving an adjoint system in addition to the original forward problem. The uncertainty related to these parameters can then be propagated deterministically to the response by linearizing the response.</p>
ISBN, ISSN	ISBN 978-951-38-7999-0 (Soft back ed.) ISBN 978-951-38-8000-2 (URL: <a href="http://www.vtt.fi/publications/index.jsp">http://www.vtt.fi/publications/index.jsp</a> ) ISSN-L 2242-119X ISSN 2242-119X (Print) ISSN 2242-1203 (Online)
Date	May 2013
Language	English
Pages	86 p. + app. 78 p.
Keywords	Burnup equations, Chebyshev rational approximation, CRAM, matrix exponential, sensitivity analysis, uncertainty analysis
Publisher	VTT Technical Research Centre of Finland P.O. Box 1000, FI-02044 VTT, Finland, Tel. +358 20 722 111



**VTT Technical Research Centre of Finland** is a globally networked multitechnological contract research organization. VTT provides high-end technology solutions, research and innovation services. We enhance our customers' competitiveness, thereby creating prerequisites for society's sustainable development, employment, and wellbeing.

Turnover: EUR 300 million

Personnel: 3,200

## **VTT publications**

VTT employees publish their research results in Finnish and foreign scientific journals, trade periodicals and publication series, in books, in conference papers, in patents and in VTT's own publication series. The VTT publication series are VTT Visions, VTT Science, VTT Technology and VTT Research Highlights. About 100 high-quality scientific and professional publications are released in these series each year. All the publications are released in electronic format and most of them also in print.

### **VTT Visions**

This series contains future visions and foresights on technological, societal and business topics that VTT considers important. It is aimed primarily at decision-makers and experts in companies and in public administration.

### **VTT Science**

This series showcases VTT's scientific expertise and features doctoral dissertations and other peer-reviewed publications. It is aimed primarily at researchers and the scientific community.

### **VTT Technology**

This series features the outcomes of public research projects, technology and market reviews, literature reviews, manuals and papers from conferences organised by VTT. It is aimed at professionals, developers and practical users.

### **VTT Research Highlights**

This series presents summaries of recent research results, solutions and impacts in selected VTT research areas. Its target group consists of customers, decision-makers and collaborators.

## Numerical methods for nuclear fuel burnup calculations

The material composition of nuclear fuel changes constantly due to nuclides transforming to other nuclides via neutron-induced transmutation reactions and spontaneous radioactive decay. The objective of burnup calculations is to simulate these changes over time. They are formulated around two basic equations in reactor physics: neutron transport criticality equation and burnup equations. This thesis considers the numerical solution of burnup equations based on computing the burnup matrix exponential, and the uncertainty analysis of neutron transport criticality equation based on perturbation theory.

In this thesis, the mathematical properties of burnup matrices are studied and the Chebyshev rational approximation method (CRAM) is proposed as a novel method for solving the burnup equations. The results suggest that the proposed approach is capable of providing a robust and accurate solution to the burnup equations with a very short computation time. Secondly, the propagation of neutron interaction data uncertainty through the criticality equation is studied on a fuel assembly level. The considered approach is deterministic and utilizes the adjoint system of the criticality equation, which allows propagating these uncertainties in an efficient manner.

ISBN 978-951-38-7999-0 (soft back ed.)  
ISBN 978-951-38-8000-2 (URL: <http://www.vtt.fi/publications/index.jsp>)  
ISSN-L 2242-119X  
ISSN 2242-119X (Print)  
ISSN 2242-1203 (Online)

